μ(I) rheology for granular flows with *Gerris* applications for avalanches and column collapse

Pierre-Yves Lagrée∗, Lydie Staron∗, Stéphane Popinet ∗o

∗Institut Jean le Rond d'Alembert, CNRS, Université Pierre & Marie Curie, 4 place Jussieu, Paris, France

o National Institute of Water and Atmospheric Research, PO Box 14-901 Kilbirnie, Wellington, New Zealand

http://gfs.sourceforge.net/wiki/index.php/Gerris_users'_meeting_registration

- What is a granular media?
- size > 100µm
- grains of sand, small rocks, glass beads, animal feed pellet, medicines, cereals, wheat, sugar, rice...
- 50 % of the traded products

FIG. 1.2 – Les milieux granulaires forment une famille extrêmement vaste.

spoil tip (boney pile, gob pile, bing or pit heap), «terril» in french

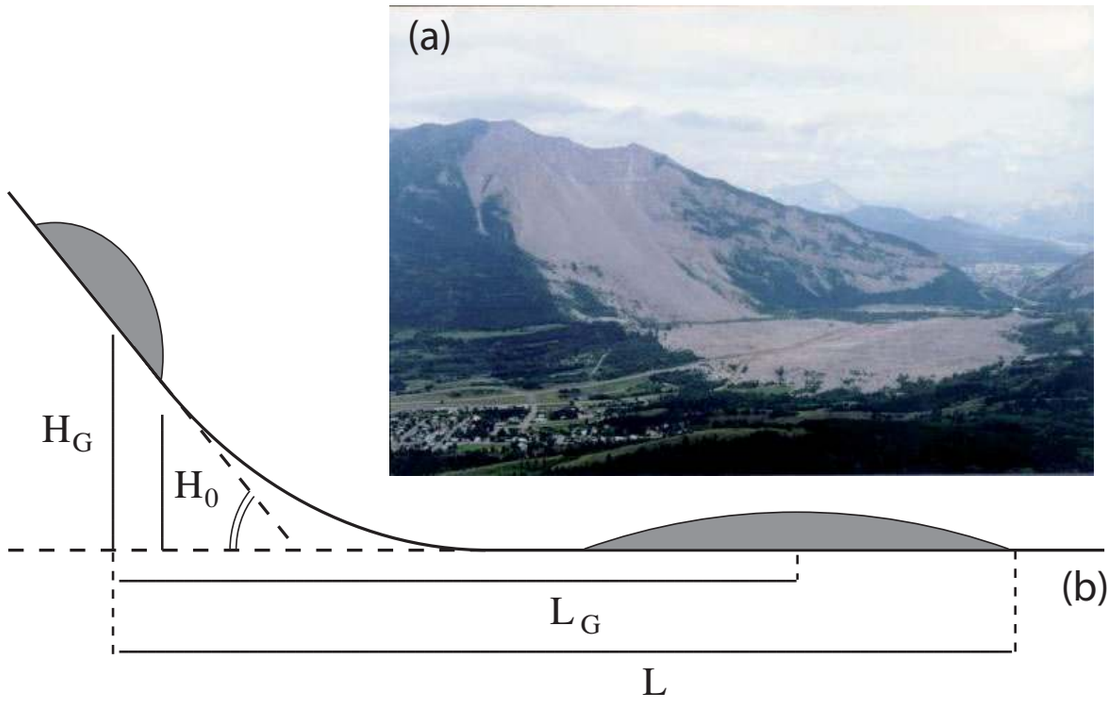

Staron

Fig. 20. Frank slide.

Environmental Modelling & Software xx (2006) 1e18
www.elsevier.com/locate/envsoft

The effect of the earth pressure coefficients on the runout of granular material

Marina Pirulli [a,*], Marie-Odile Bristeau [b], Anne Mangeney [c], Claudio Scavia

on MARS...

http://books.google.fr/books?id=HY6Z5od4-E4C&pg=PA49&dq=granular+flow&hl=fr&ei=lamtTaa_NYyVOoToldcL&sa=X&oi=book_result&ct=result&resnum=10&ved=0CFkQ6AEwCTgK#v=onepage&q&f=true

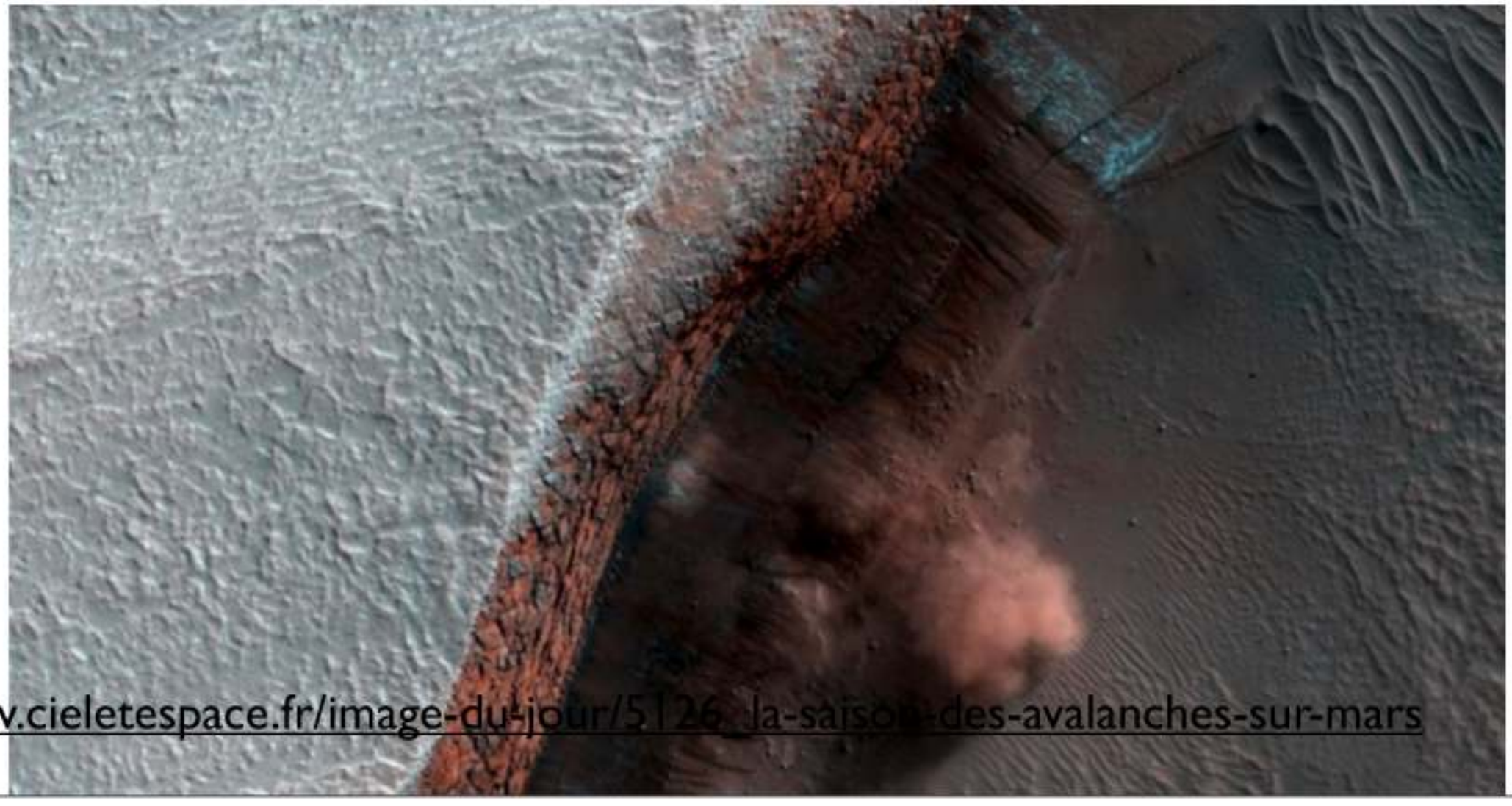

http://www.cieletespace.fr/image-du-jour/5126_la-saison-des-avalanches-sur-mars

sorry it is a fake, I a have no photos of my children playing with sand !

The sand pit problem: quickly remove the bucket of sand

http://www.mylot.com/w/photokeywords/pail.asp

Granular Column Collapse

Lajeunesse 04

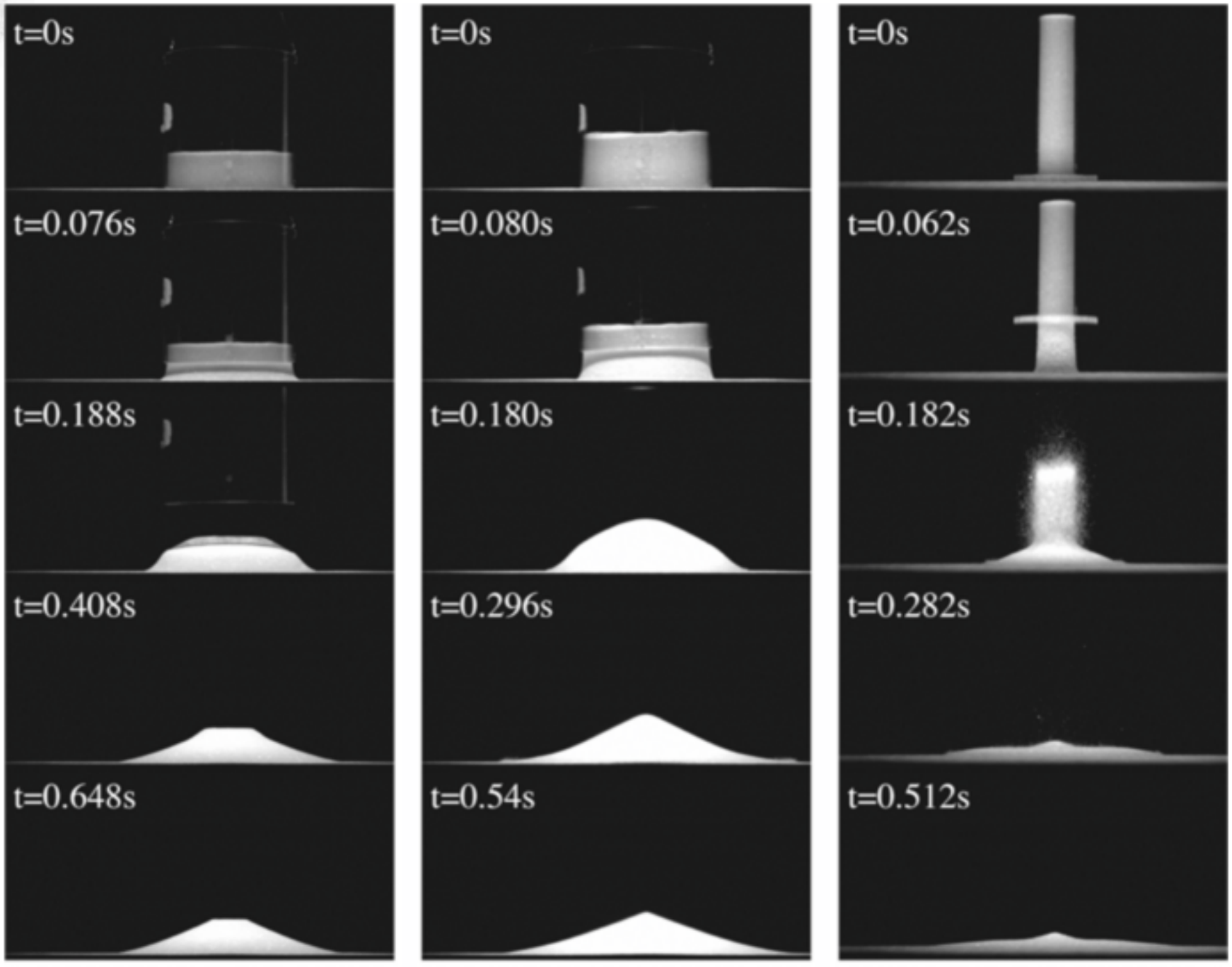

The sand pit problem: quickly remove the bucket of sand

http://www.mylot.com/w/photokeywords/pail.asp

Granular Column Collapse

aspect ratio $a = H_0/R_0 = H_0/L_0$

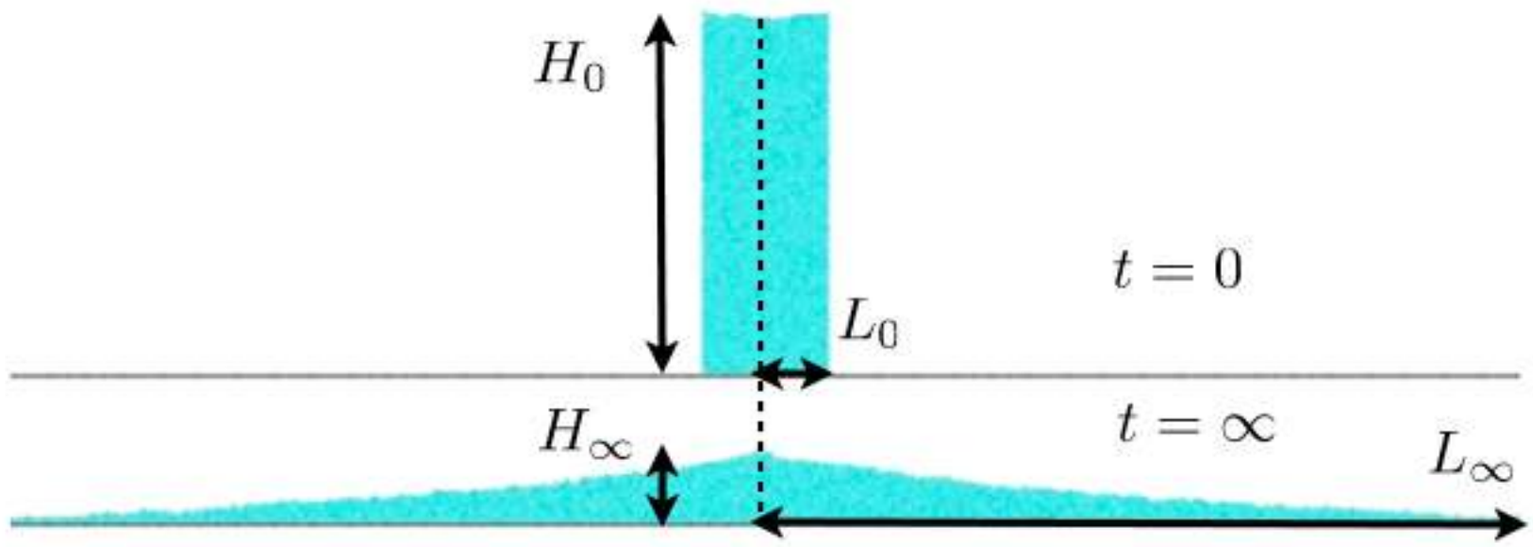

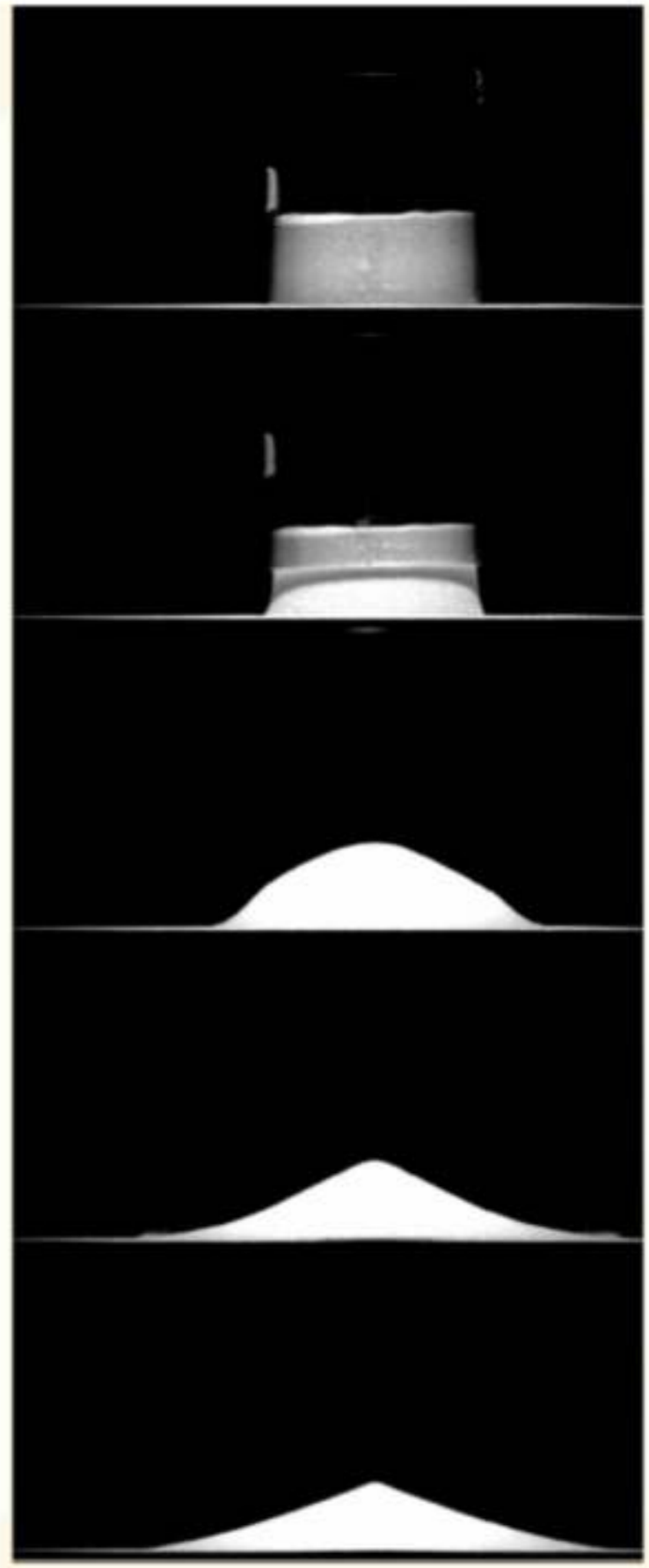

Lajeunesse et al., 2004

The sand pit problem: quickly remove the bucket of sand

Granular Column Collapse

A possible experimental set up is a container filled by sand (left), the aspect ratio (height/length) is *a*. At initial time, the gate is opened quickly. After the avalanche, the grains stop, the final configuration is at rest (right). We compare results from Discrete Contact Method Simulations (simulation of the displacement of each grain) to a continuum Navier Stokes simulation with the μ(I) rheology *Gerris*.

The sand pit problem: quickly remove the bucket of sand

- Looking for a continuum description
- Lot of recent experiments
- Simulation with Contact Dynamics

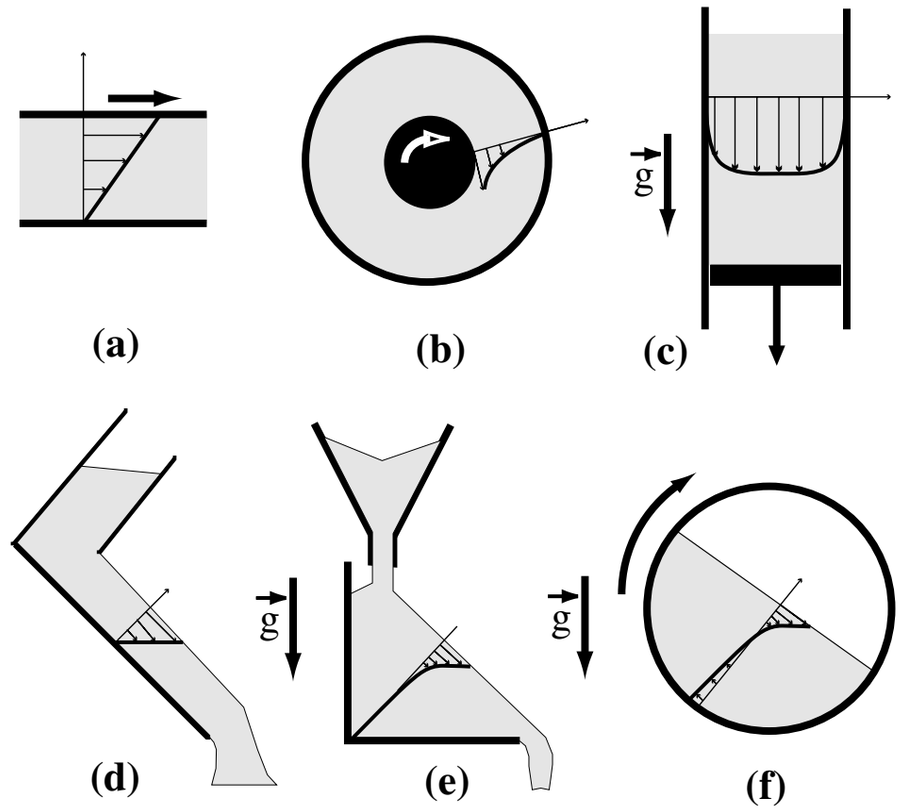

Fig. 1. The six configurations of granular flows: (a) plane shear, (b) annular shear, (c) vertical-chute flows, (d) inclined plane, (e) heap flow, (f) rotating drum.

GDR MiDi EPJ E 04

- Looking for a continuum description
- Lot of recent experiments
- Simulation with Contact Dynamics

- Defining a «viscosity»
- Implement it in *Gerris*
- Test on exact «Bagnold» avalanche solution
- Test on granular collapse

$V(z)$

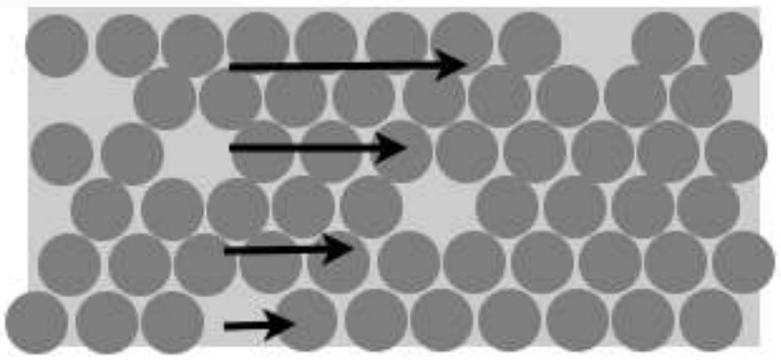

$V(z)$

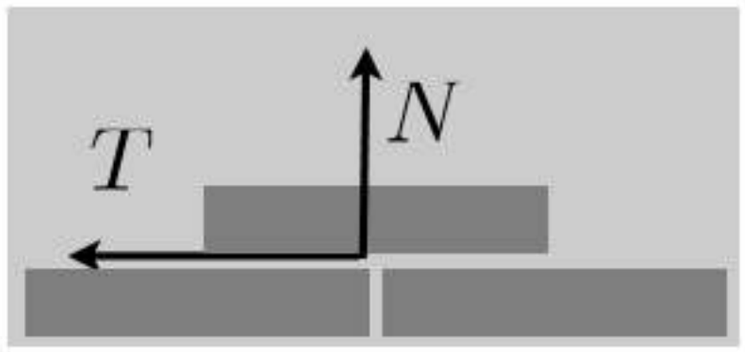

$$T = \mu N$$

constitutive law?

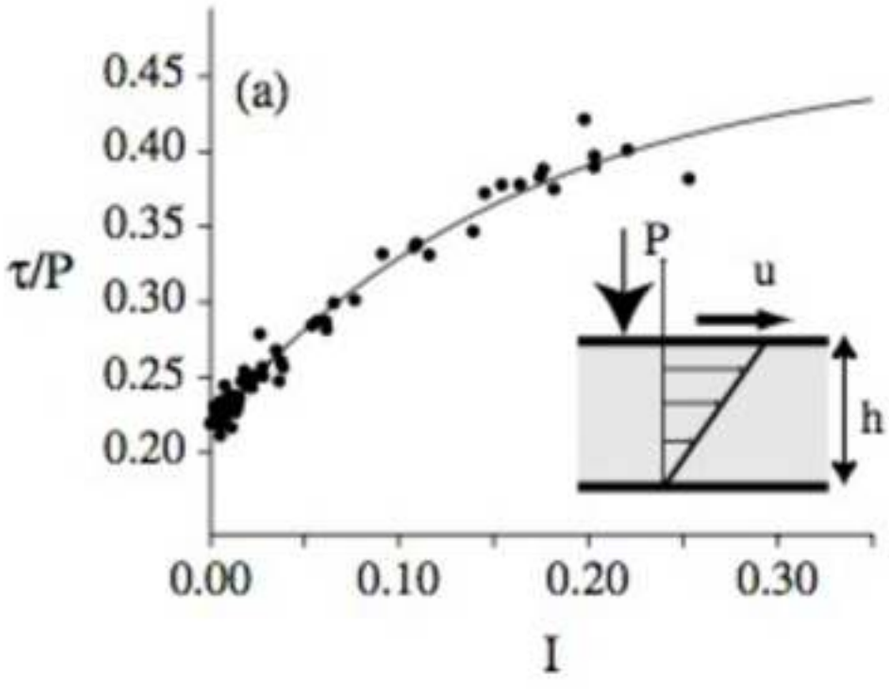

Coulomb dry friction

Coulomb friction law

$$\tau = \mu P$$

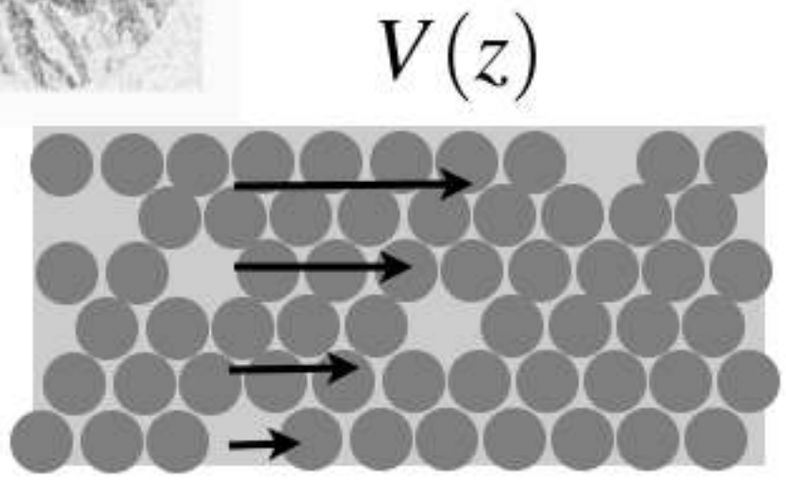

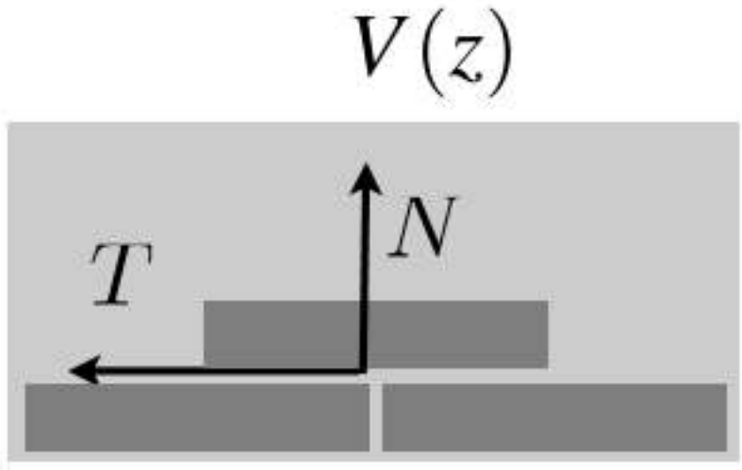

$$T = \mu N$$

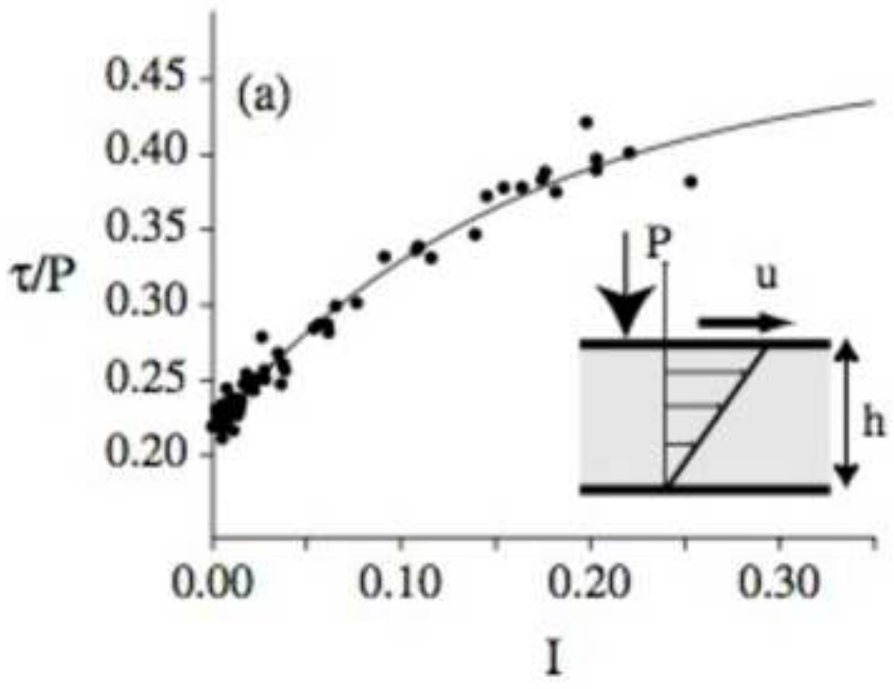

Coulomb friction law

$$I = \frac{d\frac{\partial u}{\partial y}}{\sqrt{P/\rho}}$$

$$\tau = \mu(I)P$$

non dimensional number: «Froude»

local «Inertial Number» (Da Cruz 04-05)

$V(z)$

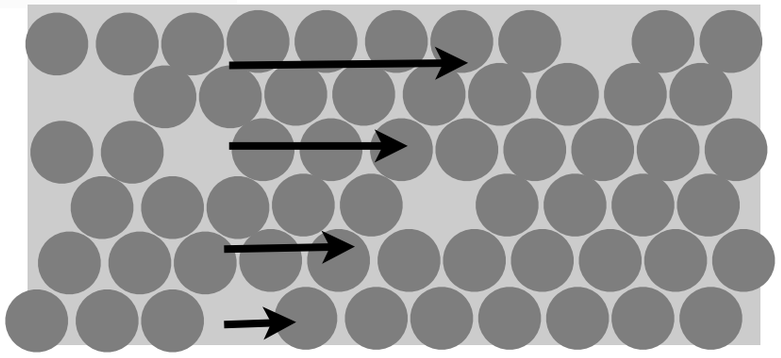

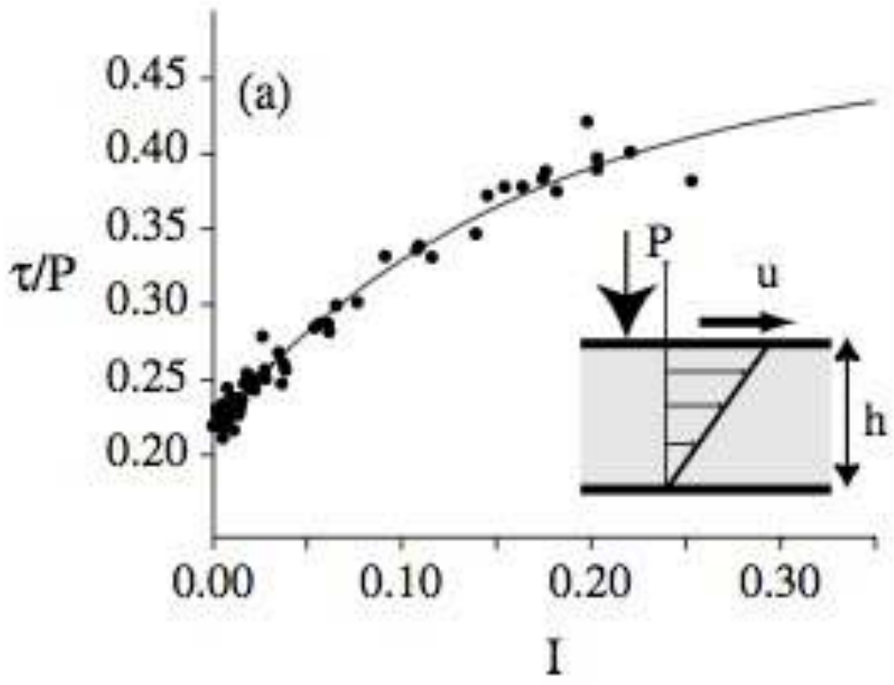

$$\frac{\text{falling time}}{\text{displacement time}} \qquad I = \frac{d\frac{\partial u}{\partial y}}{\sqrt{P/\rho}}$$

non dimensional number: «Froude»
local «Inertial Number» (Da Cruz 04-05)

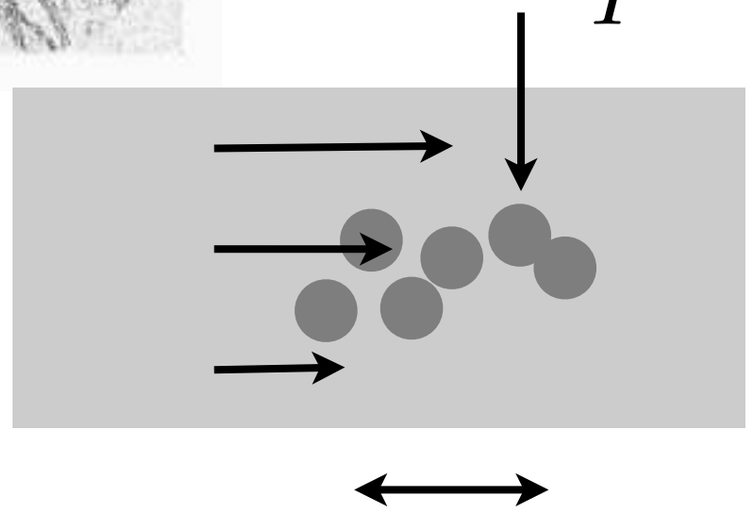

$$P$$

$$md^2y/dt^2 = Pd^2$$

$$t^2 = \rho d^2/(P)$$

$$\frac{dx}{dt} = d\frac{\partial u}{\partial y} \qquad t = 1/\frac{\partial u}{\partial y}$$

$$\frac{\text{falling time}}{\text{displacement time}} \qquad I = \frac{d\frac{\partial u}{\partial y}}{\sqrt{P/\rho}}$$

$V(z)$

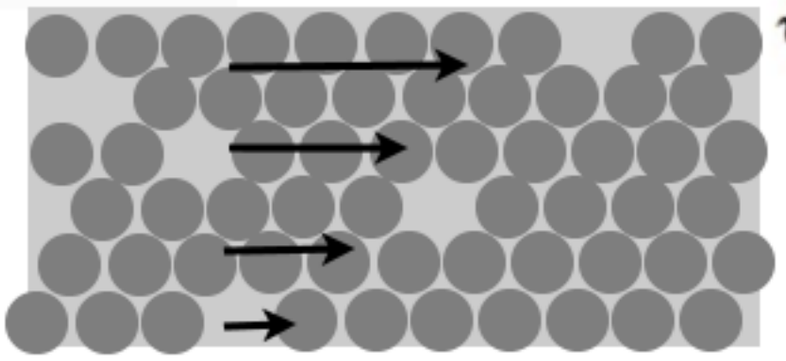

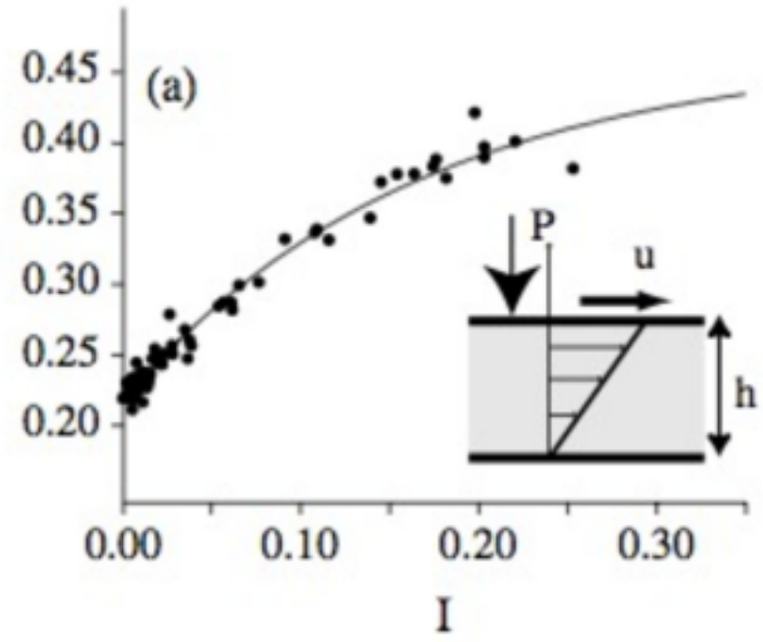

by grain dynamics

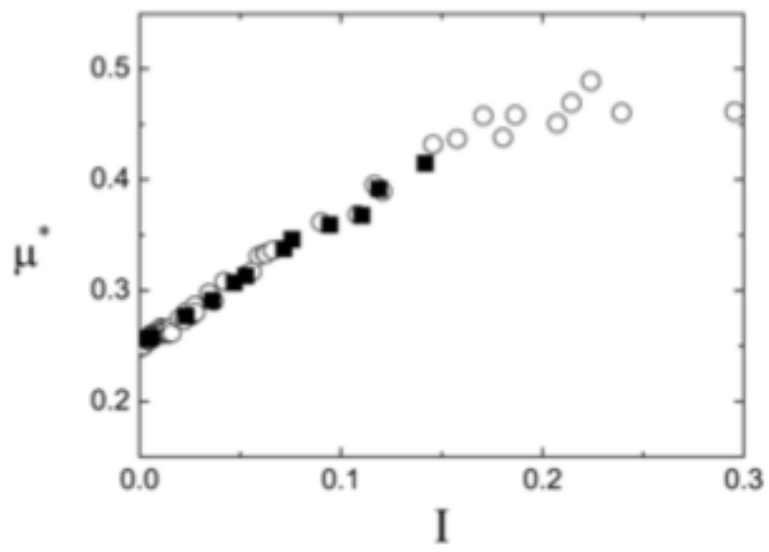

Da Cruz PRE 05

Coulomb friction law

$$\tau = \mu(I) P$$

$$\frac{\text{falling time}}{\text{displacement time}} \qquad I = \frac{d\frac{\partial u}{\partial y}}{\sqrt{P/\rho}}$$

Pouliquen 99
Pouliquen Forterre JSM 06
Da Cruz 04-05
GDR Midi 04
Josserand Lagrée Lhuillier 04

$V(z)$

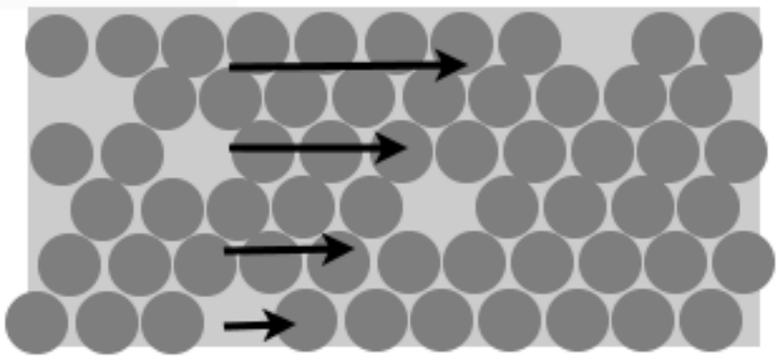

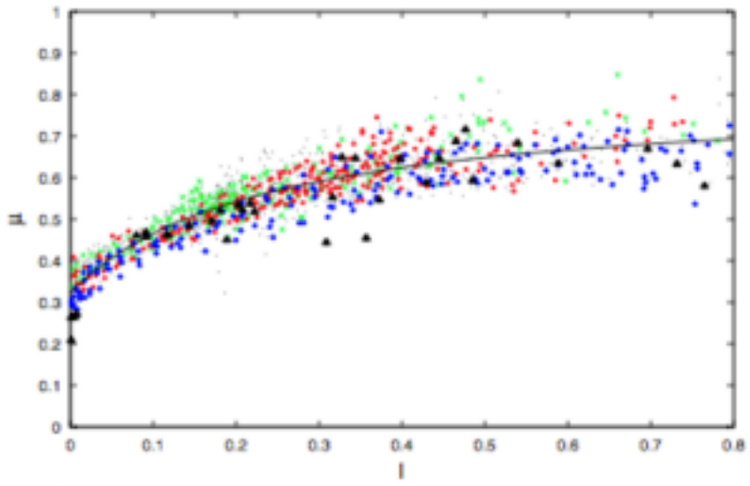

by grain dynamics

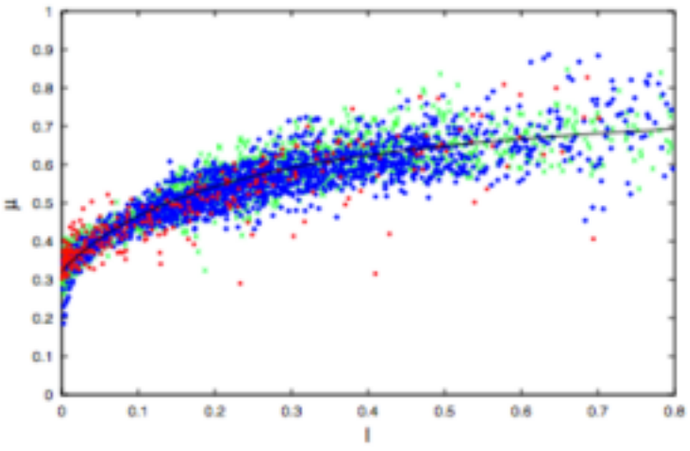

Lacaze Kerswell 09

Coulomb friction law

$$\tau = \mu(I) P$$

$$I = \frac{d\frac{\partial u}{\partial y}}{\sqrt{P/\rho}}$$

$$\mu(I) = \mu_1 + \frac{\mu_2 - \mu_1}{I_0/I + 1}$$

$$\mu_1 \simeq 0.32 \quad (\mu_2 - \mu_1) \simeq 0.23 \quad I_0 \simeq 0.3$$

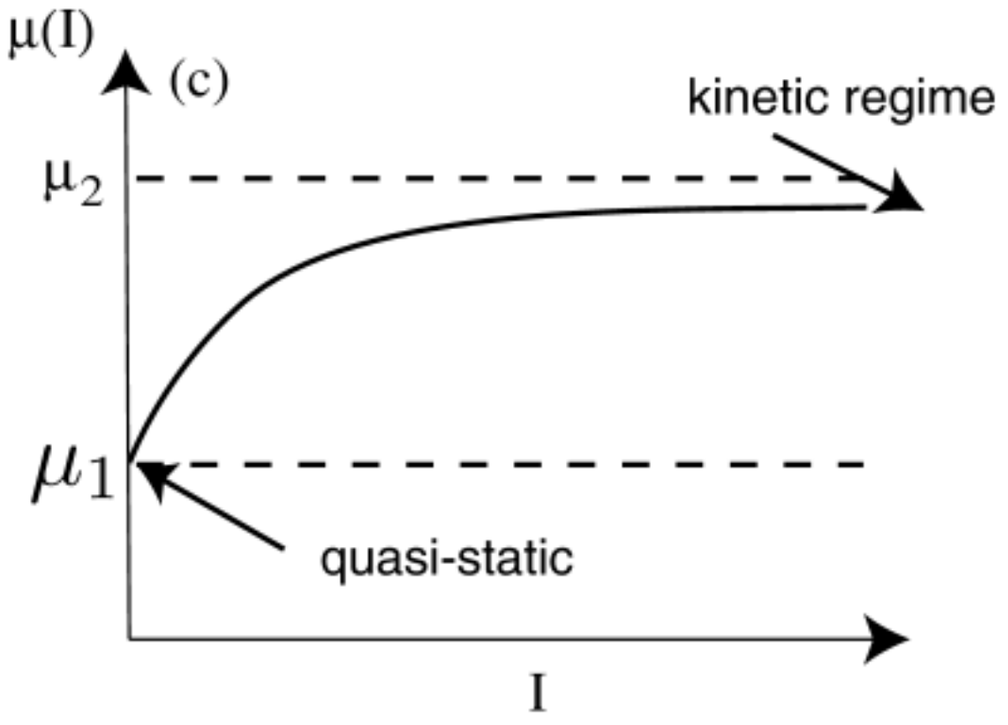

rheology; defining a viscosity

$$\mu(I) = \mu_1 + \frac{\mu_2 - \mu_1}{I_0/I + 1}$$

$$\eta \frac{\partial u}{\partial y} = \mu(I) P$$

local equilibrium

$$\eta = \frac{\mu(\frac{d\frac{\partial u}{\partial y}}{\sqrt{P/\rho}})P}{\frac{\partial u}{\partial y}}$$

construction of a viscosity

P. Jop, Y. Forterre, O. Pouliquen, (2006) "A rheology for dense granular flows", Nature 441, pp. 727-730

implementation in *Gerris* flow solver?

$$\mu(I) = \mu_1 + \frac{\mu_2 - \mu_1}{I_0/I + 1}$$

$$D_2 = \sqrt{D_{ij} D_{ij}} \qquad D_{ij} = \frac{u_{i,j} + u_{j,i}}{2}$$

construction of a viscosity based on the D_2 invariant and redefinition of I

$$\eta = \min(\eta_{max}, \max\left(\frac{\mu(I)}{\sqrt{2}D_2} p \ , \ 0\right)) \qquad I = d\sqrt{2}D_2/\sqrt{(|p|/\rho)}.$$

- the «min» limits viscosity to a large value
- always flow, even slow

$$\nabla \cdot \mathbf{u} = 0, \quad \rho\left(\frac{\partial \mathbf{u}}{\partial t} + \mathbf{u} \cdot \nabla \mathbf{u}\right) = -\nabla p + \nabla \cdot (2\eta \mathbf{D}) + \rho g,$$

$$\frac{\partial c}{\partial t} + \nabla \cdot (c\mathbf{u}) = 0, \quad \rho = c\rho_1 + (1-c)\rho_2, \quad \eta = c\eta_1 + (1-c)\eta_2$$

The granular fluid is covered by a passive light fluid (it allows for a zero pressure boundary condition at the surface, bypassing an up to now difficulty which was to impose this condition on a unknown moving boundary).

Boundary Conditions: no slip and *P=0* at the top

Projection Method

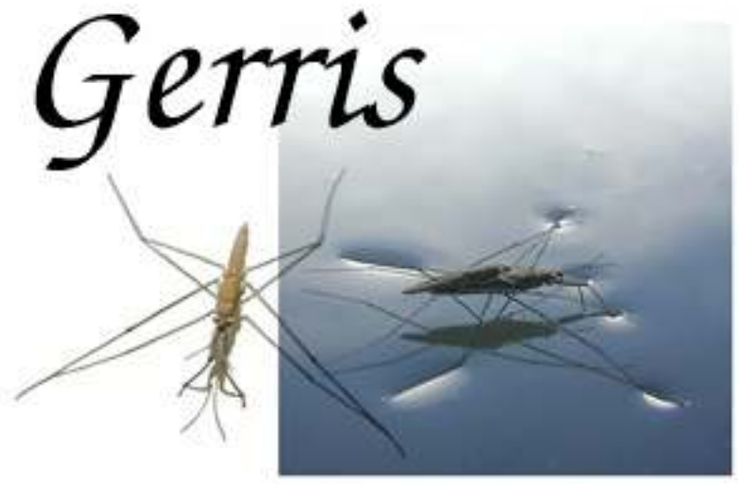

$$\rho_{n+\frac{1}{2}}\left(\frac{\mathbf{u}_*-\mathbf{u}_n}{\Delta t}+\mathbf{u}_{n+\frac{1}{2}}\cdot\boldsymbol{\nabla}\mathbf{u}_{n+\frac{1}{2}}\right)=\boldsymbol{\nabla}\cdot(\eta_{n+\frac{1}{2}}\mathbf{D}_*)-\boldsymbol{\nabla}p_{n-\frac{1}{2}},$$

$$\mathbf{u}_{n+1}=\mathbf{u}_*-\frac{\Delta t}{\rho_{n+\frac{1}{2}}}(\boldsymbol{\nabla}p_{n+\frac{1}{2}}-\boldsymbol{\nabla}p_{n-\frac{1}{2}}),$$

$$\boldsymbol{\nabla}\cdot\mathbf{u}_{n+1}=0.$$

multigrid solver for Laplacien of pressure

$$\boldsymbol{\nabla}\cdot\left(\frac{\Delta t}{\rho_{n+\frac{1}{2}}}\boldsymbol{\nabla}p_{n+\frac{1}{2}}\right)=\boldsymbol{\nabla}\cdot\left(\mathbf{u}_*+\frac{\Delta t}{\rho_{n+\frac{1}{2}}}\boldsymbol{\nabla}p_{n-\frac{1}{2}}\right)$$

implicit for u*

$$\frac{\rho_{n+\frac{1}{2}}}{\Delta t}\mathbf{u}_\star-\frac{1}{2}\nabla\cdot(\eta_{n+\frac{1}{2}}\nabla\mathbf{u}_\star)\quad=\quad\rho_{n+\frac{1}{2}}\left[\frac{\mathbf{u}_n}{\Delta t}-\mathbf{u}_{n+\frac{1}{2}}\cdot\nabla\mathbf{u}_{n+\frac{1}{2}}\right]-\nabla p_{n-\frac{1}{2}}+\frac{1}{2}\nabla\mathbf{u}_n^T\nabla\eta_{n+\frac{1}{2}}.$$

VOF reconstruction

$$\frac{c_{n+\frac{1}{2}}-c_{n-\frac{1}{2}}}{\Delta t}+\nabla\cdot(c_n\mathbf{u}_n)=0$$

precise equilibrium between pressure gradient and viscous terms, in particular for large time steps.

Gerris scripting

```
AdvectionParams { gc = 1 }

# mu(I) granular rheology
  SourceViscosity {} {
   double In = sqrt(2.)*D*D2/sqrt(fabs(P));
   double mul = .38 + (.26)*In/(.3 + In);
   return MAX((mul*P)/(sqrt(2.)*D2), 0.);
  } { beta = 1 }
```

$$I = \frac{d\sqrt{2}D_2}{\sqrt{(|p|/\rho)}} \qquad \mu(I) = \mu_1 + \frac{\mu_2 - \mu_1}{I_0/I + 1} \qquad \eta = \max\left(\frac{\mu(I)}{\sqrt{2}D_2}p\ ,\ 0\right)$$

Test of the code: «Bagnold» avalanche

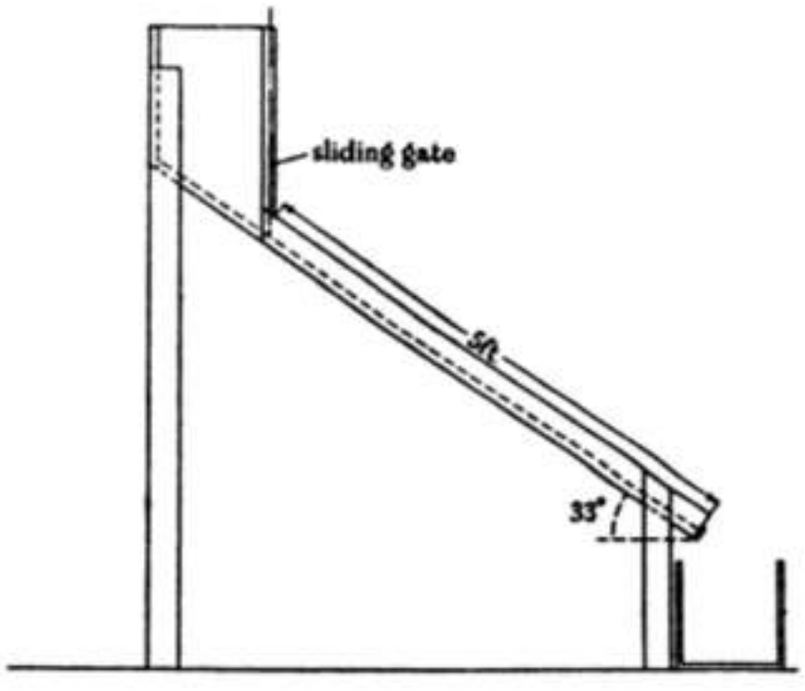

kind of Nuβelt solution

$$T \propto \sigma(\lambda D)^2 \, (dU/dy)^2$$

$$U = \frac{2}{3} \times 0.165 \, (g \sin \beta)^{1/2} \, \frac{y'^{3/2}}{D} \, ,$$

Bagnold 1954

TABLE 1.

flow height Y (cm)	measured speed (cm/sec)	speed, from (9) (cm/sec)	ratio
0.5	17.2	26.4	1.53
0.65	27.5	38.8	1.41
0.75	30.0	48.0	1.6
0.9	39.0	63.0	1.61

Test of the code: «Bagnold» avalanche

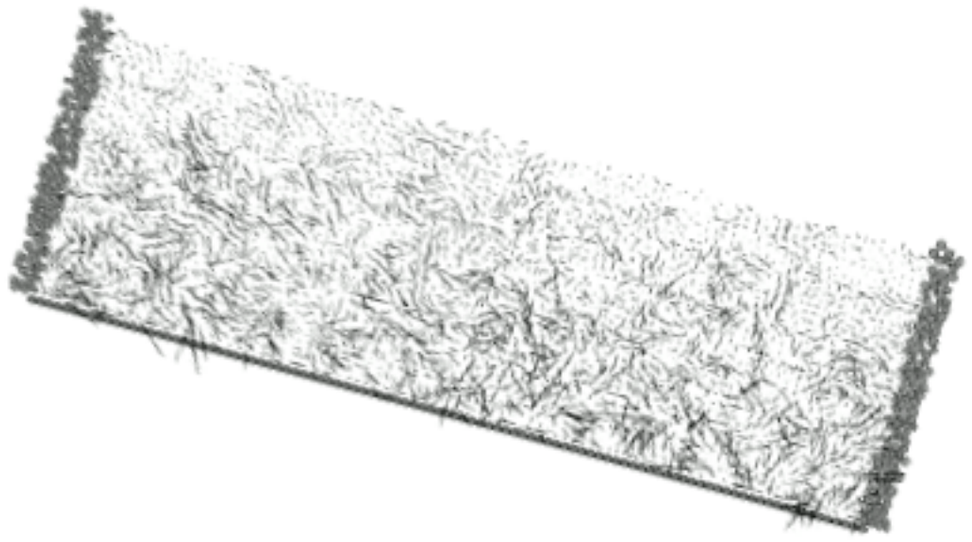

kind of Nuβelt solution

Contact Dynamic simulation Lydie Staron

Test of the code: «Bagnold» avalanche

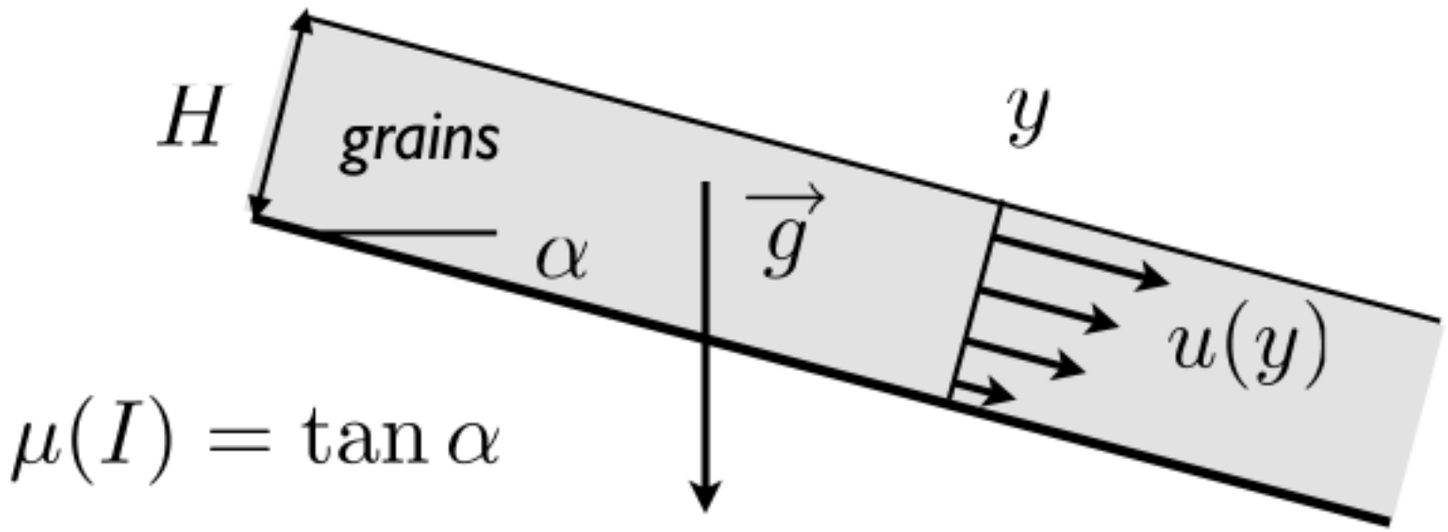

$$u = \frac{2}{3} I_\alpha \sqrt{gd\cos\alpha \frac{H^3}{d^3}} \left(1 - \left(1 - \frac{y}{H}\right)^{3/2}\right),$$

$$v = 0, \quad p = \rho g H \left(1 - \frac{y}{H}\right) \cos\alpha.$$

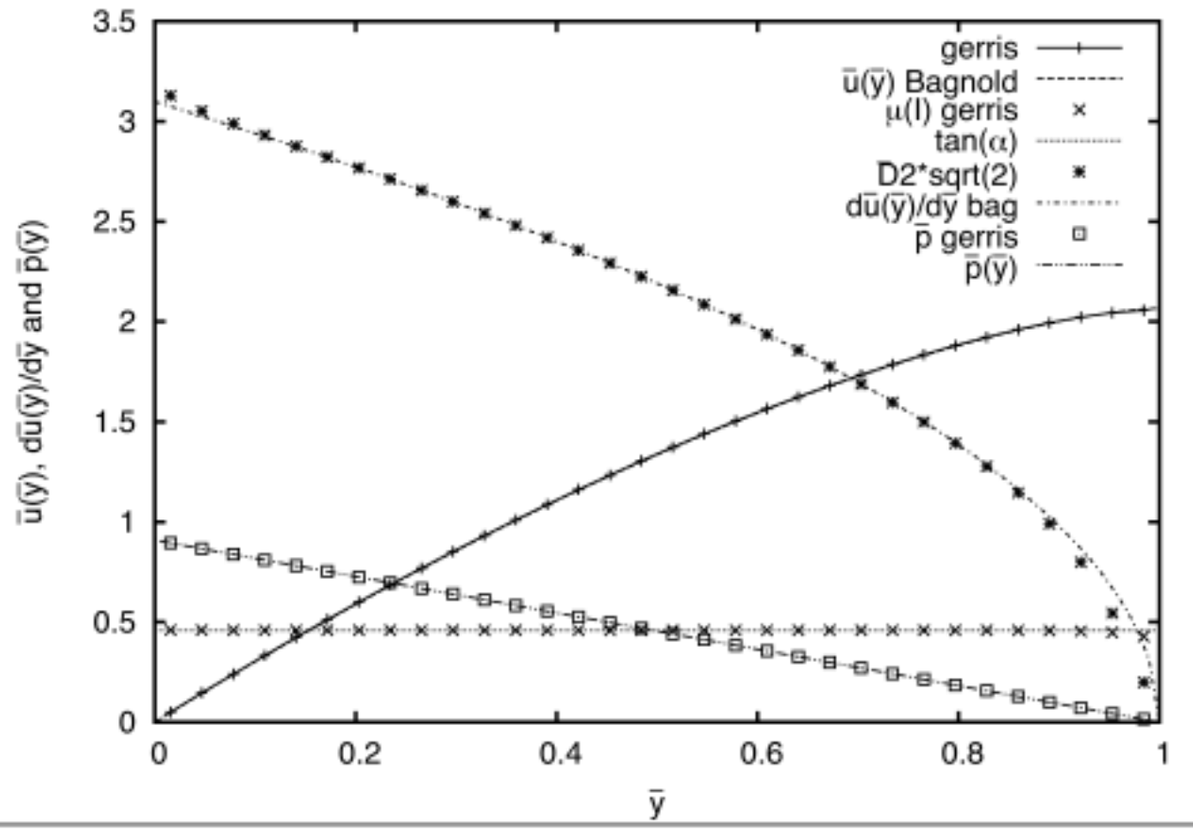

Test of the code: «Bagnold» avalanche

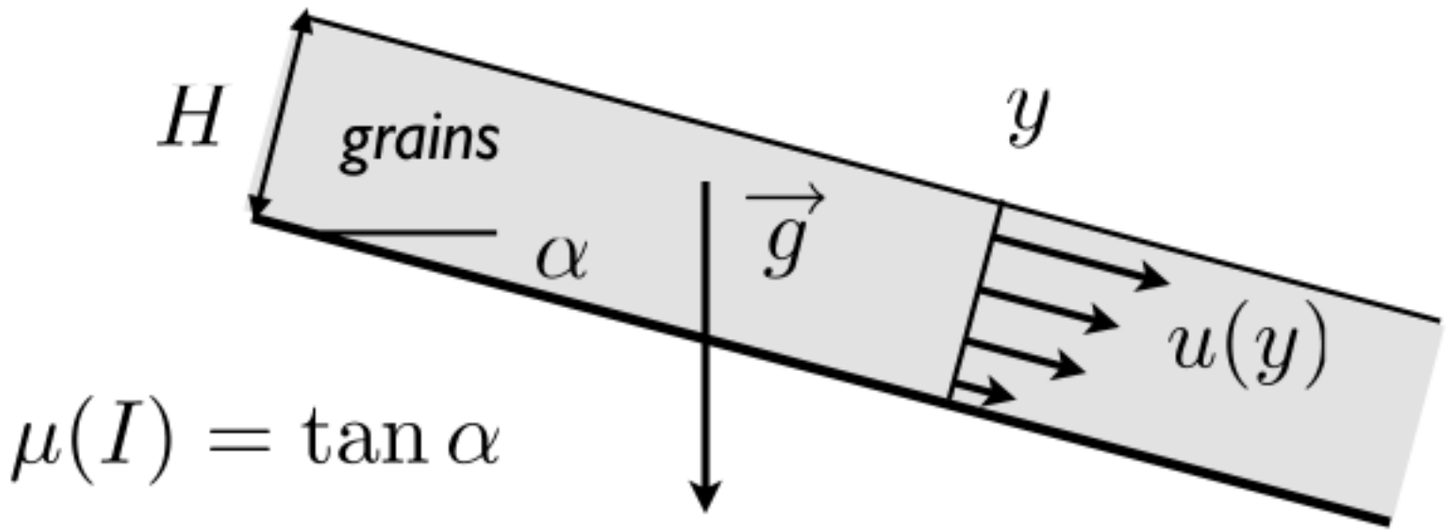

$$\mu(I) = \tan\alpha$$

$$u = \frac{2}{3} I_\alpha \sqrt{gd\cos\alpha \frac{H^3}{d^3}} \left(1 - \left(1 - \frac{y}{H}\right)^{3/2}\right),$$

$$v = 0, \quad p = \rho g H \left(1 - \frac{y}{H}\right) \cos\alpha.$$

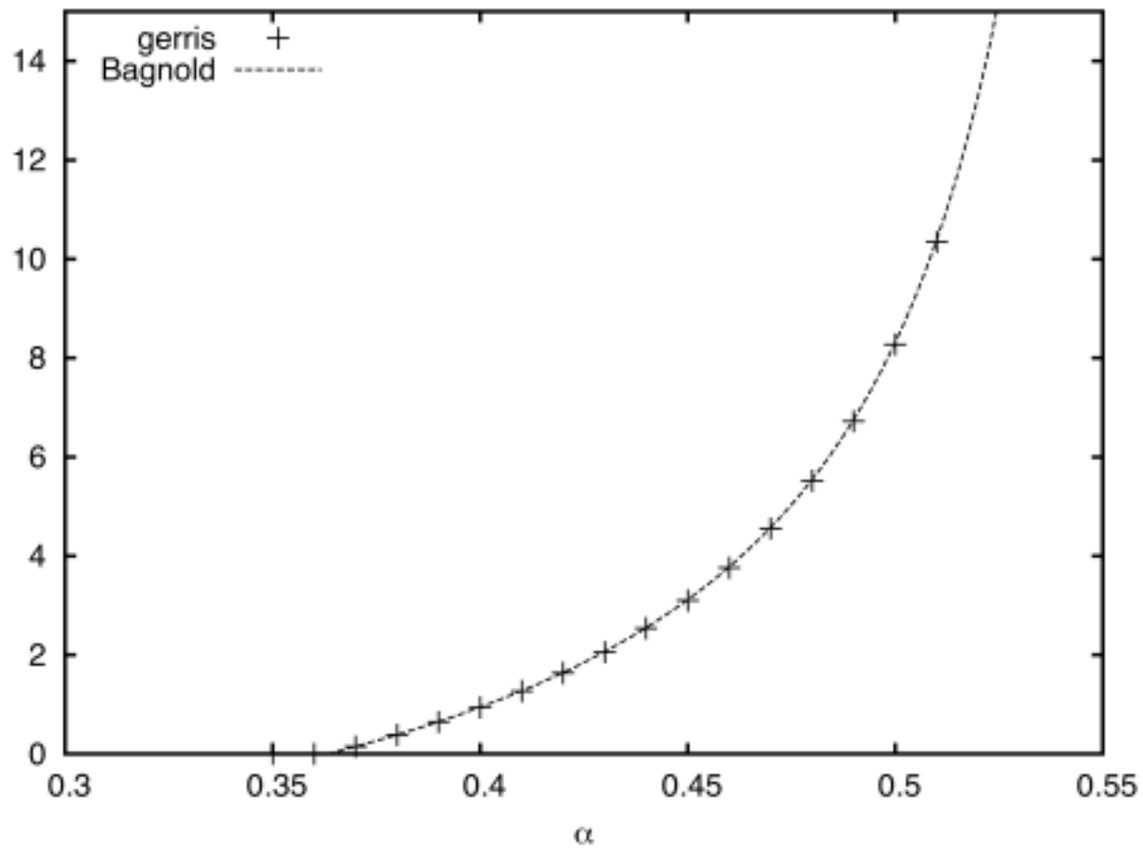

Test of the code: «Bagnold» avalanche

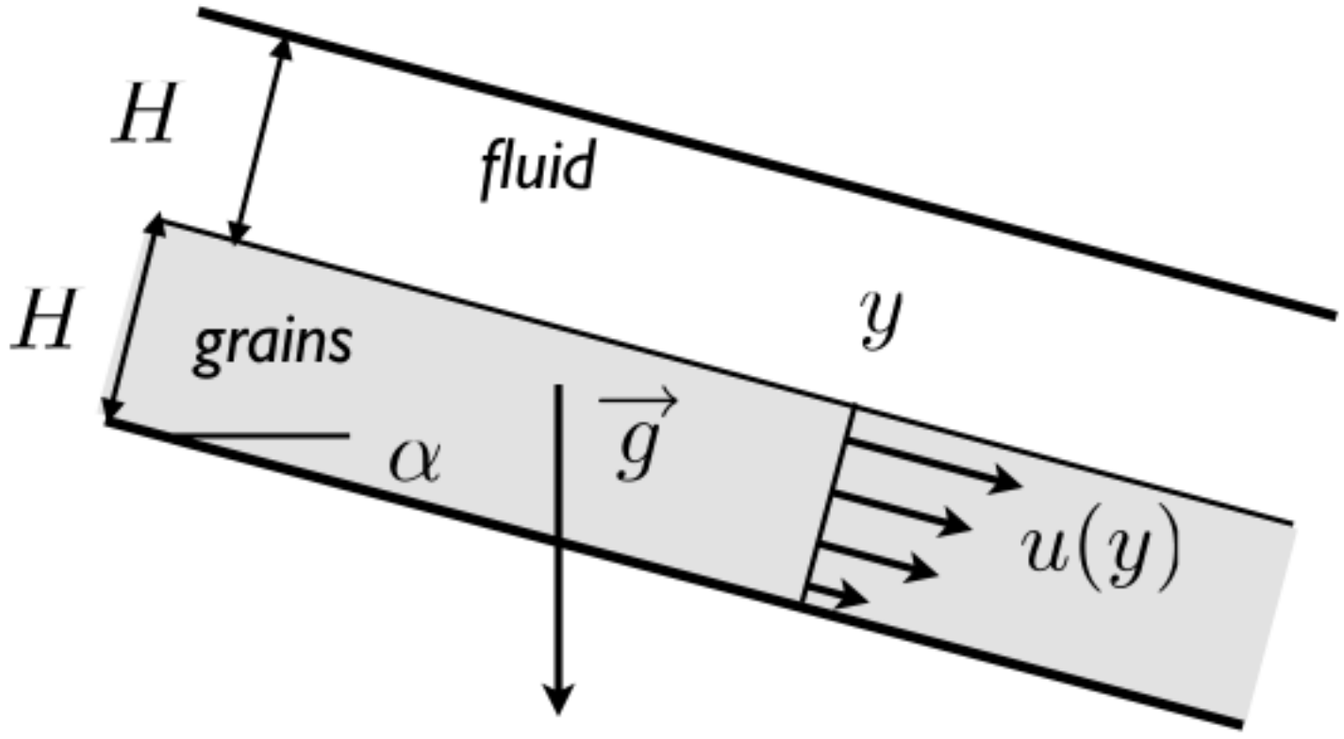

$$u(y) = \frac{(2H - y)\left(\rho_f g y \sin\alpha - 2\tau_0\right)}{2\mu_f}$$

$$d\frac{\partial u}{\partial y} = \max\left[\sqrt{p_0/\rho + gH\left(1 - \frac{y}{H}\right)\cos\alpha} \times \mu^{-1}\left(\frac{\tau_0 + \rho g H\left(1 - \frac{y}{H}\right)\sin\alpha}{p_0 + \rho g H\left(1 - \frac{y}{H}\right)\cos\alpha}\right), 0\right].$$

$$u(H^-) - u(H^+) = 0$$

Test of the code: «Bagnold» avalanche

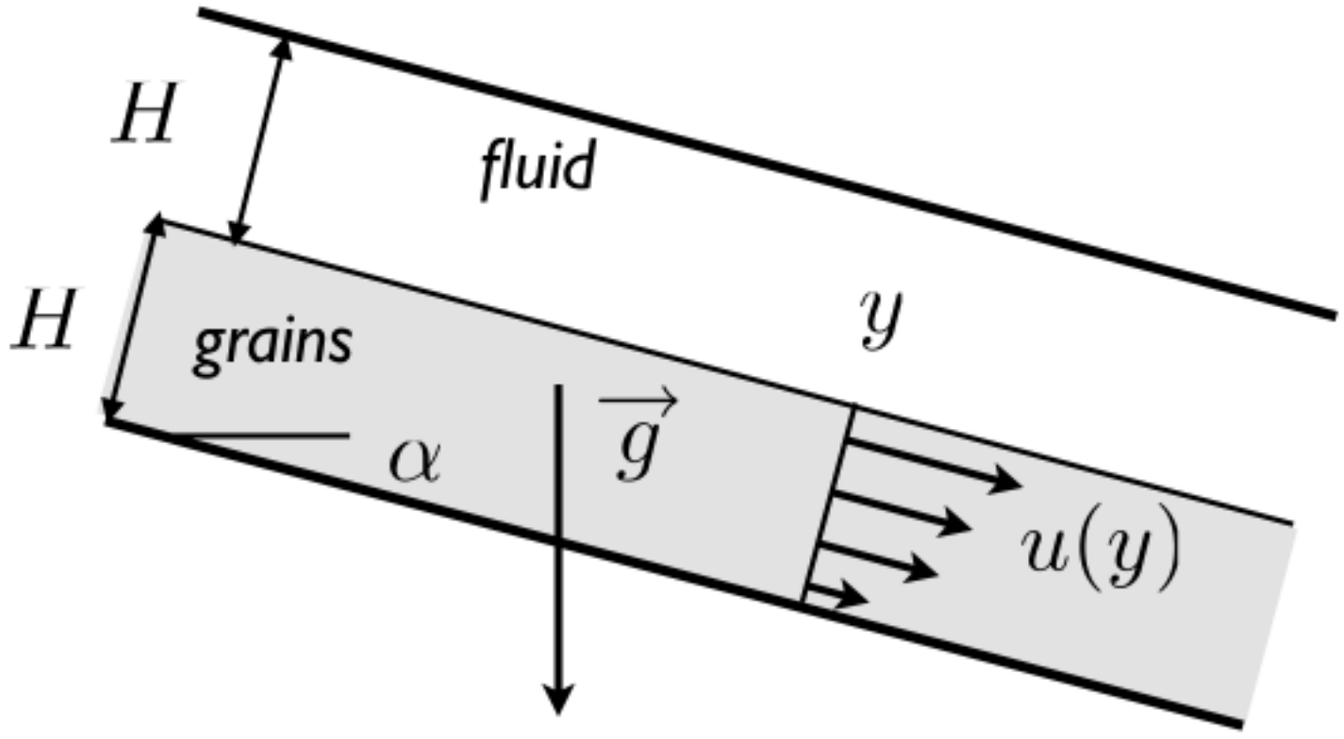

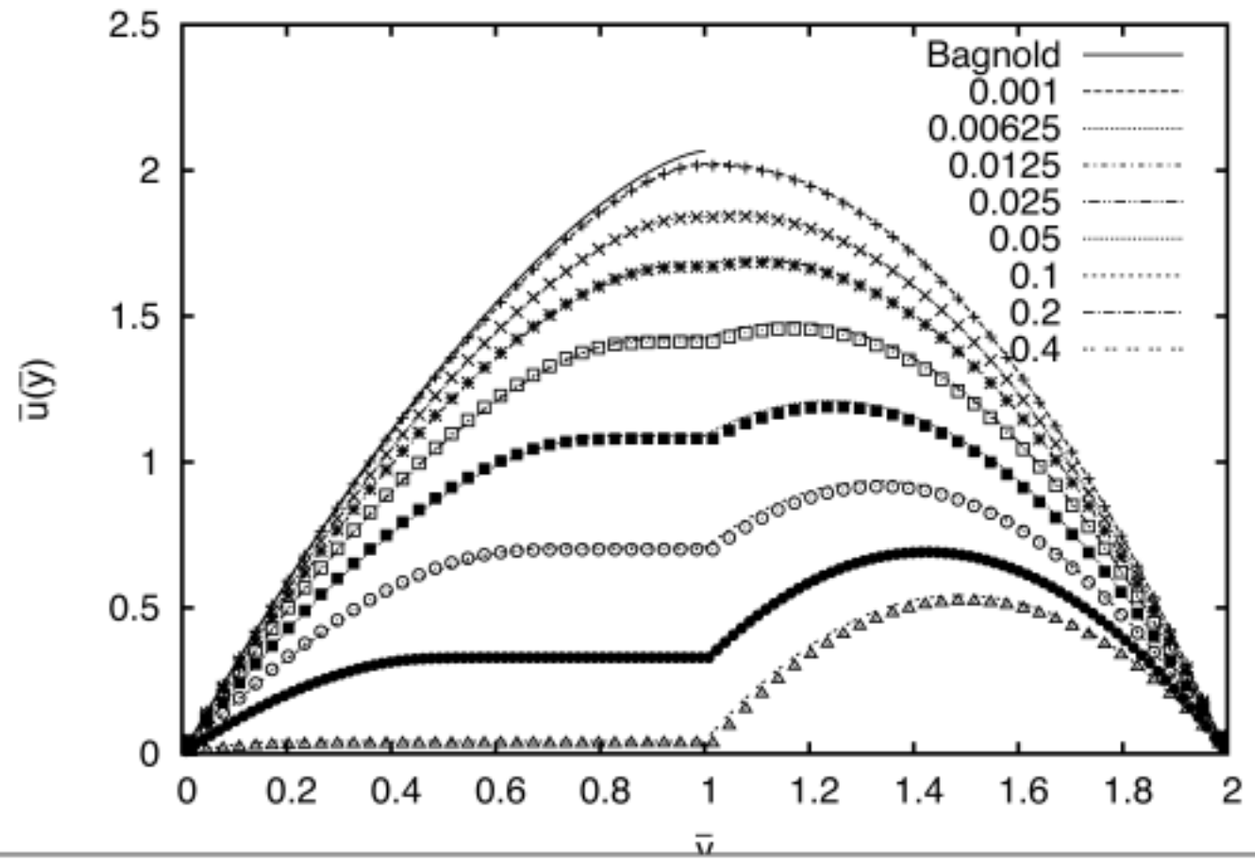

Collapse of columns

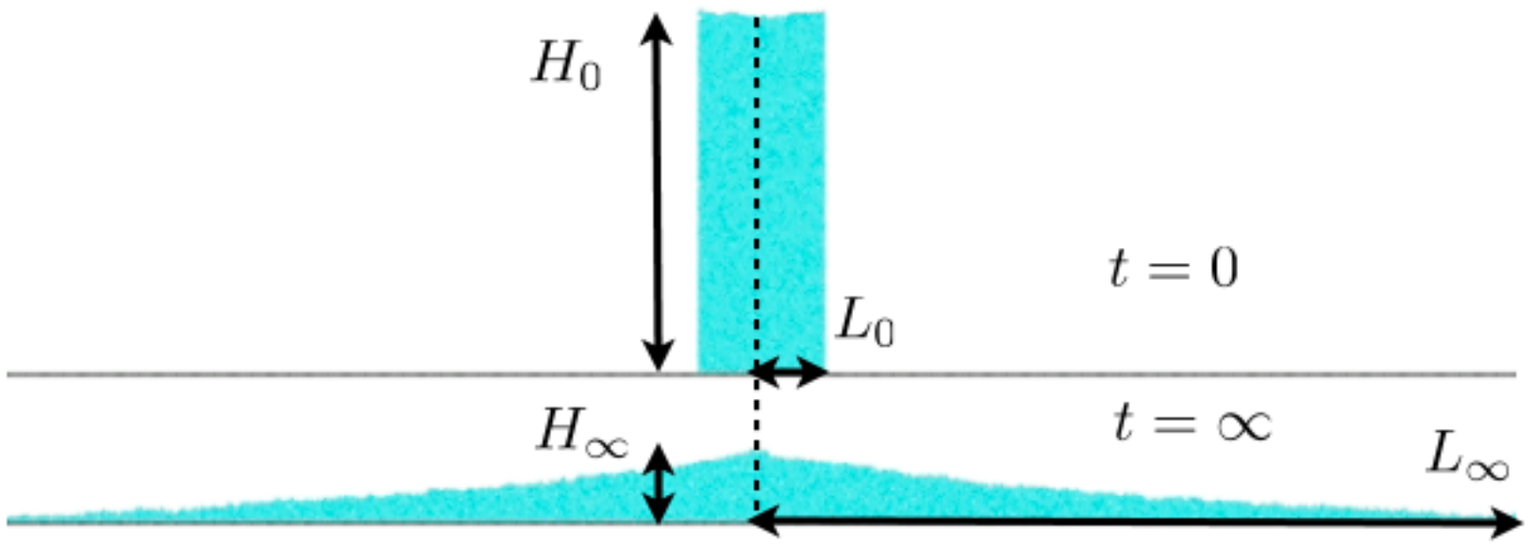

Collapse of columns

a=0.37

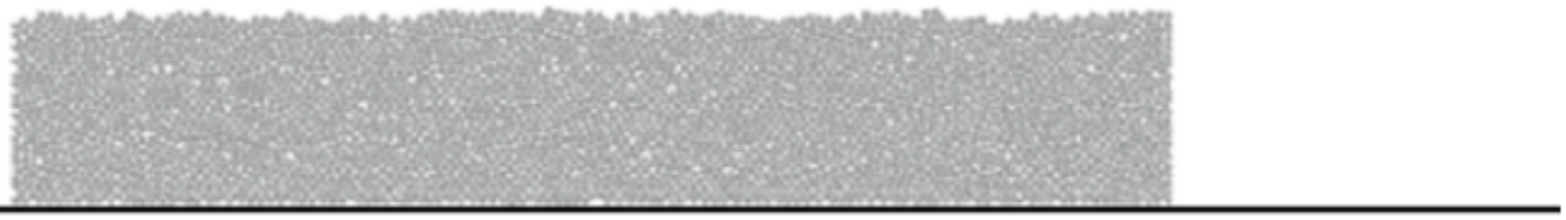

Contact Dynamic simulation Lydie Staron

Collapse of columns

a=0.90

Contact Dynamic simulation Lydie Staron

Collapse of columns simulation *Gerris μ(I)*

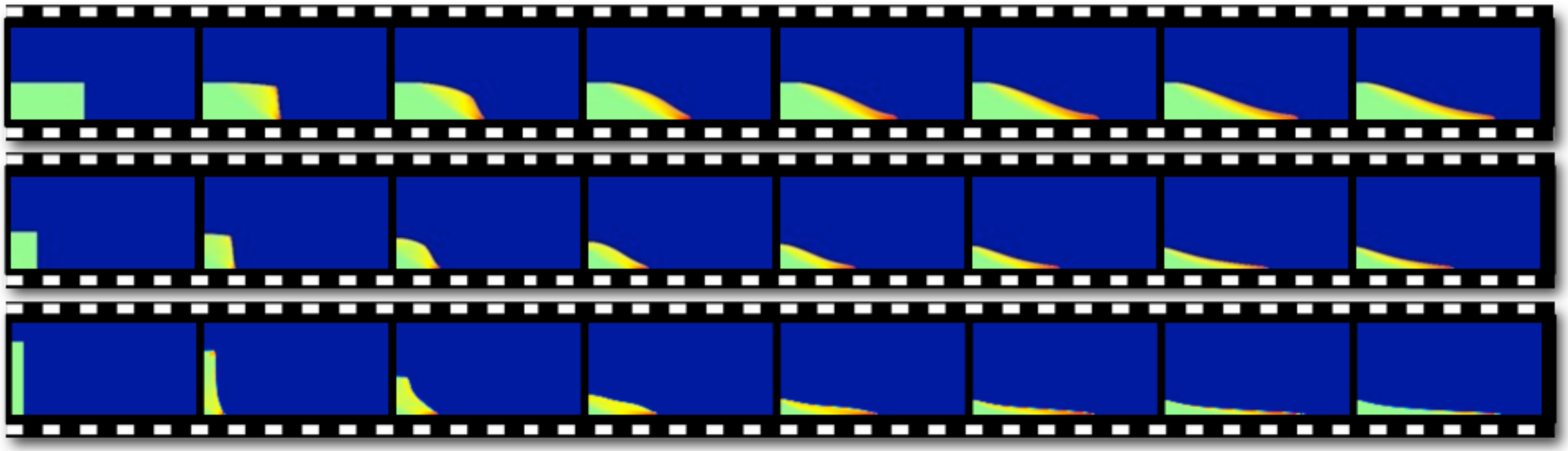

Snapshots of collapse of three columns of aspect ration 0.5 1.42 and 6.26 (top to bottom)

Collapse of columns simulation *Gerris μ(I)*

Collapse of columns of aspect ratio 0.5 comparison of Discrete Simulation Contact Method and Navier Stokes gerris, shape at time 0, 1, 2, 3, 4 and position of the front of the avalanche as function of time (time measured with $\sqrt{H_0/g}$ and space with aH_0)

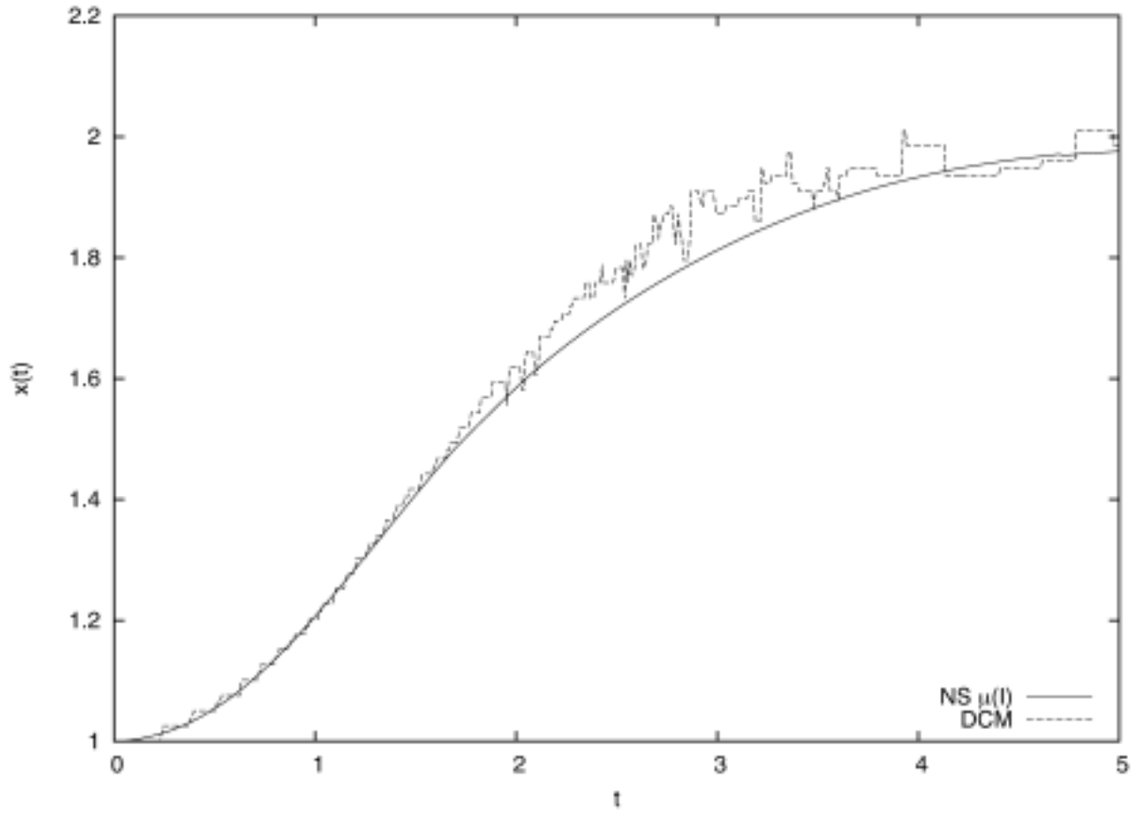

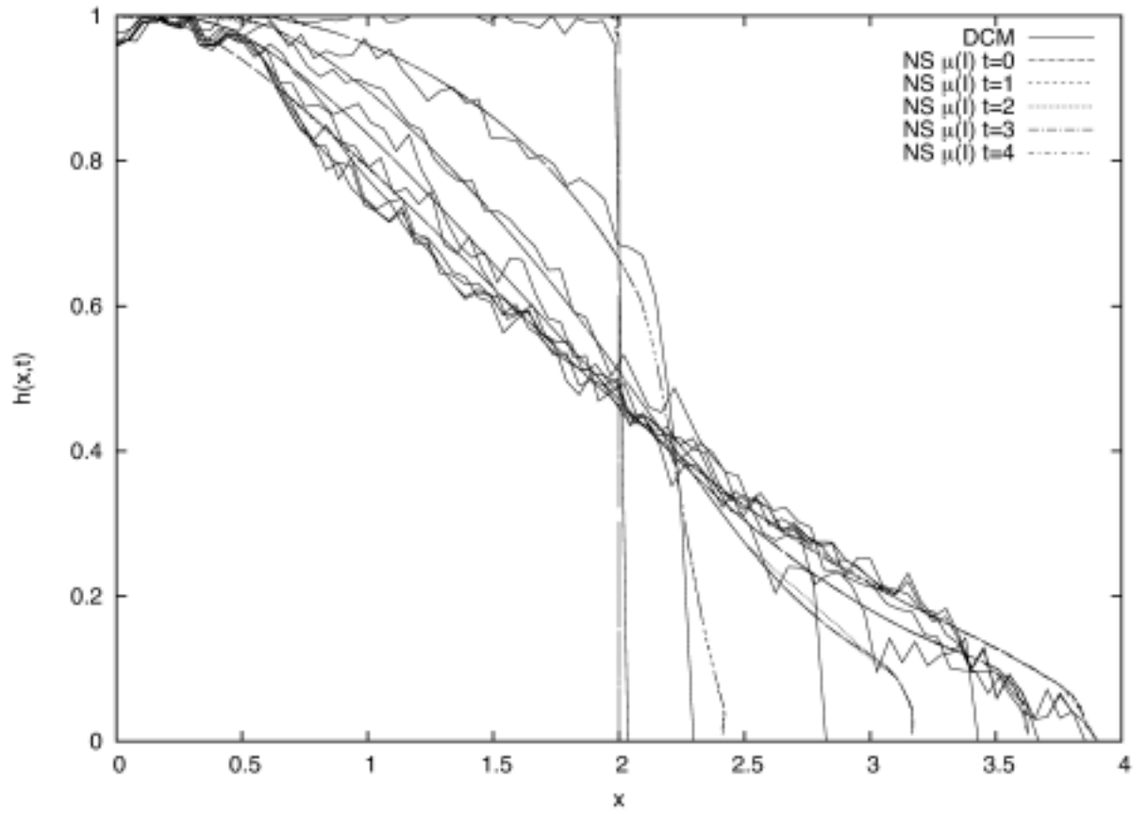

Collapse of columns simulation *Gerris μ(I)*

Collapse of columns of aspect ratio 1.42 comparison of Discrete Simulation Contact Method and Navier Stokes gerris, shape at time 0, 1, 2, 3, 4 and position of the front of the avalanche as function of time (time measured with $\sqrt{H_0/g}$ and space with aH_0)

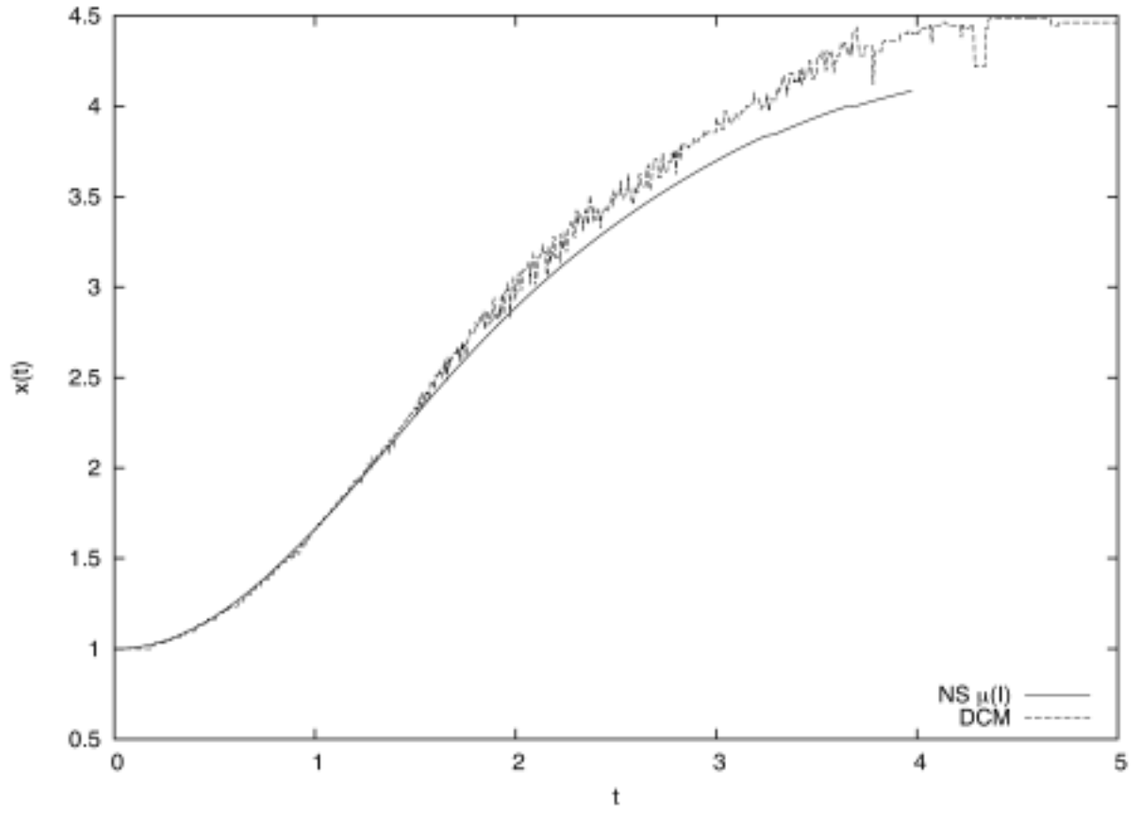

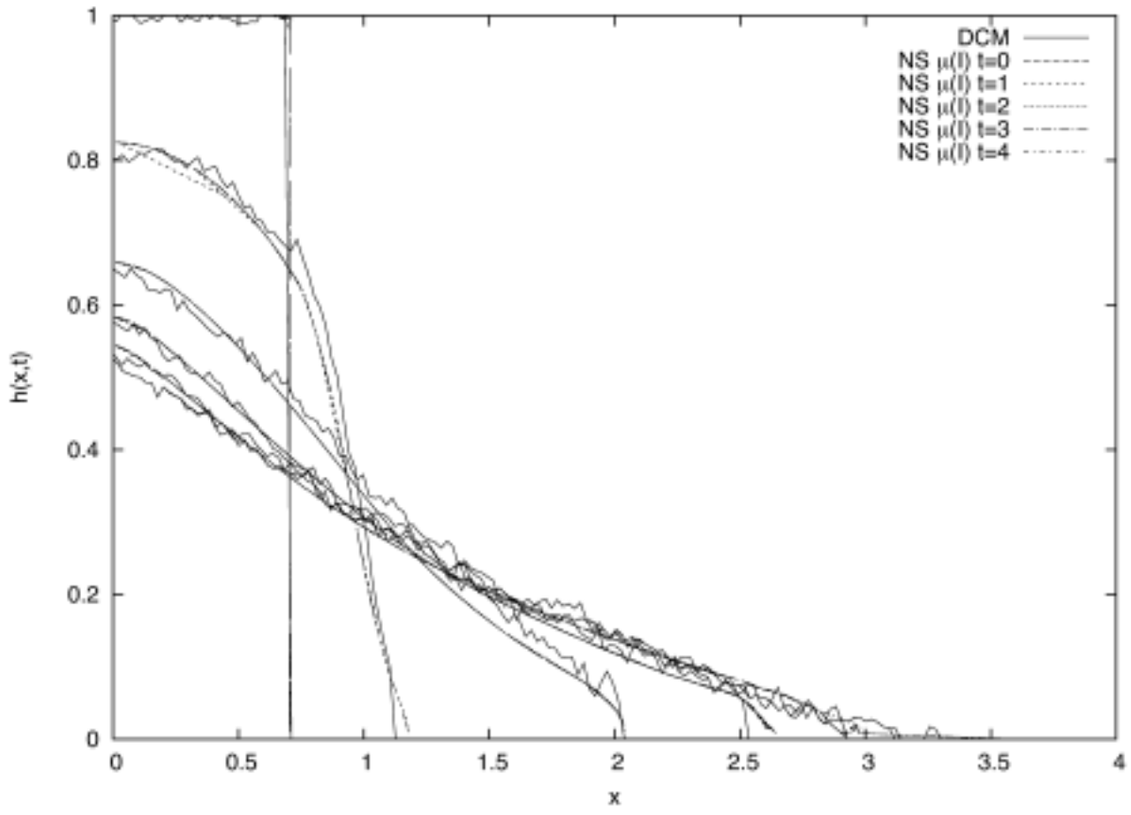

Collapse of columns simulation *Gerris μ(I)*

Collapse of columns of aspect ratio 6.26 comparison of Discrete Simulation Contact Method and Navier Stokes gerris, shape at time 0, 1, 2, 3, 4 and position of the front of the avalanche as function of time (time measured with $\sqrt{H_0/g}$ and space with aH_0)

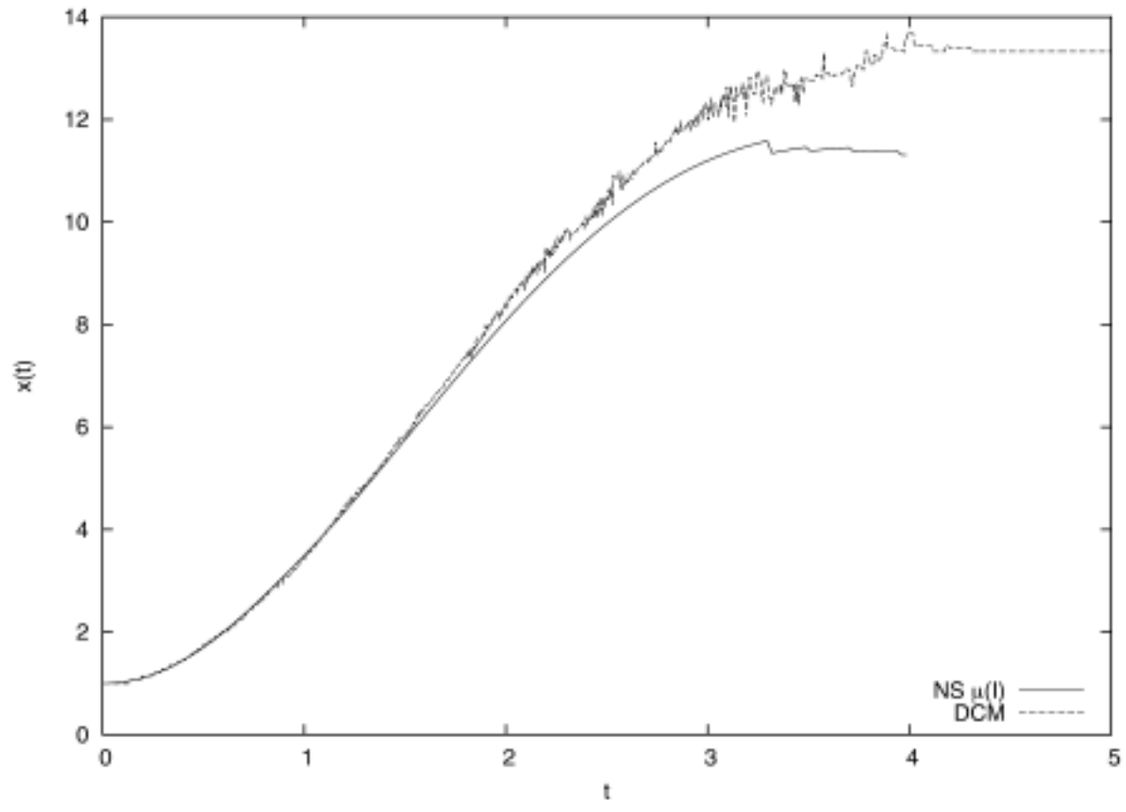

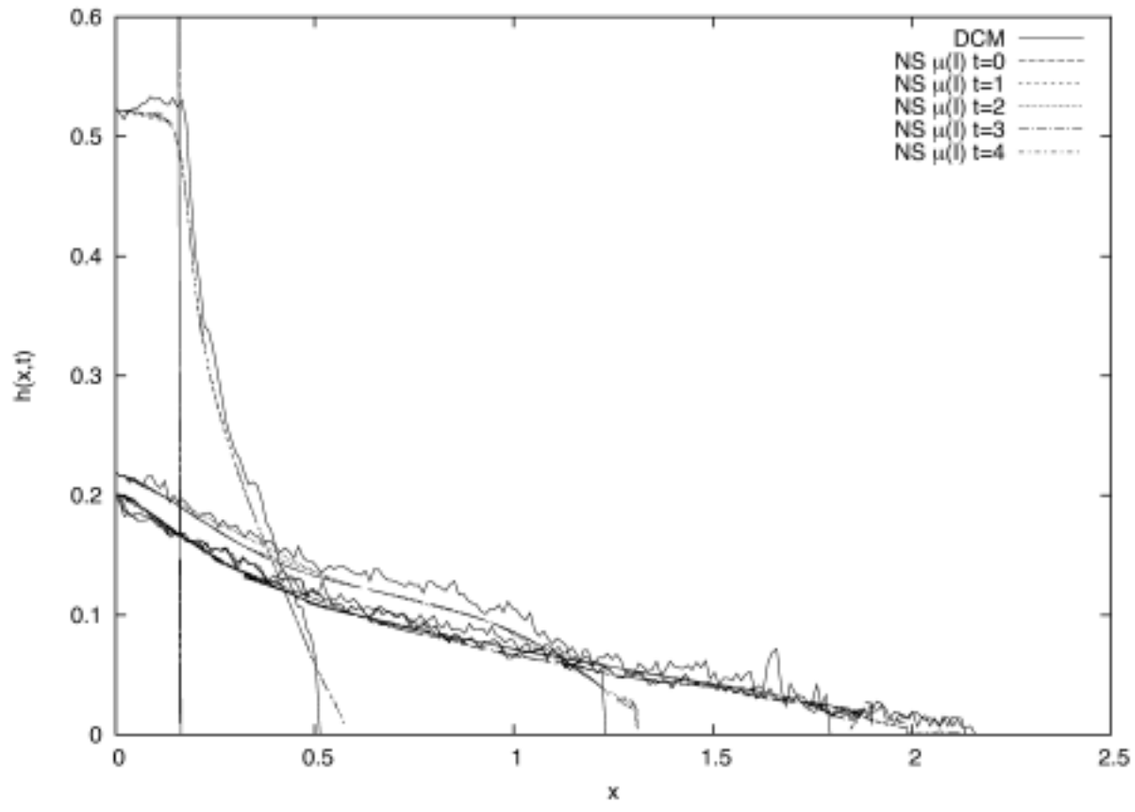

Collapse of columns simulation *Gerris μ(I)*

optimisation

$$\mu(I) = \mu_s + \frac{\Delta\mu}{\frac{I_0}{I} + 1}$$

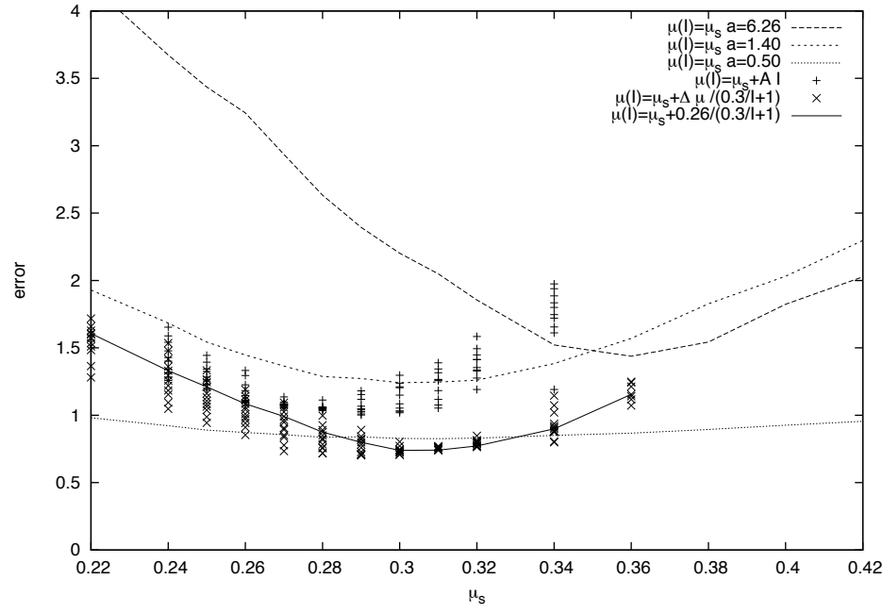

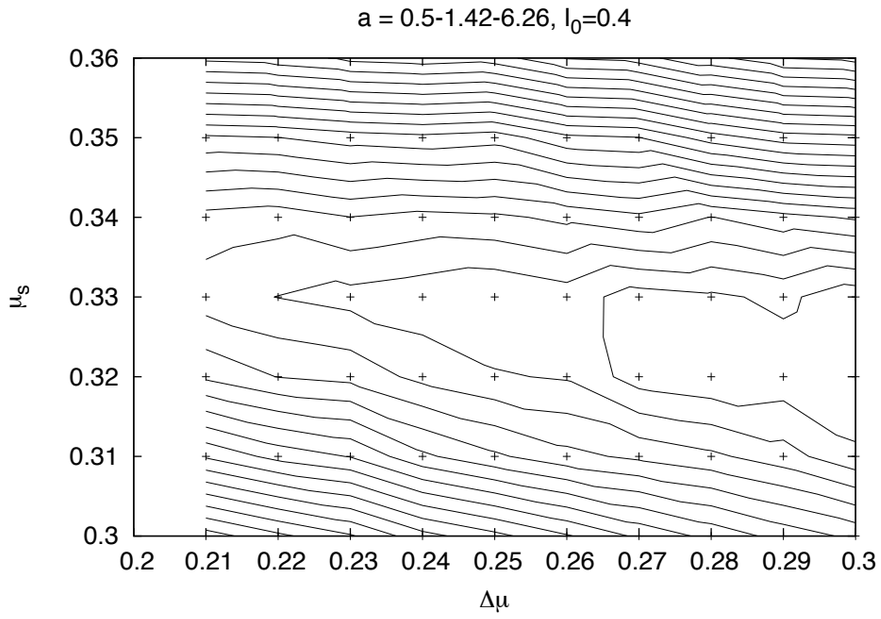

final values

$$\mu_s = 0.32\ \Delta\mu = 0.28\ I_0 = 0.4$$

Collapse of columns simulation *Gerris μ(I)*

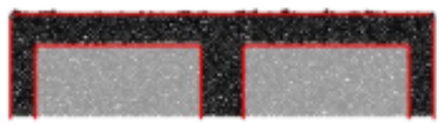

$a = 0.5$ DCM vs *Gerris μ(I)*

Collapse of columns simulation *Gerris μ(I)*

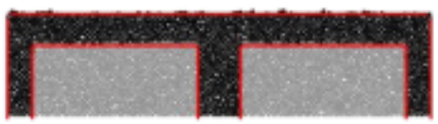

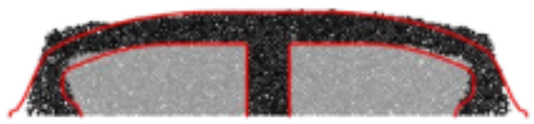

$a = 0.5$ DCM vs *Gerris μ(I)*

Collapse of columns simulation *Gerris μ(I)*

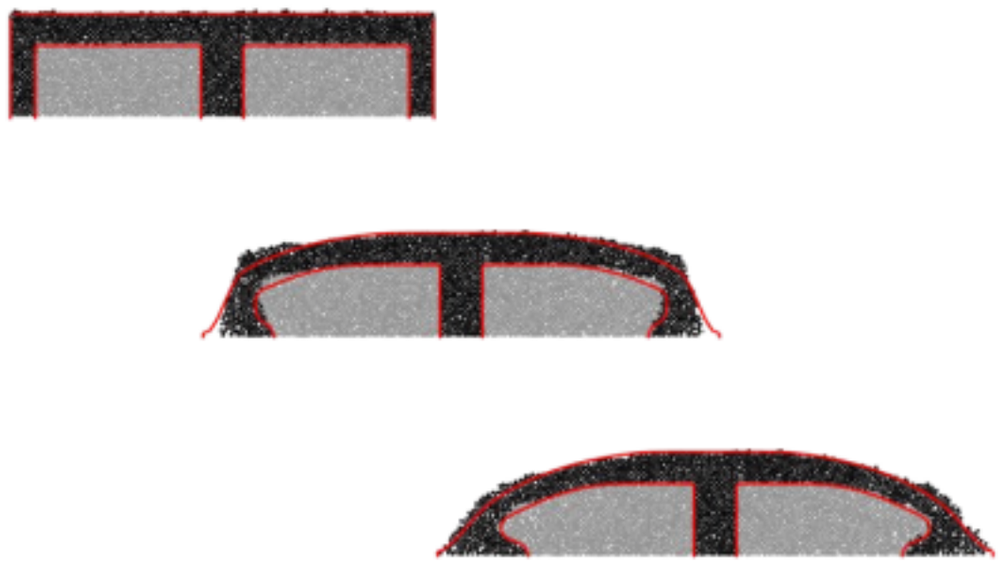

$a = 0.5$ DCM vs *Gerris μ(I)*

Collapse of columns simulation *Gerris* $\mu(I)$

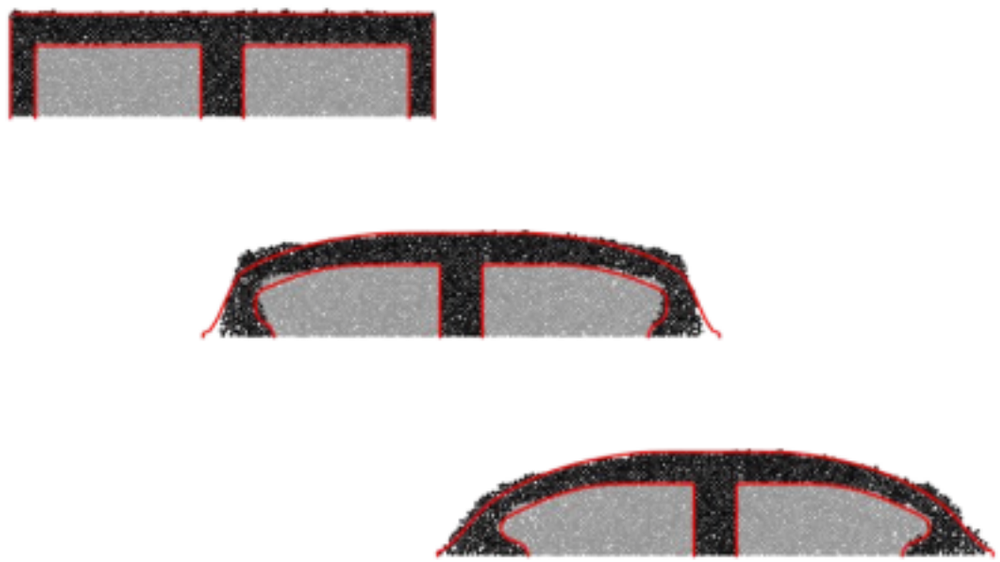

$a = 0.5$ DCM vs *Gerris* $\mu(I)$

Collapse of columns simulation *Gerris μ(I)*

$a = 0.5$ DCM vs *Gerris μ(I)*

Collapse of columns simulation *Gerris μ(I)*

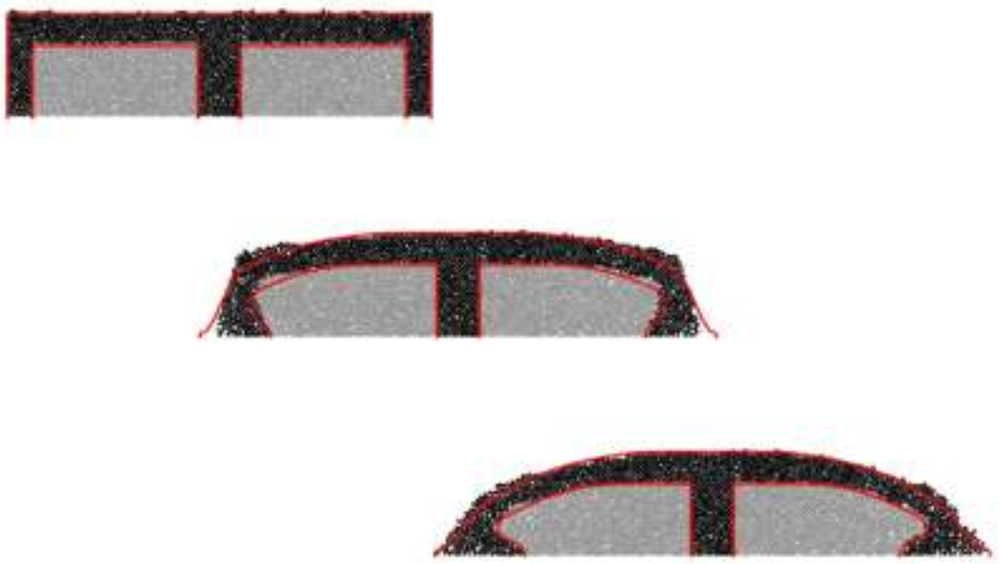

$a = 0.5$ DCM vs *Gerris μ(I)*

Collapse of columns simulation *Gerris μ(I)*

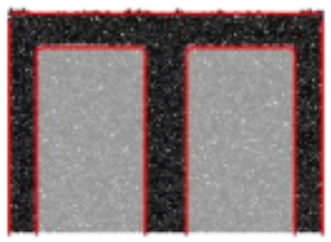

$a = 1.42$ DCM vs *Gerris μ(I)*

Collapse of columns simulation *Gerris μ(I)*

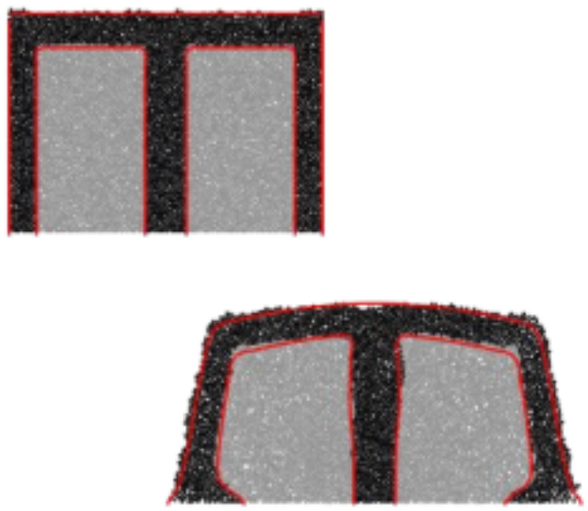

$a = 1.42$ DCM vs *Gerris μ(I)*

Collapse of columns simulation *Gerris μ(I)*

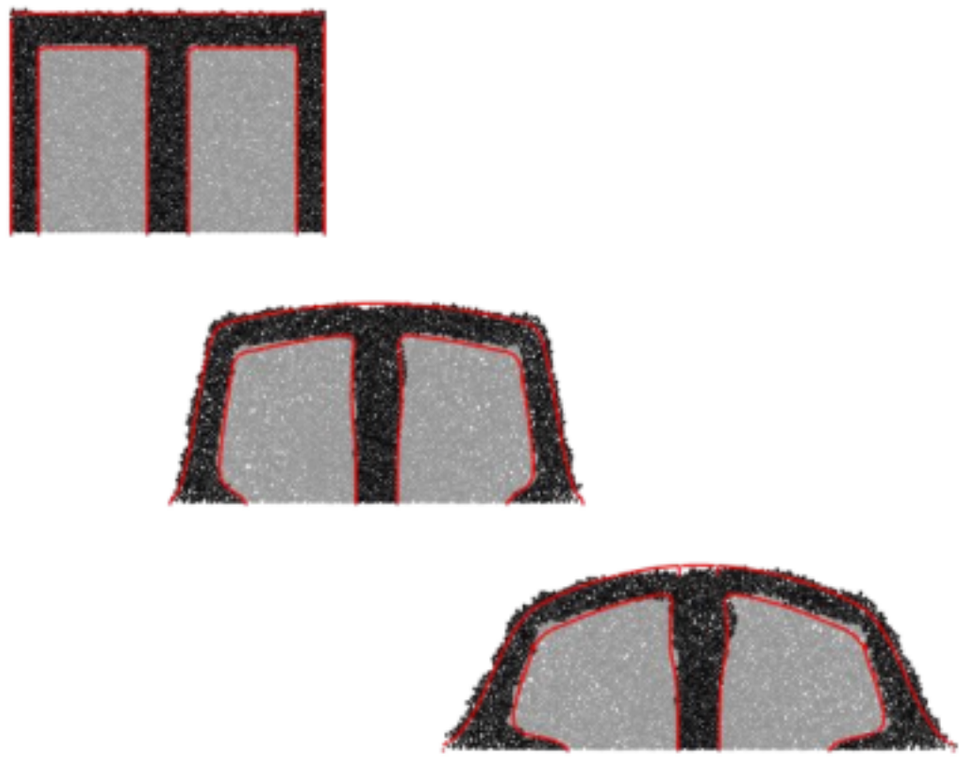

$a = 1.42$ DCM vs *Gerris μ(I)*

Collapse of columns simulation *Gerris μ(I)*

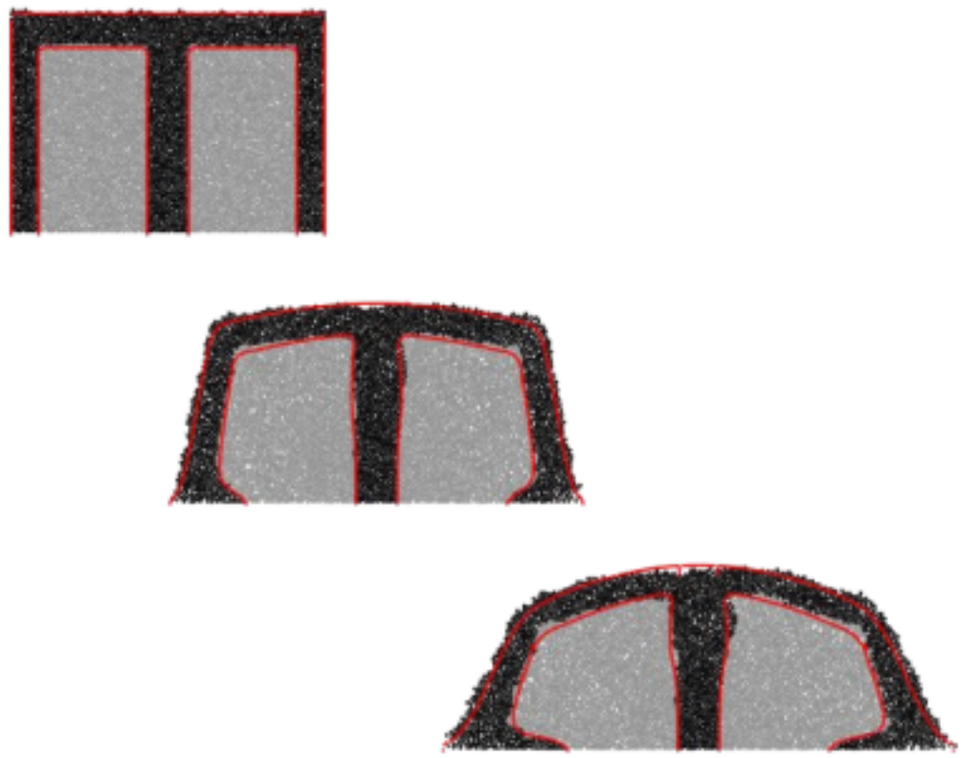

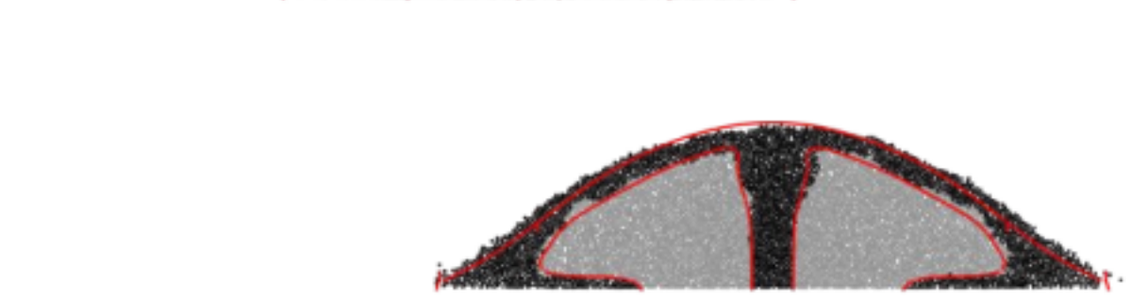

$a = 1.42$ DCM vs *Gerris μ(I)*

Collapse of columns simulation *Gerris μ(I)*

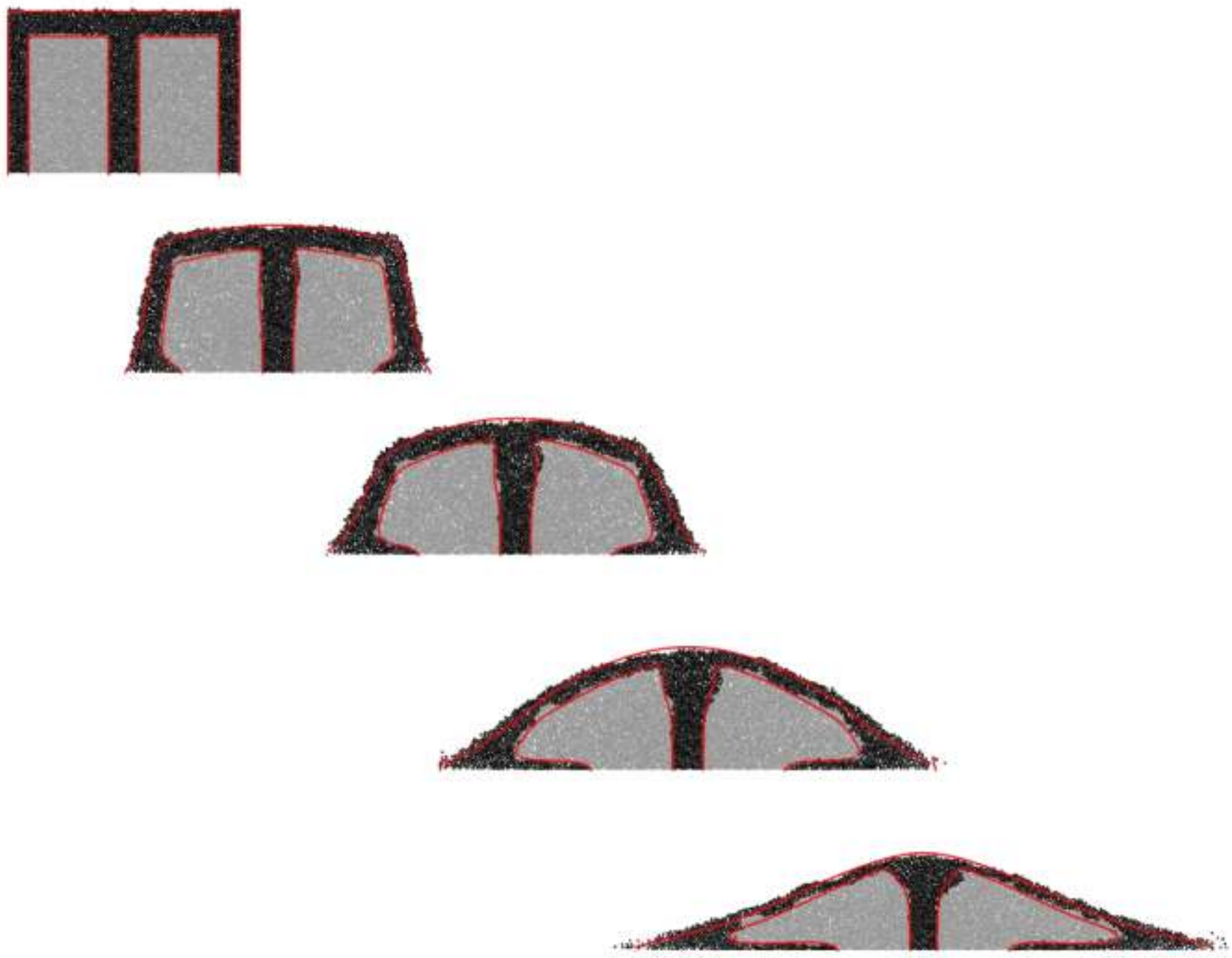

$a = 1.42$ DCM vs *Gerris μ(I)*

Collapse of columns simulation *Gerris μ(I)*

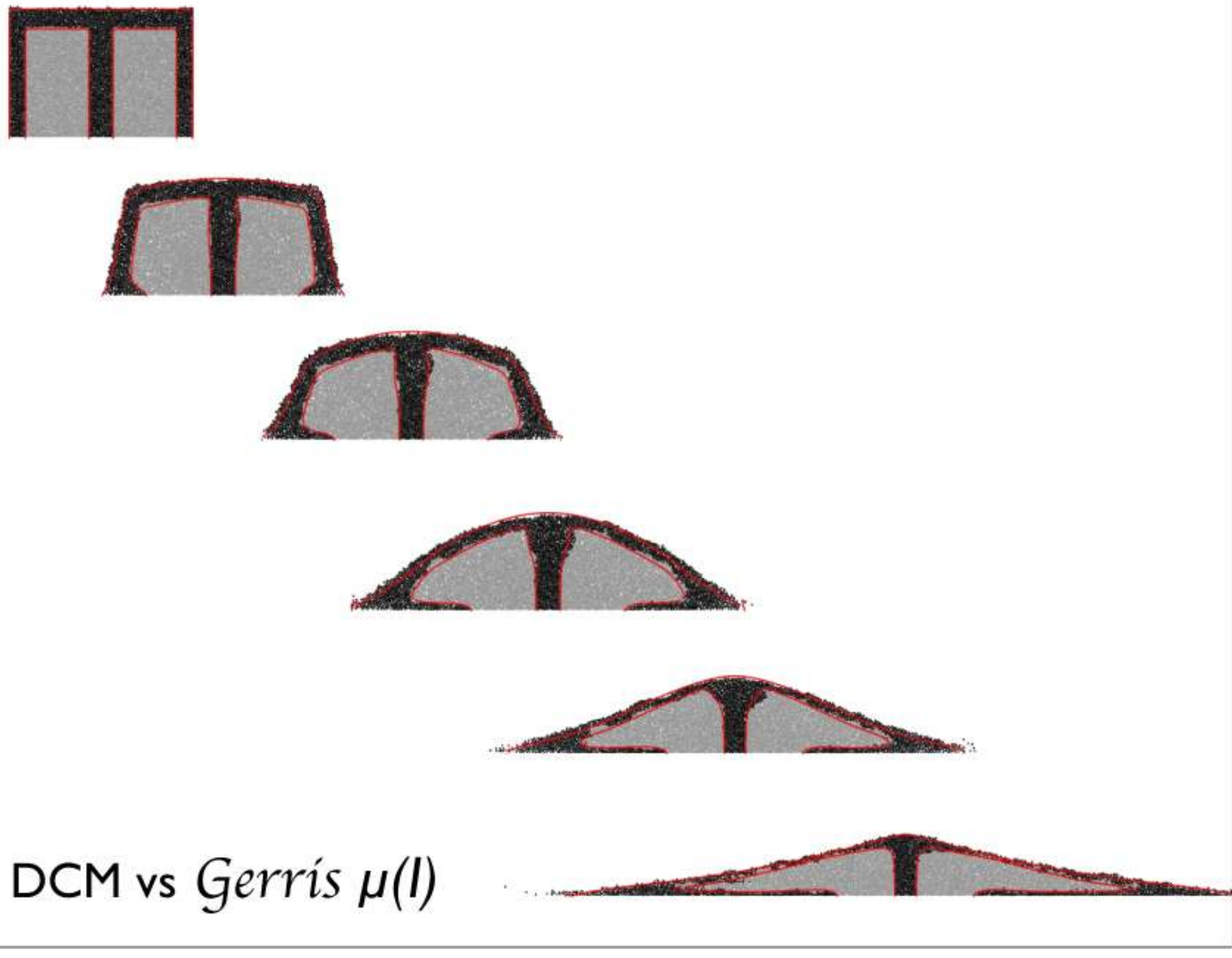

$a = 1.42$ DCM vs *Gerris μ(I)*

Collapse of columns simulation *Gerris μ(I)*

$a = 6.6$ DCM vs *Gerris μ(I)*

Collapse of columns simulation *Gerris* $\mu(I)$

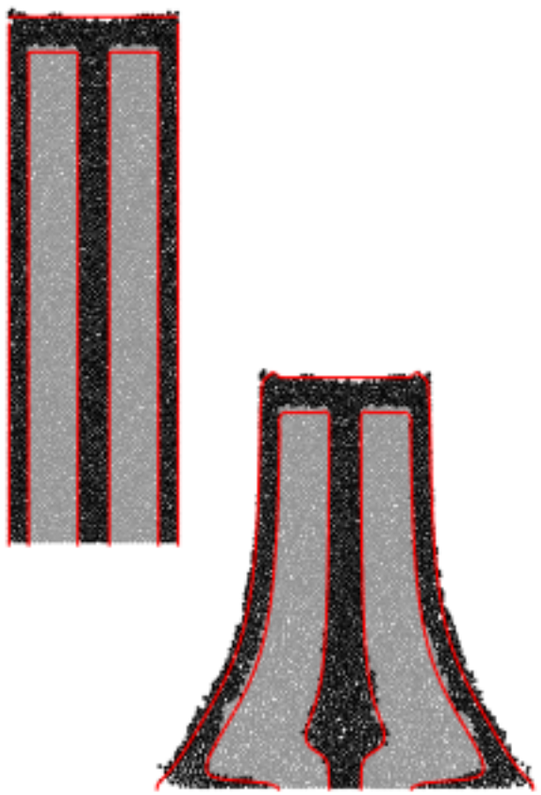

$a = 6.6$ DCM vs *Gerris* $\mu(I)$

Collapse of columns simulation *Gerris* $\mu(I)$

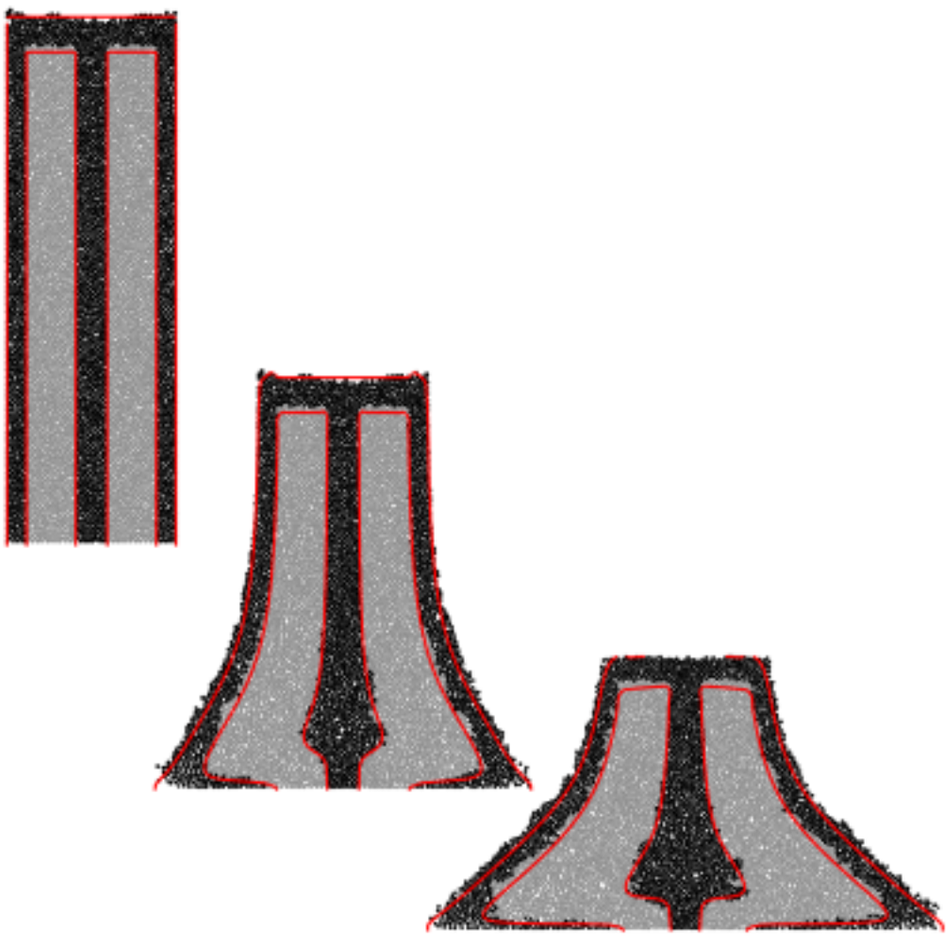

$a = 6.6$ DCM vs *Gerris* $\mu(I)$

Collapse of columns simulation *Gerris* $\mu(I)$

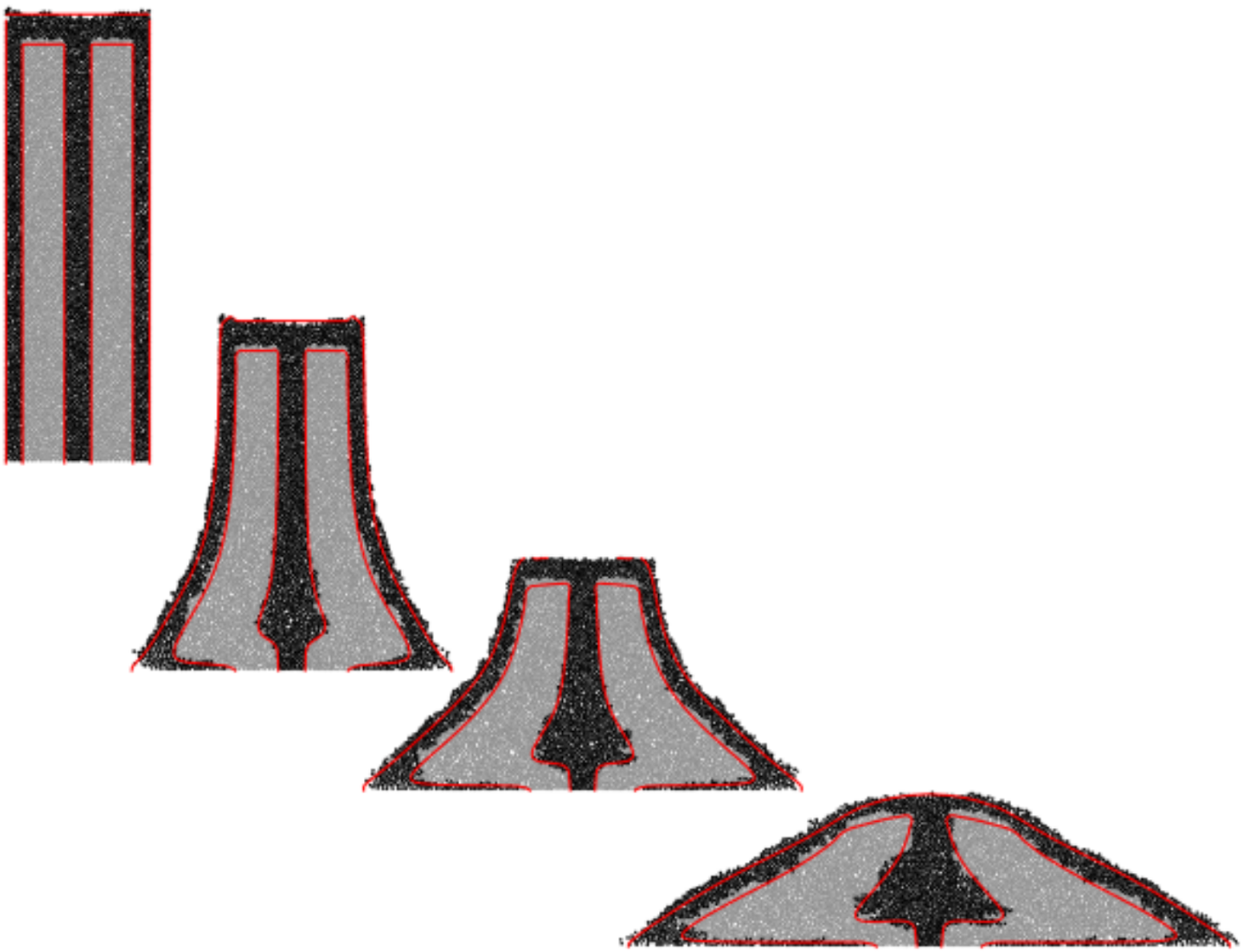

$a = 6.6$ DCM vs *Gerris* $\mu(I)$

Collapse of columns simulation *Gerris μ(I)*

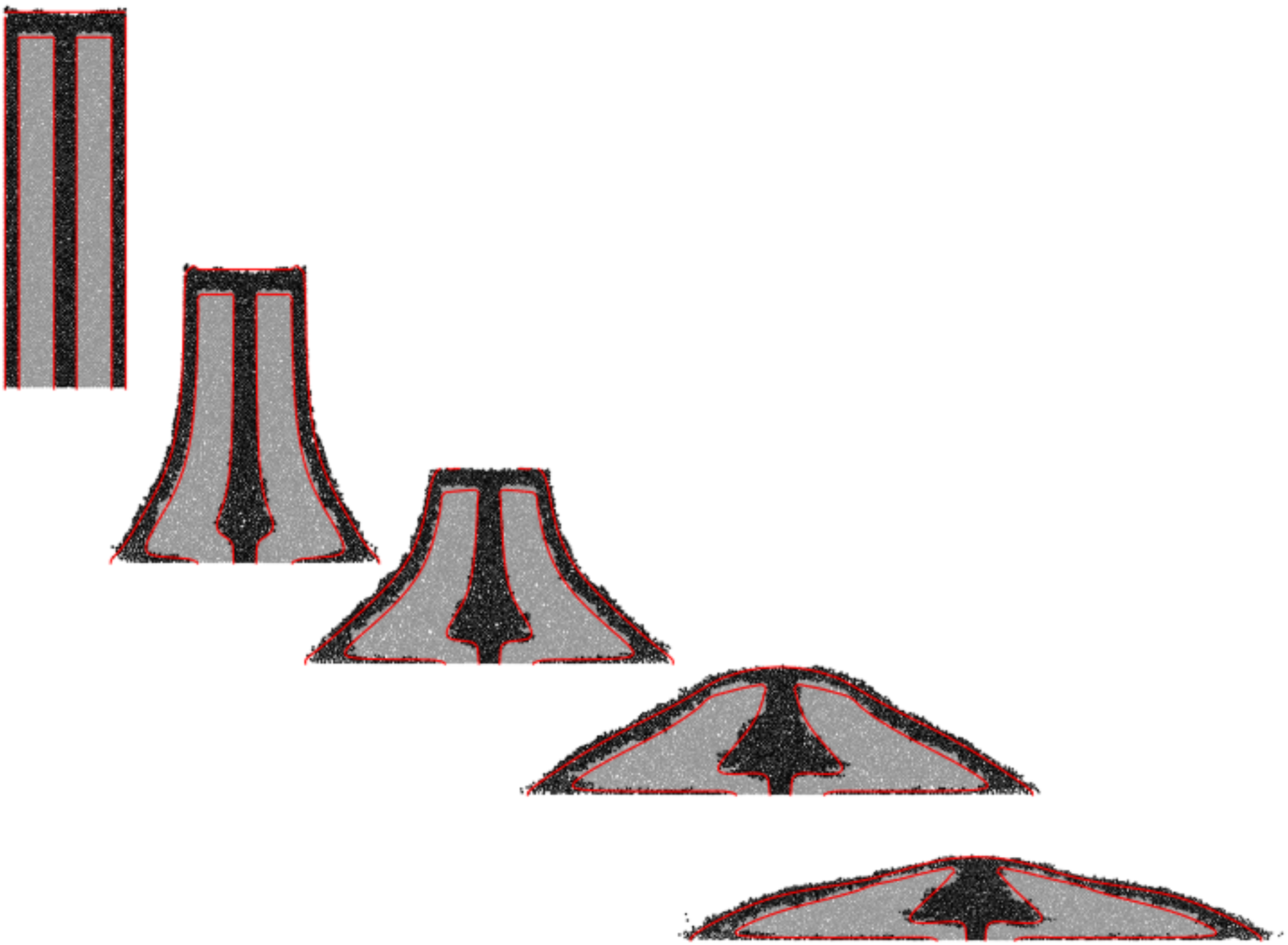

$a = 6.6$ DCM vs *Gerris μ(I)*

Collapse of columns simulation *Gerris μ(I)*

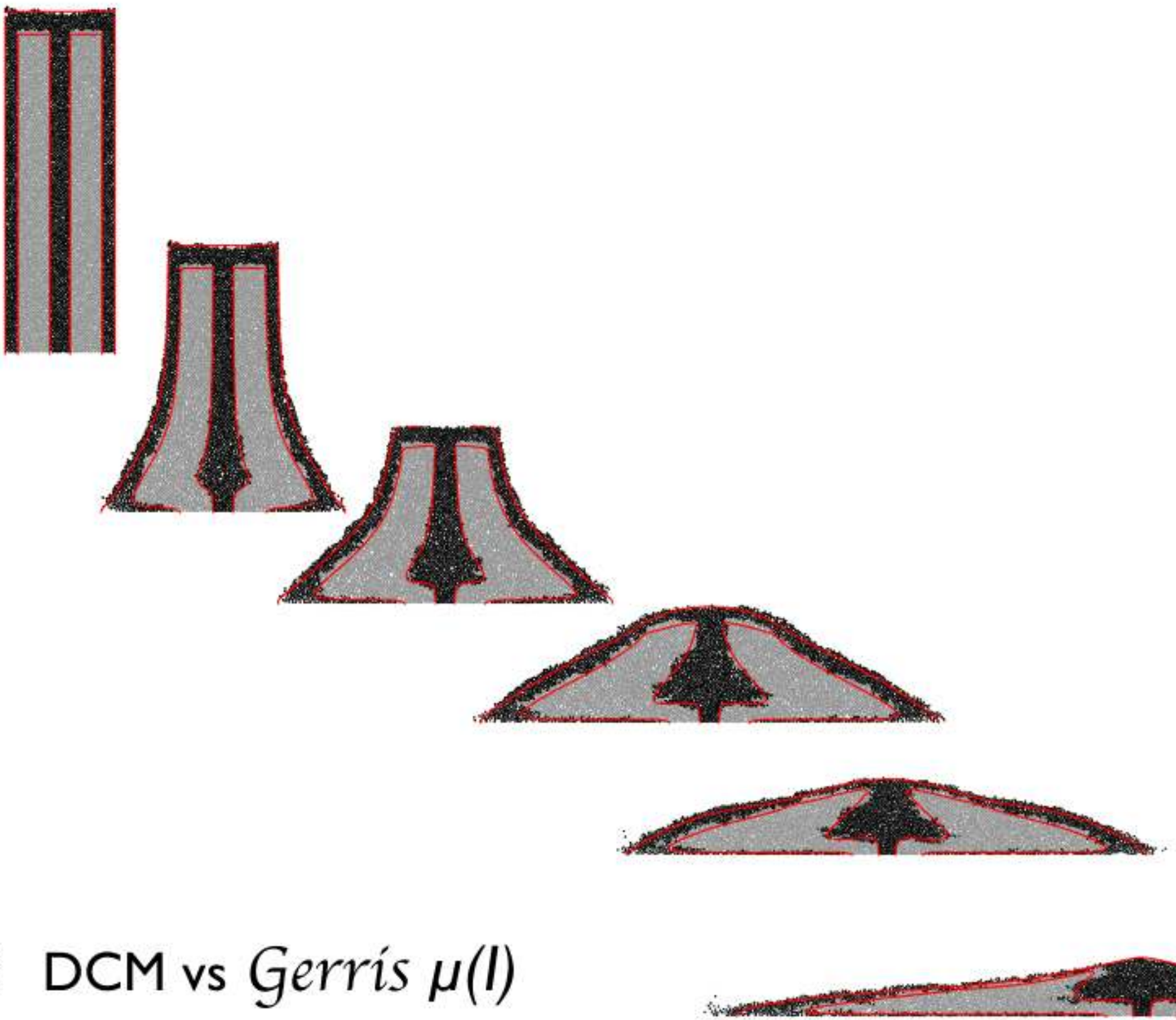

$a = 6.6$ DCM vs *Gerris μ(I)*

Collapse of columns simulation *Gerris μ(I)*

DCM vs *Gerris μ(I)*

Collapse of columns simulation *Gerris μ(I)*

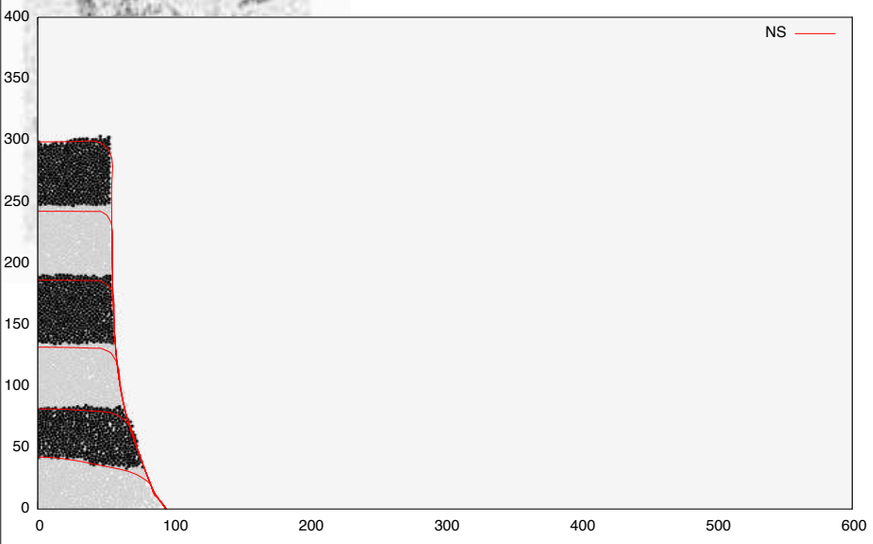

DCM vs *Gerris μ(I)*

Collapse of columns simulation *Gerris μ(I)*

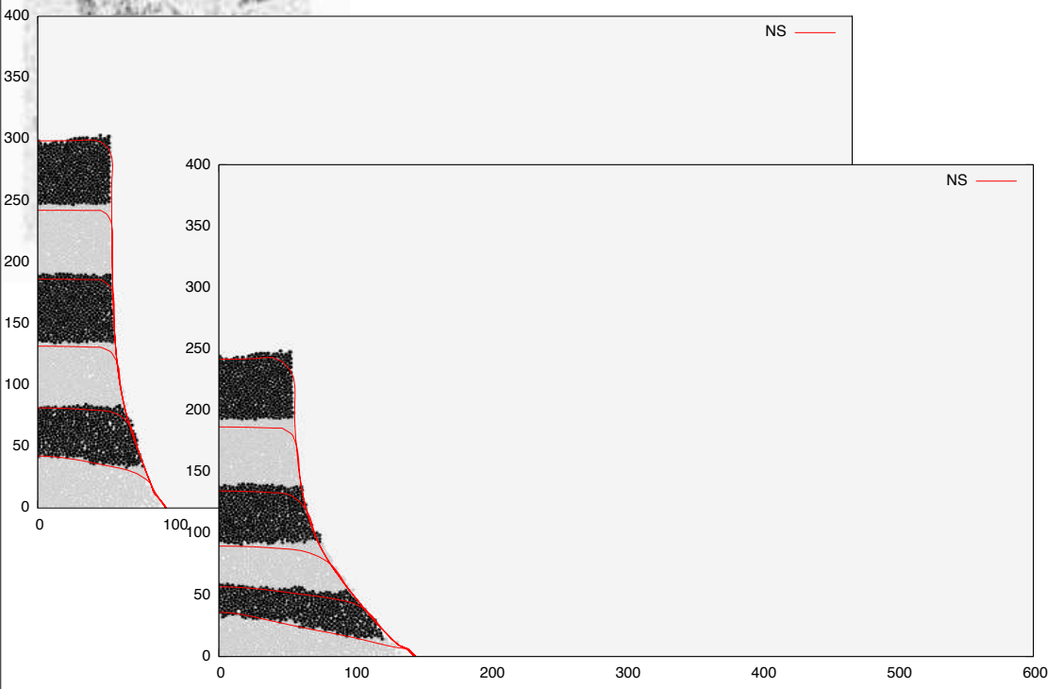

DCM vs *Gerris μ(I)*

Collapse of columns simulation *Gerris μ(I)*

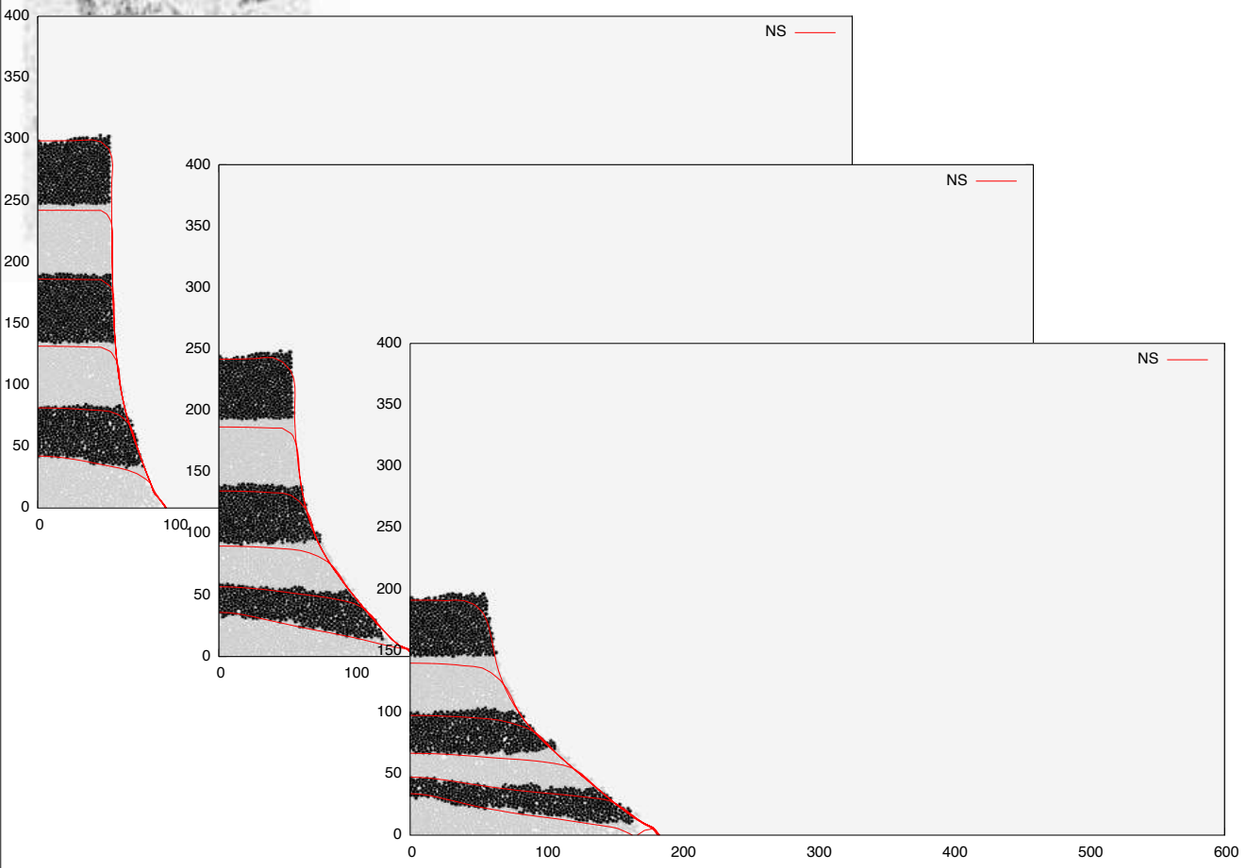

DCM vs *Gerris μ(I)*

Collapse of columns simulation *Gerris μ(I)*

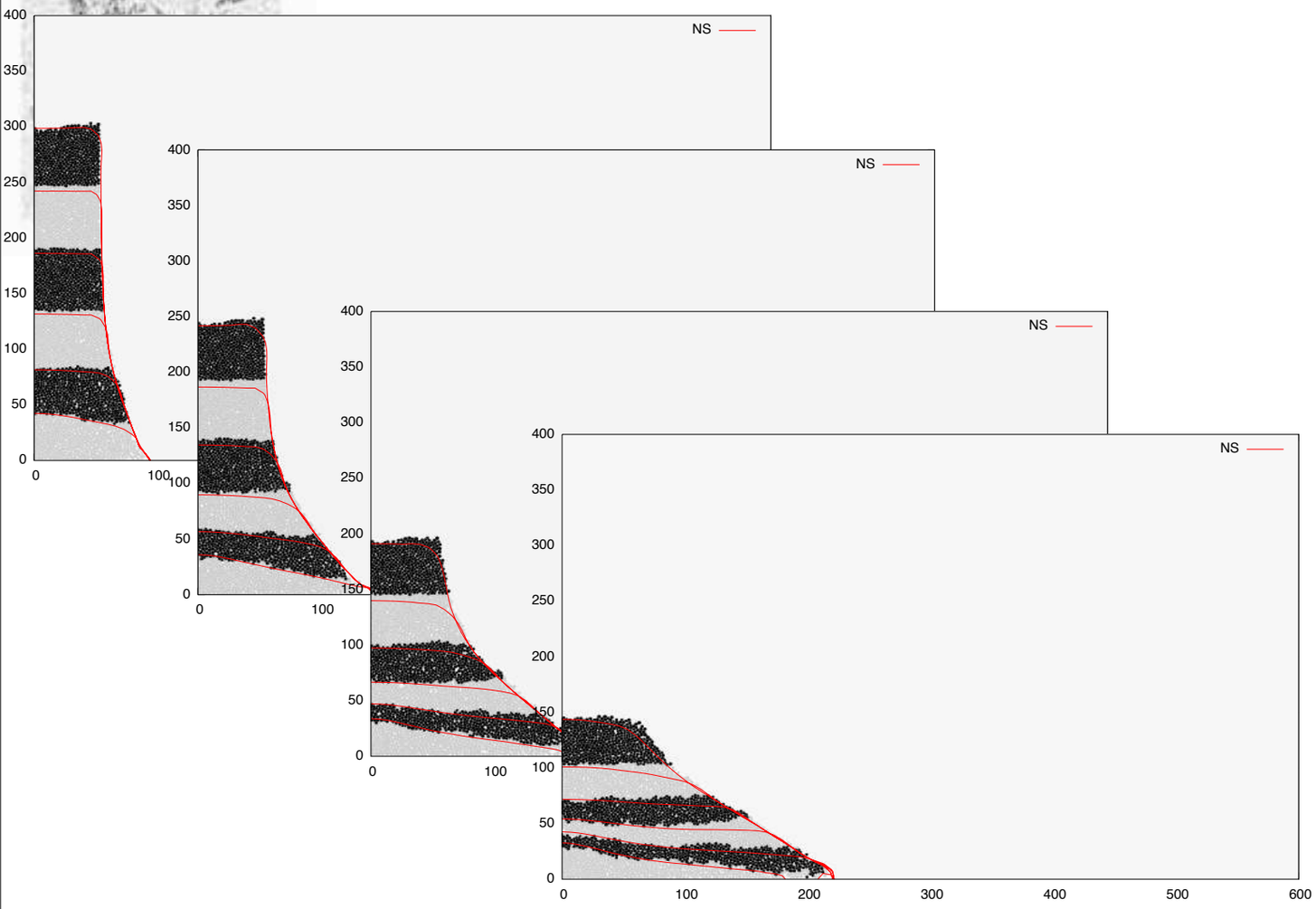

DCM vs *Gerris μ(I)*

Collapse of columns simulation *Gerris μ(I)*

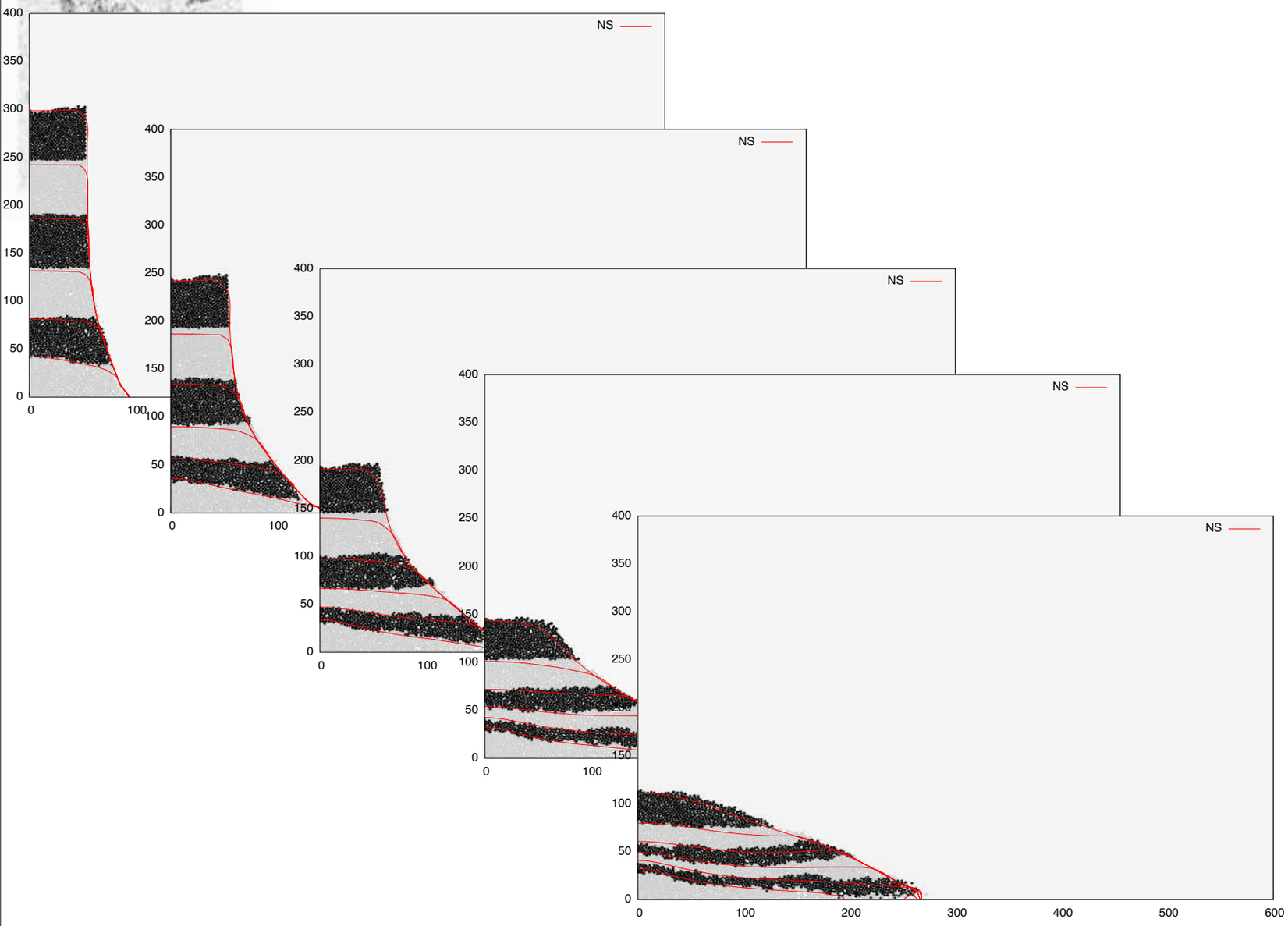

DCM vs *Gerris μ(I)*

Collapse of columns simulation *Gerris μ(I)*

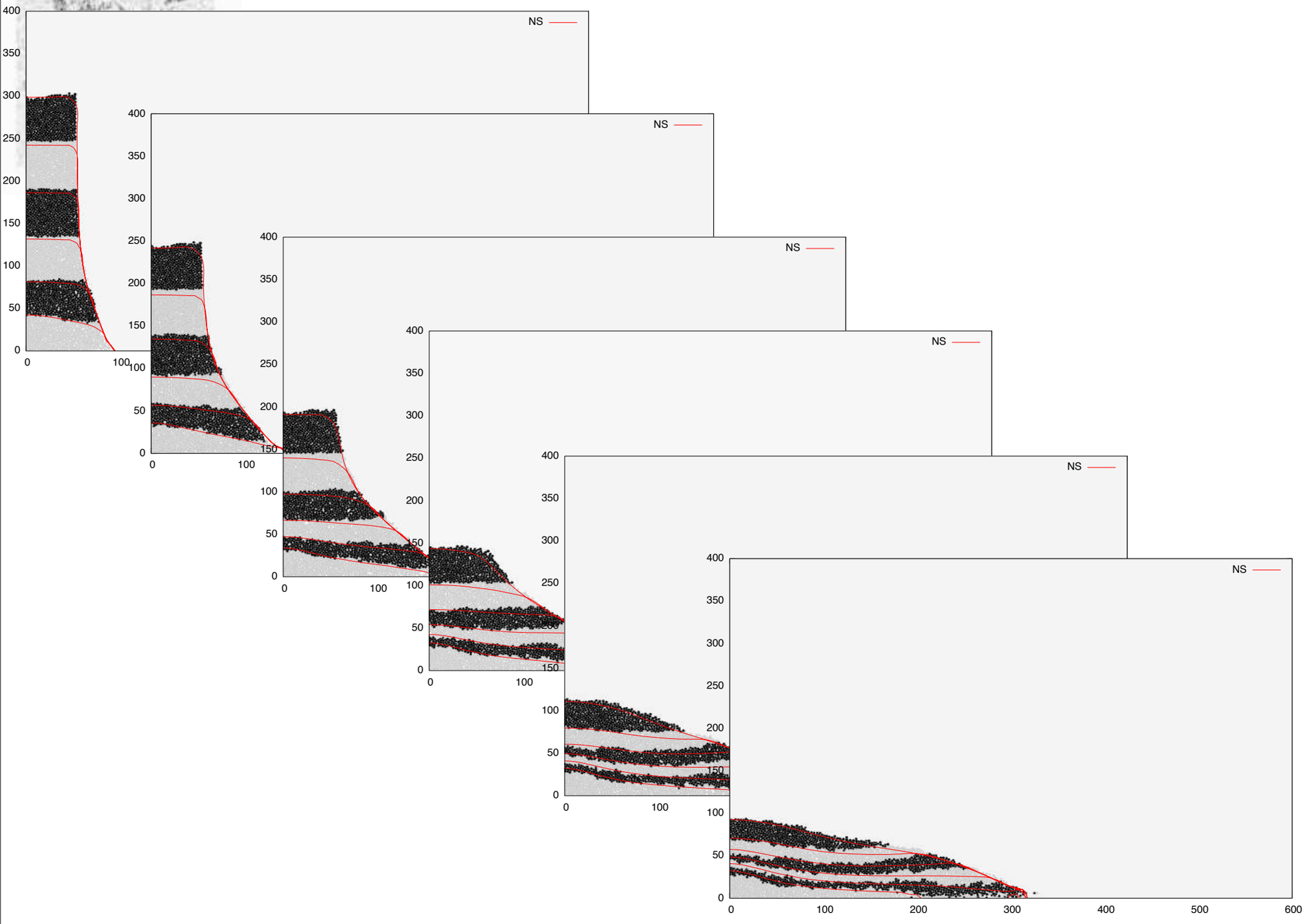

DCM vs *Gerris μ(I)*

Collapse of columns simulation *Gerris μ(I)*

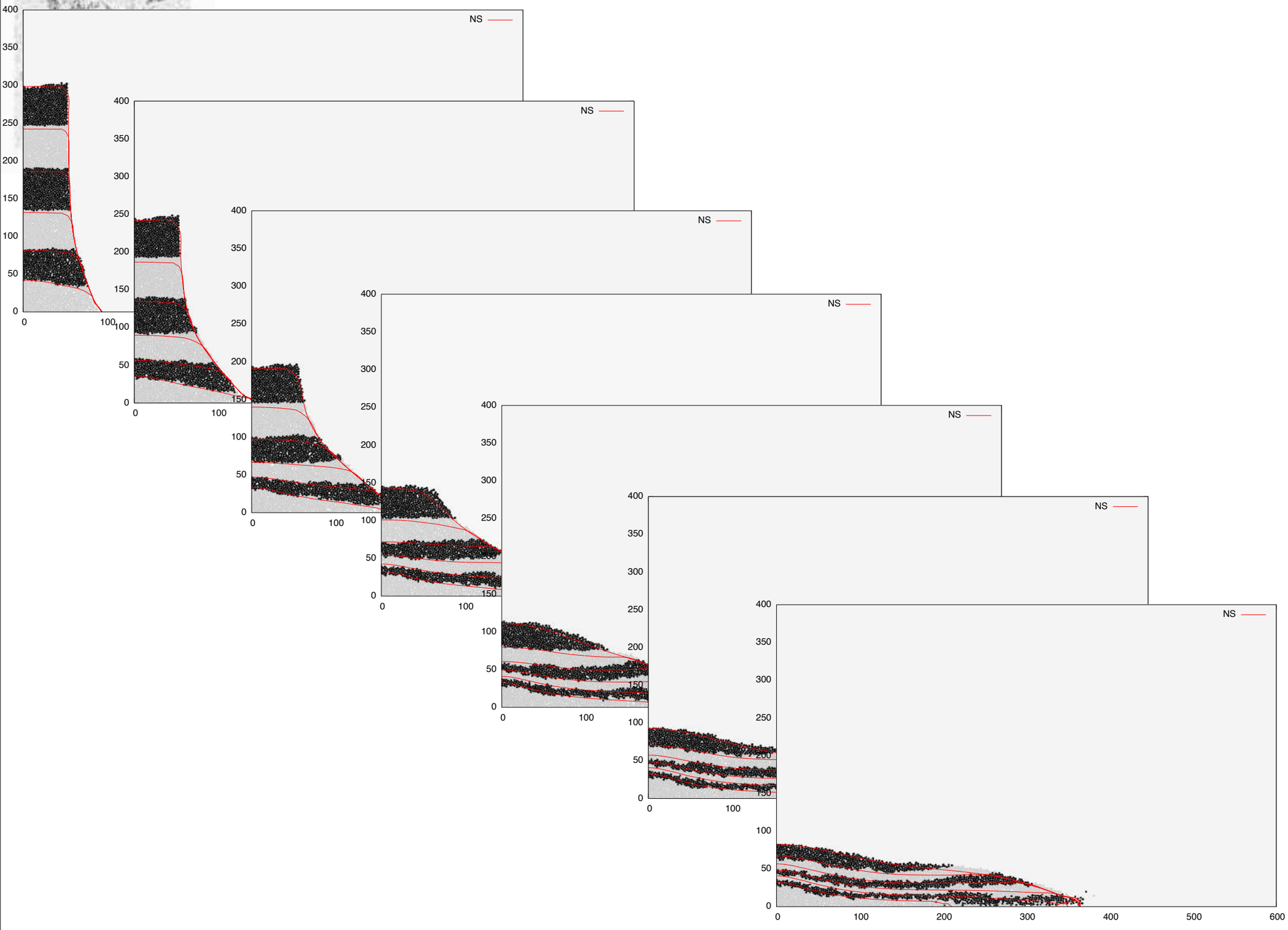

DCM vs *Gerris μ(I)*

Collapse of columns simulation *Gerris μ(I)*

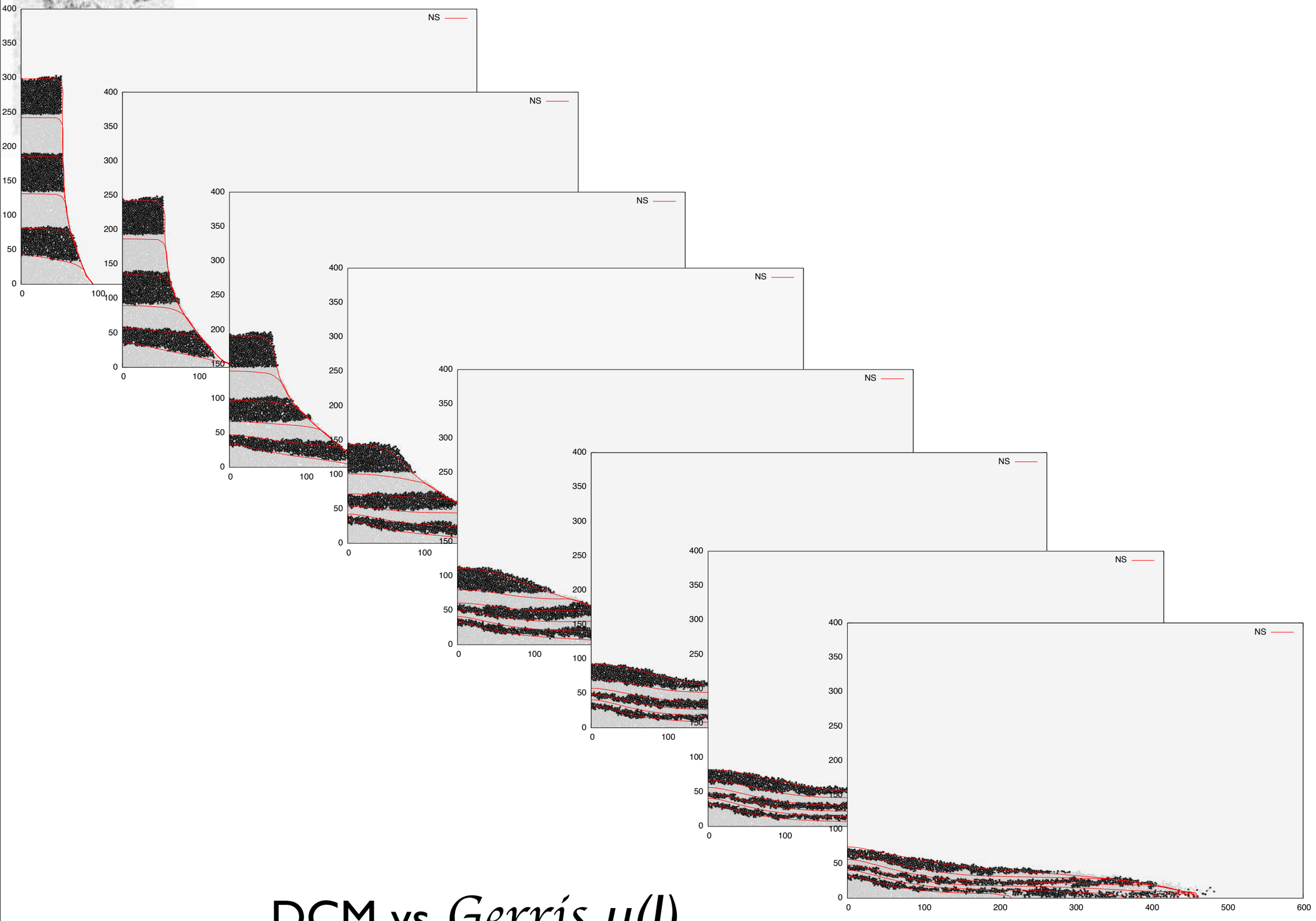

DCM vs *Gerris μ(I)*

Collapse of columns simulation *Gerris μ(I)*

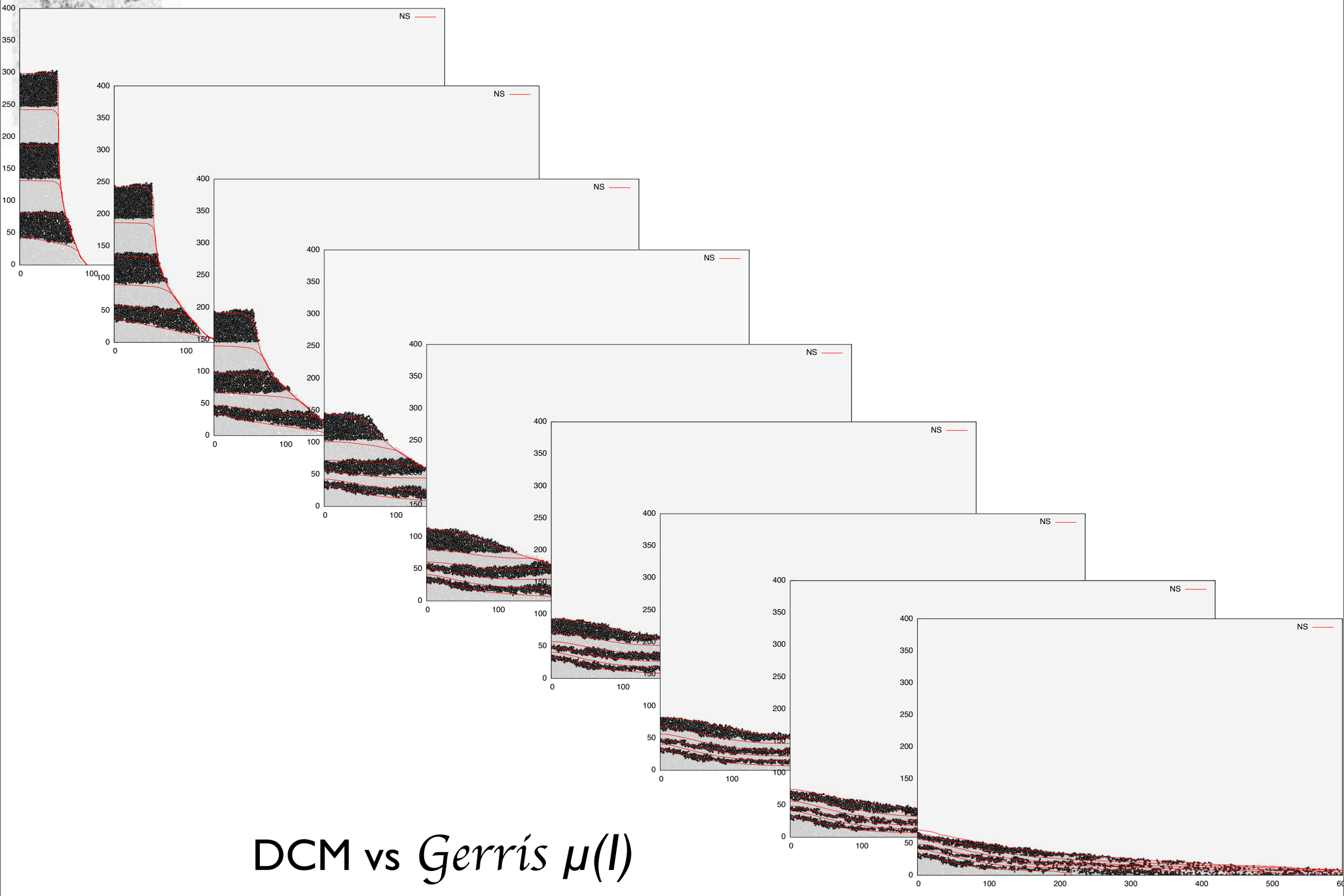

DCM vs *Gerris μ(I)*

Collapse of columns simulation *Gerris μ(I)*

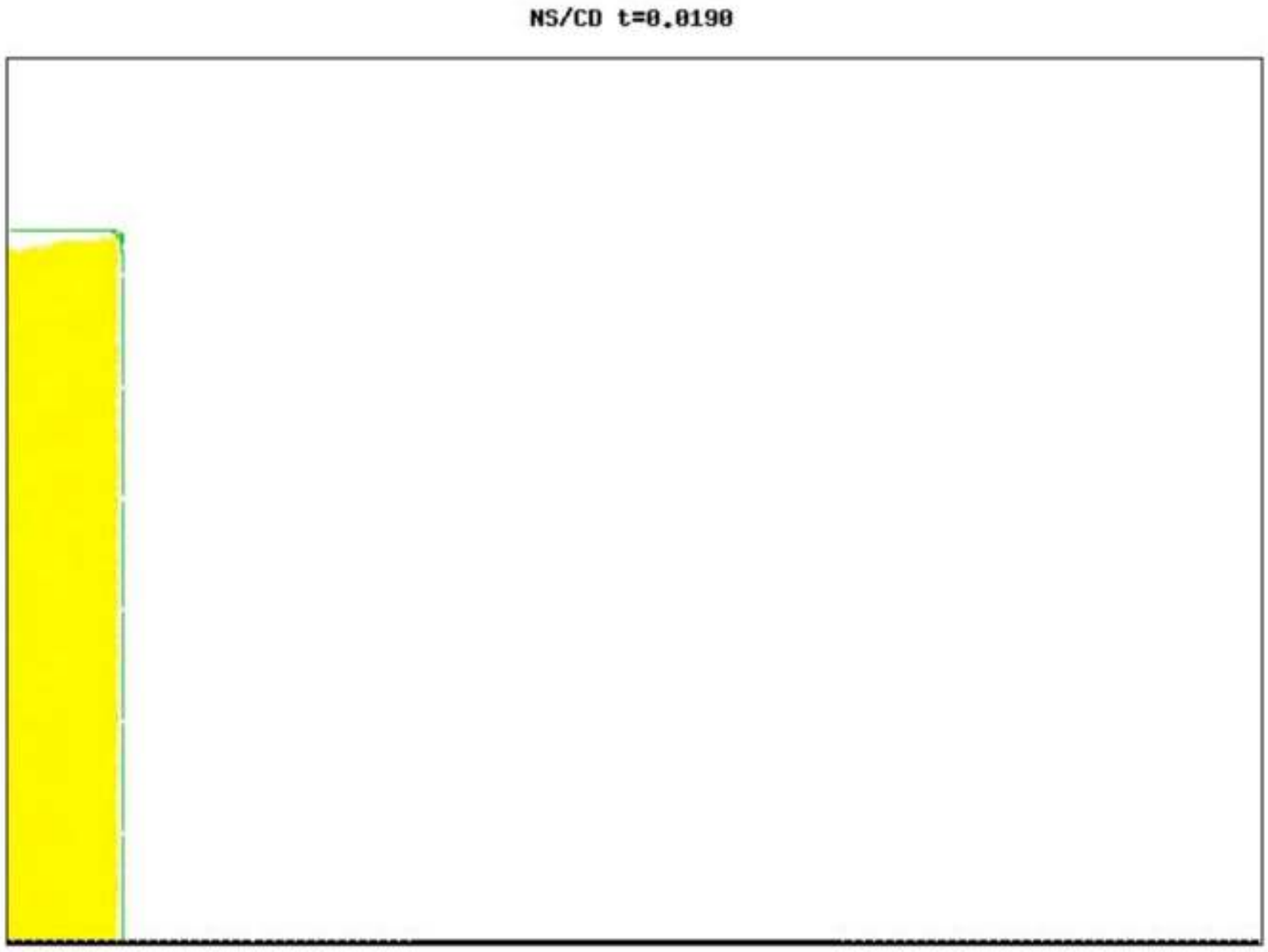

DCM vs *Gerris μ(I)*

Collapse of columns simulation *Gerris μ(I)*

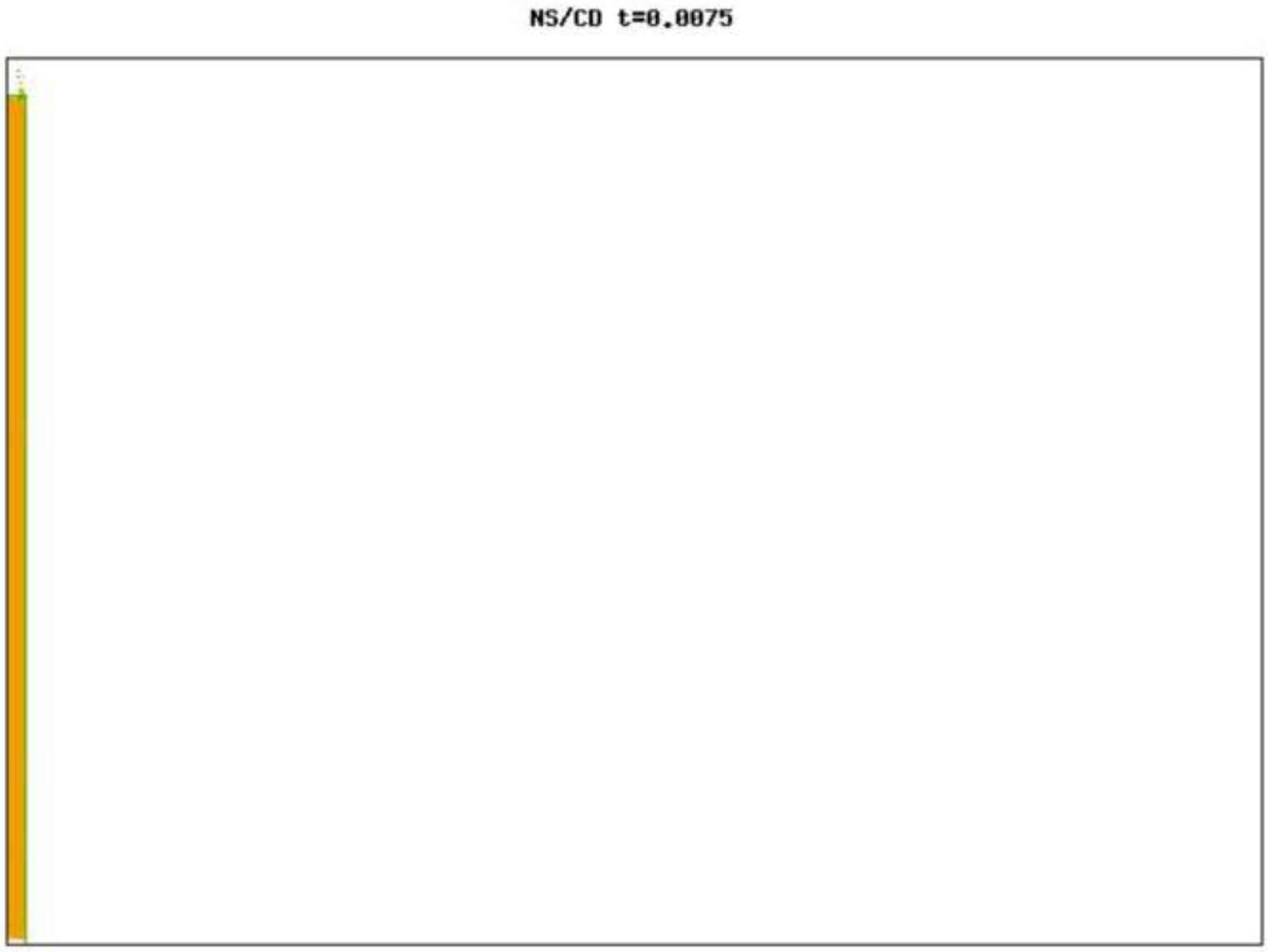

DCM vs *Gerris μ(I)*

Collapse of columns simulation *Gerris μ(I)*

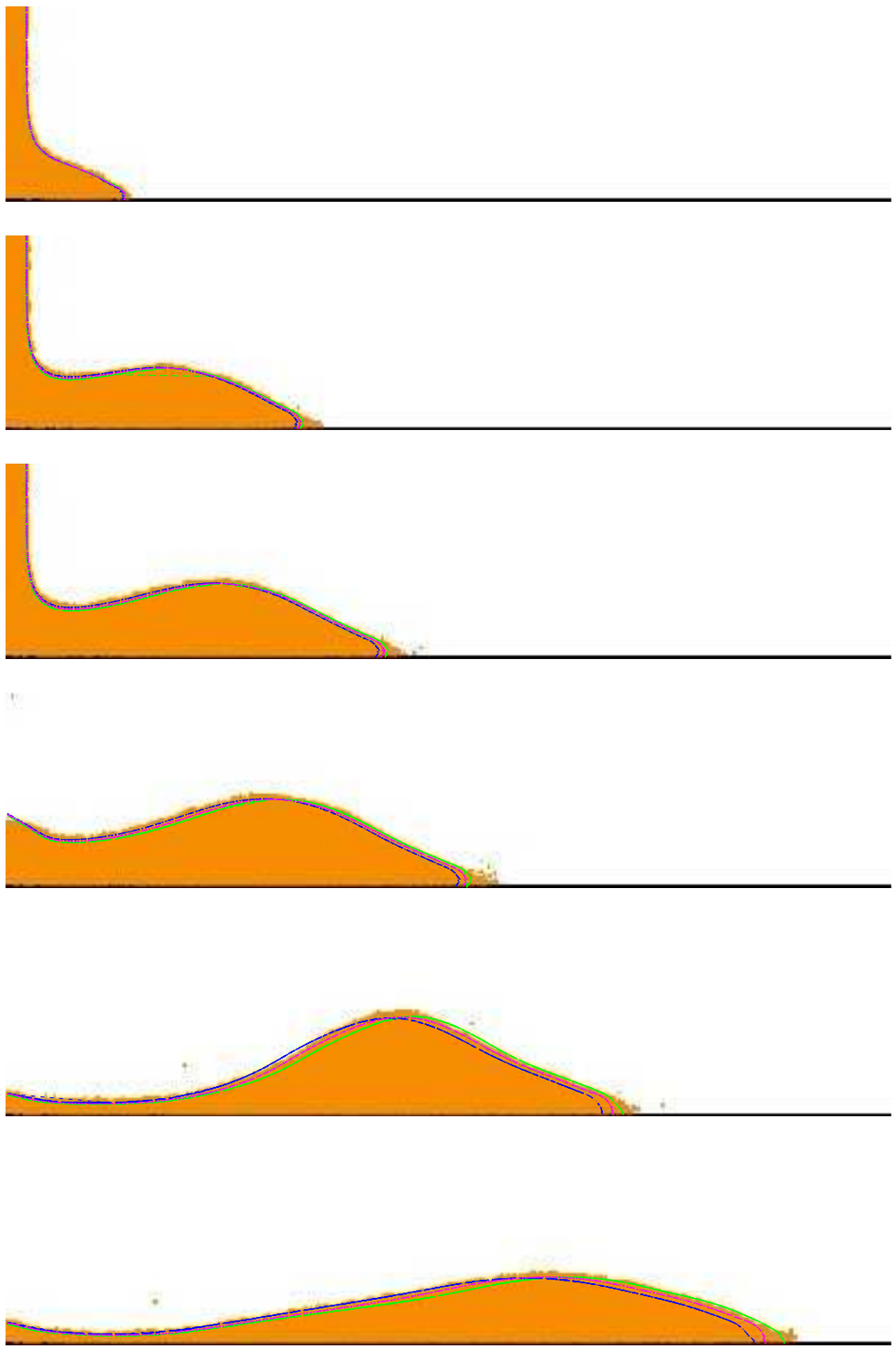

Figure 10: Strip representing a series of snapshots ($t = 0.5, 1.0, 1.2, 1.4, 1.7$, and 2.0) of a column collapse with aspect ratio $a = 68$. The most advanced curve (in green) corresponds to $\mu_s = 0.3$ $\Delta mu = 0.26$ and $I_0 = 0.30$. the less advanced (in blue) $\mu_s = 0.32$ $\Delta mu = 0.28$ and $I_0 = 0.30$ fits better the end of the heap. The curve in between (in cyan) corresponds to $\mu_s = 0.32$ $\Delta mu = 0.28$ and $I_0 = 0.40$ and fits better the top of the surge.

DCM vs *Gerris μ(I)*

- comparaison of velocity profiles

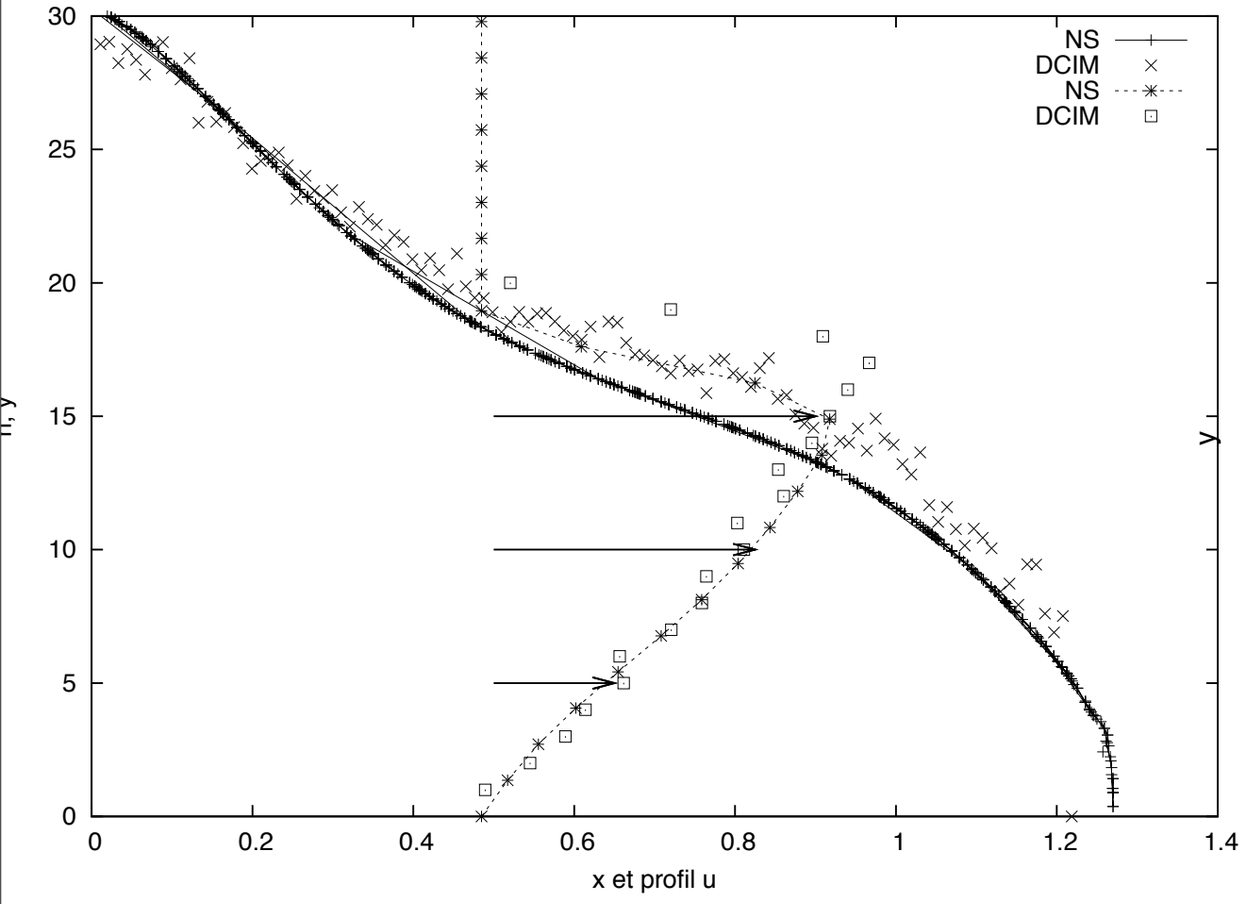

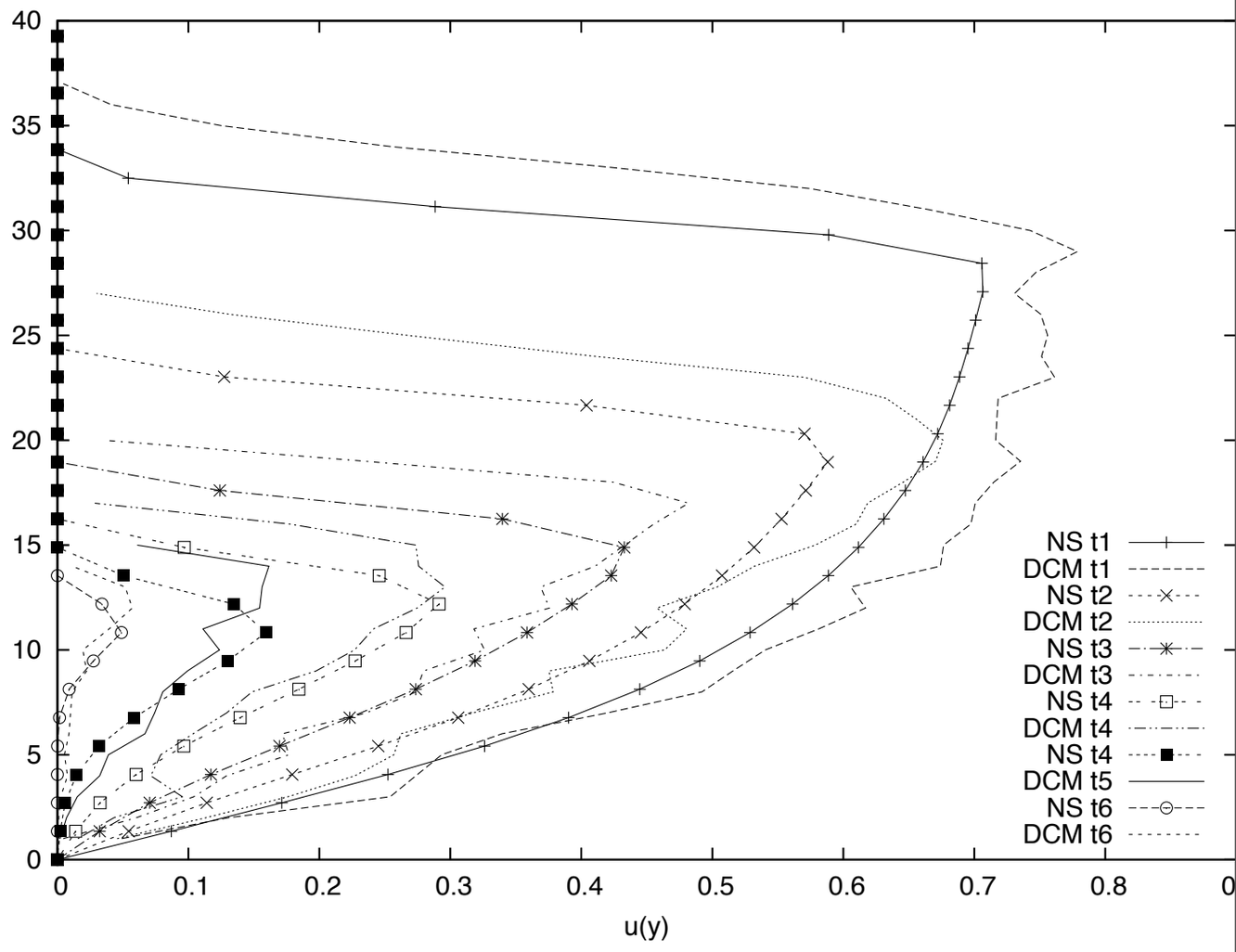

DCM vs *Gerris μ(I)*

- comparaison of velocity profiles

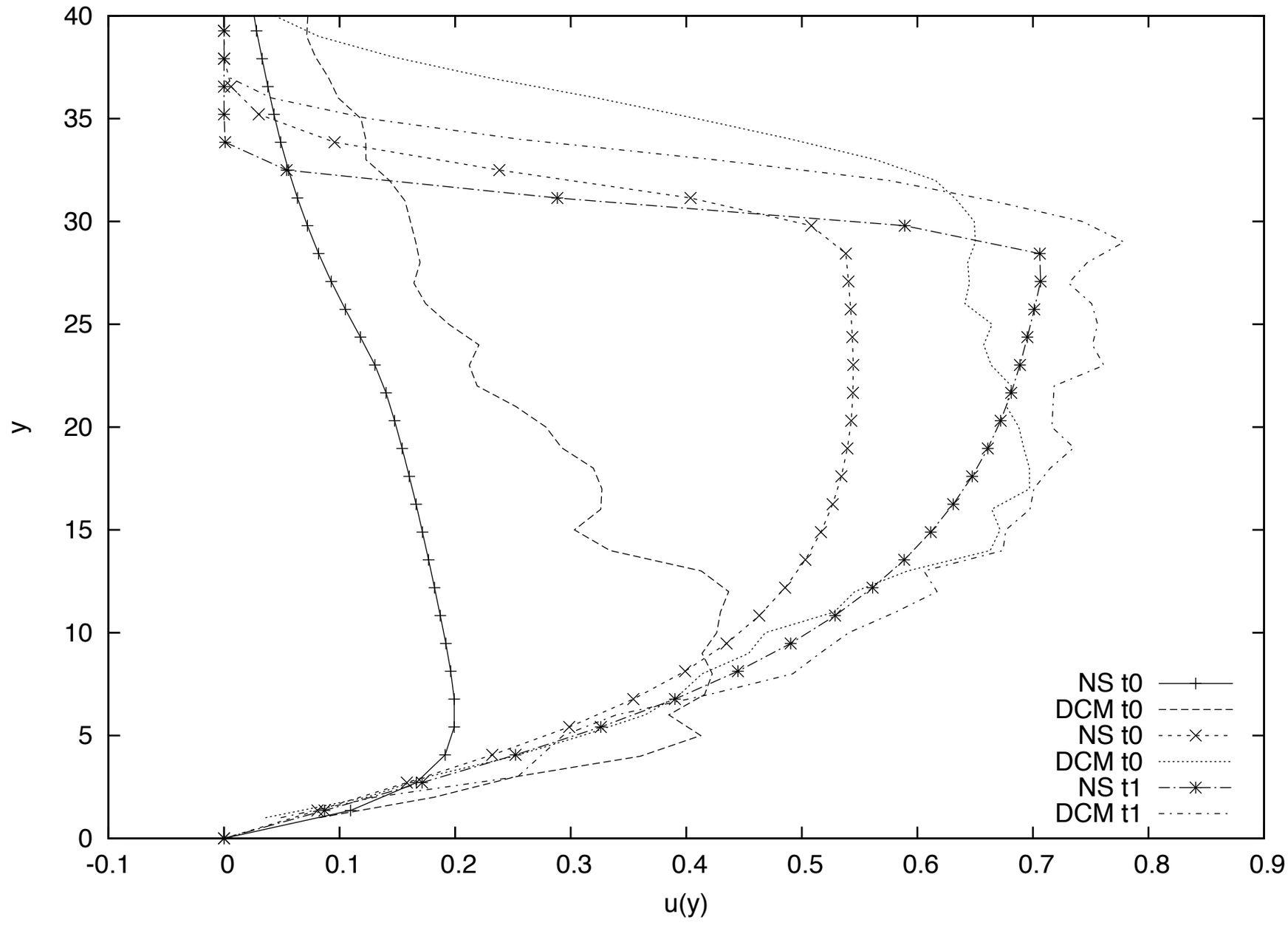

DCM vs *Gerris μ(I)*

- comparaison of velocity profiles

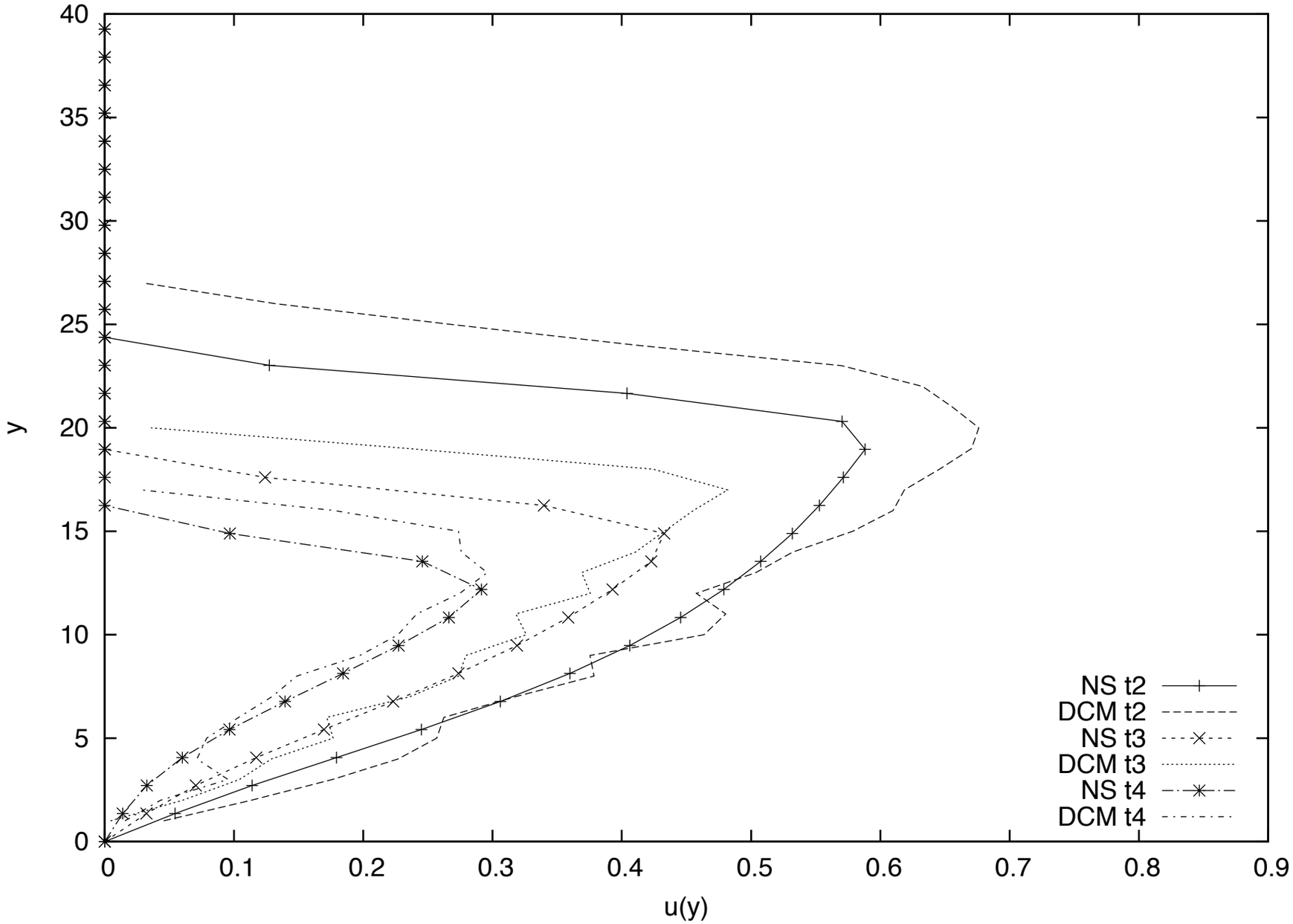

DCM vs *Gerris μ(I)*

- comparaison of velocity profiles

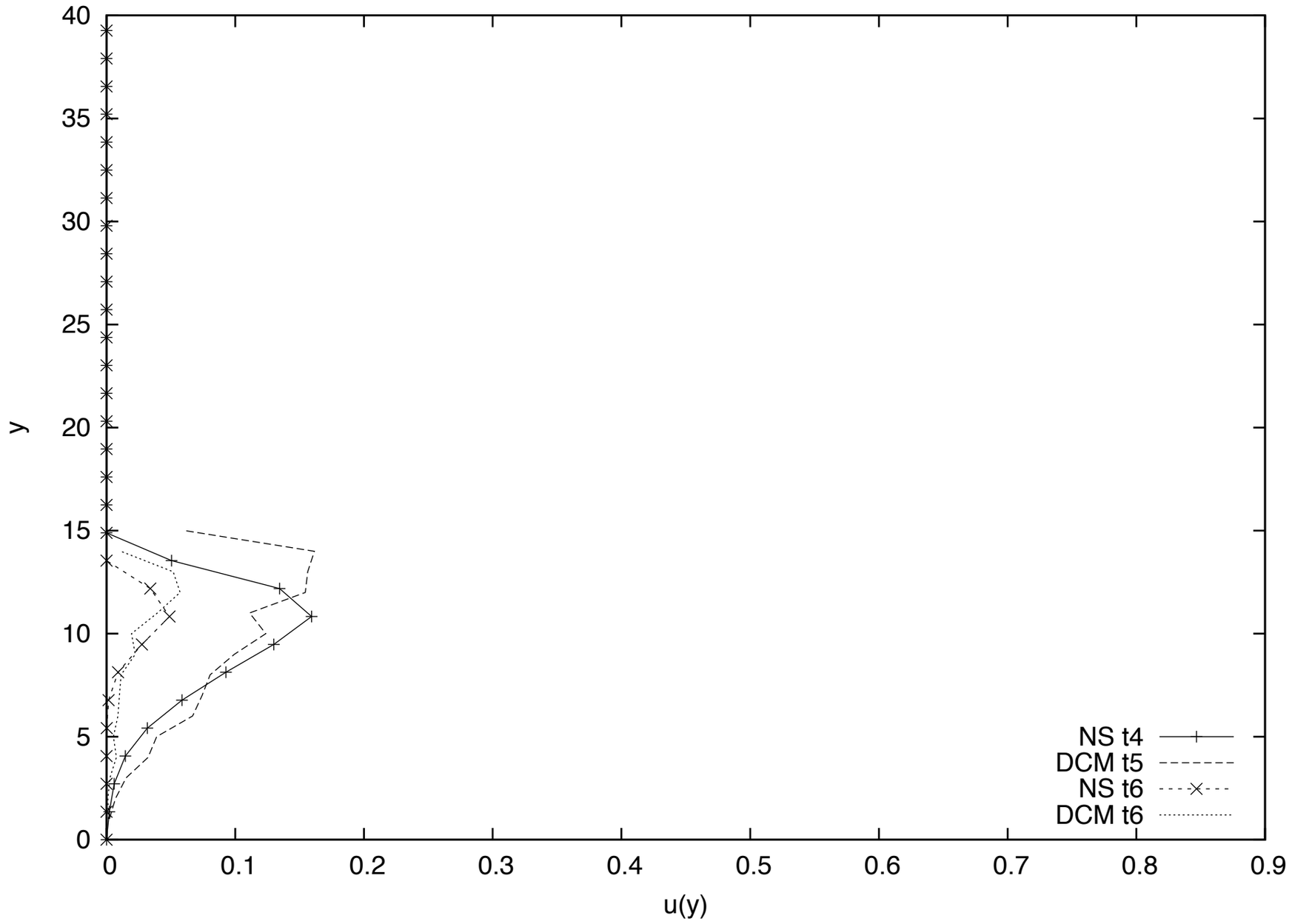

DCM vs *Gerris μ(I)*

Collapse of columns simulation *Gerris μ(I)*

at the tip, a=6.6 t=1.33 2 2.66

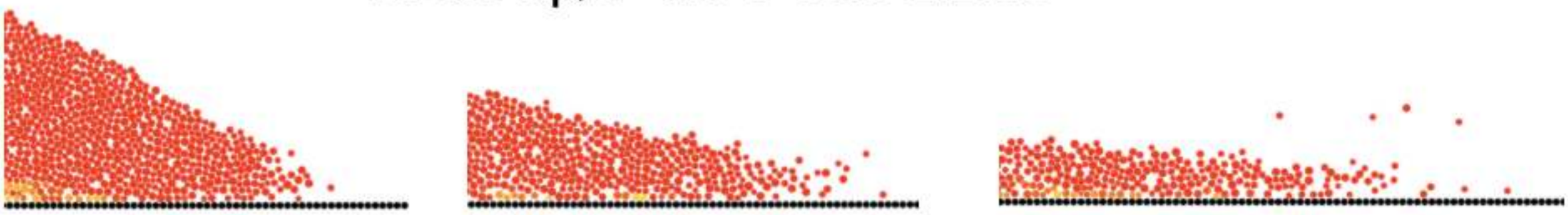

DCM vs *Gerris μ(I)*

Collapse of columns simulation *Gerris μ(I)*

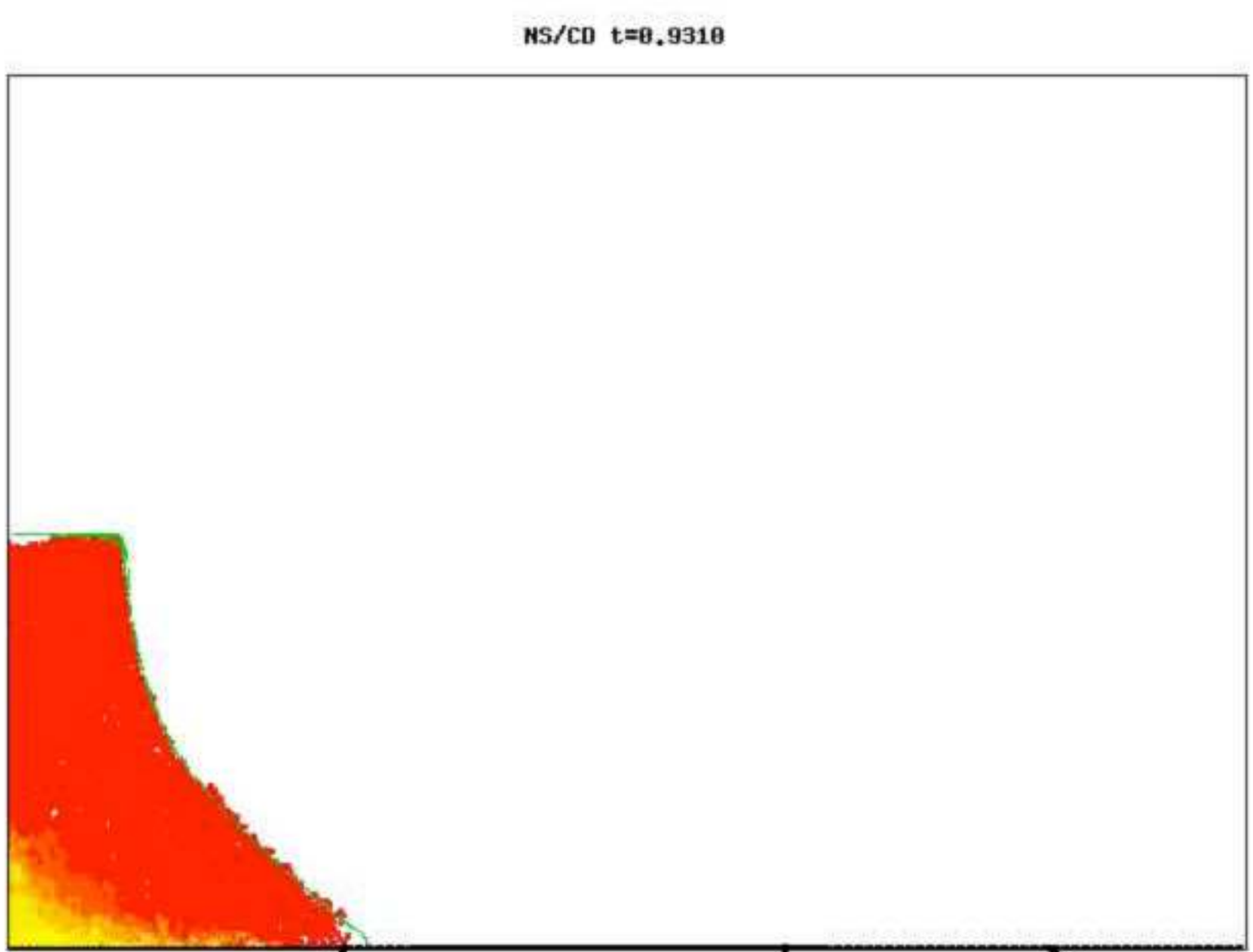

at the tip, a=6.6 t=1.33 2 2.66

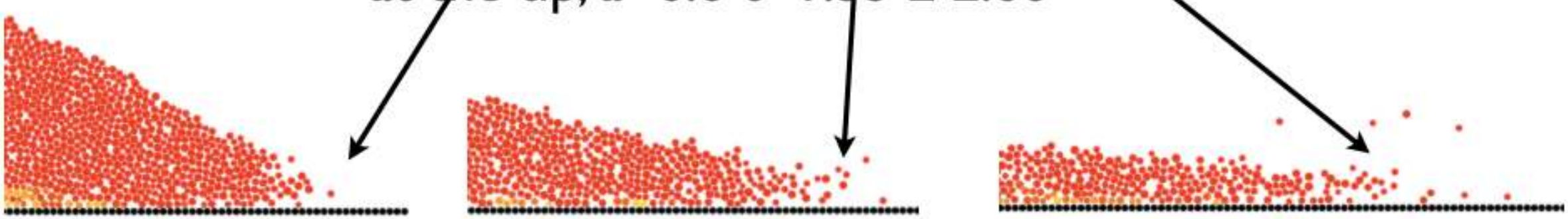

DCM vs *Gerris μ(I)*

Collapse of columns simulation *Gerris μ(I)*

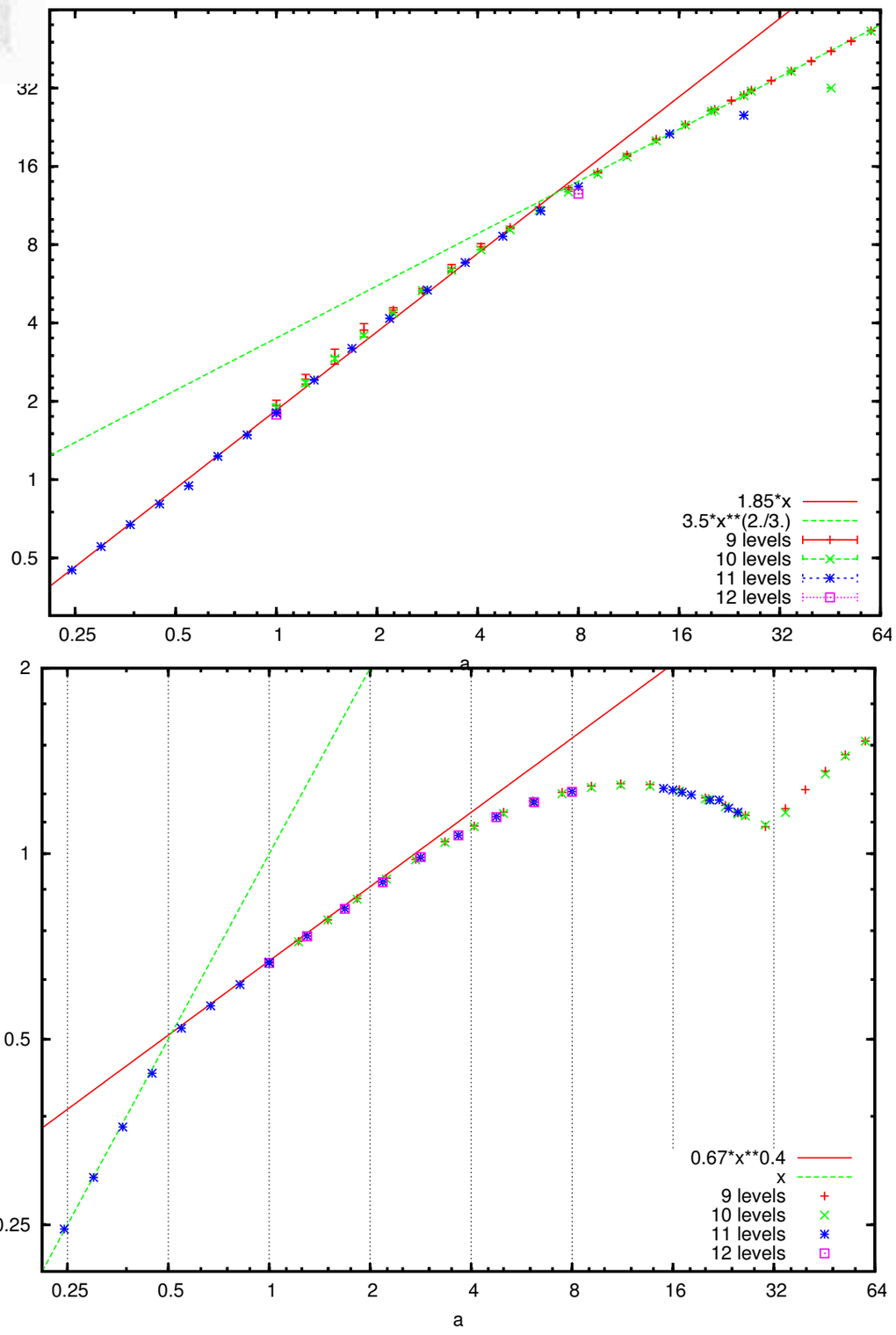

Normalised final deposit extent as a function of aspect ratio *a*.

Well-defined power law dependencies with exponents of 1 and 2/3 respectively.

We recover the experimental scaling [Lajeunesse et al. 04] and [Staron et al. 05]. Differences between the values of the prefactors are due to the difficulties to obtain the run out length: friction in the Navier Stokes code tends to underestimate it, whereas direct simulation shows that the tip is very gazeous, it can no longer explained by a continuum mechanic description.

Saint-Venant Savage Hutter *Gerris*

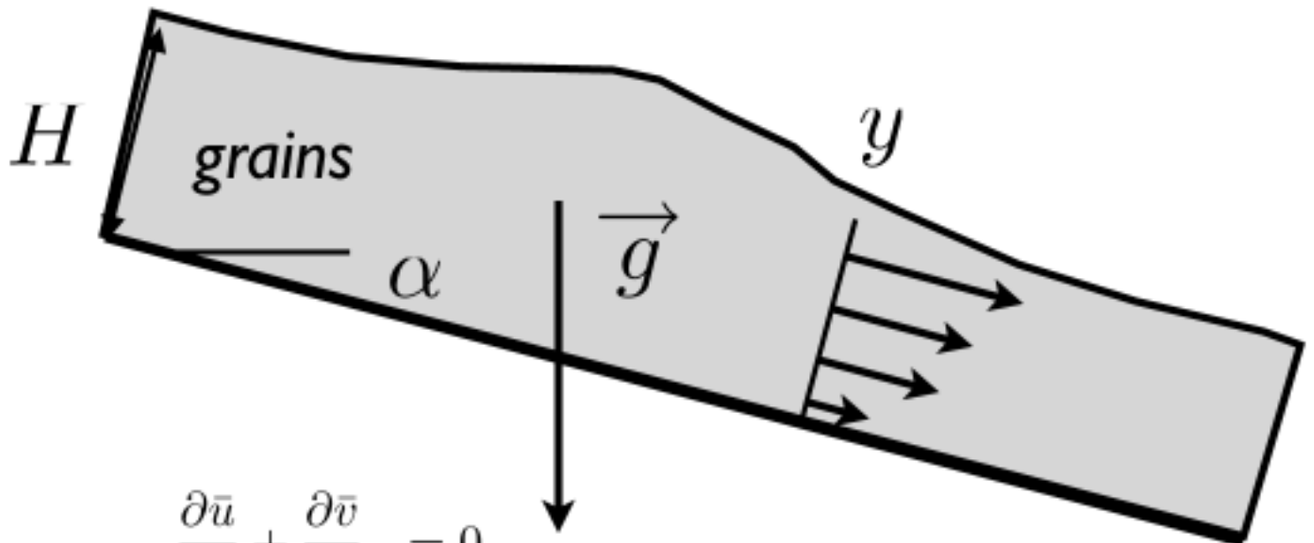

$$\varepsilon = \dot{H}/L$$

$$\begin{cases} \dfrac{\partial \bar{u}}{\partial \bar{x}} + \dfrac{\partial \bar{v}}{\partial \bar{y}} = 0 \\ \varepsilon(\dfrac{\partial \bar{u}}{\partial \bar{t}} + \dfrac{\partial \bar{u}^2}{\partial \bar{x}} + \dfrac{\partial \bar{u}\bar{v}}{\partial \bar{y}}) = -\sin\alpha - \varepsilon\dfrac{\partial \bar{p}}{\partial \bar{x}} + \sin\alpha\varepsilon\dfrac{\partial \bar{\tau}_{xx}}{\partial \bar{x}} + \sin\alpha\dfrac{\partial \bar{\tau}_{xy}}{\partial \bar{y}} \\ \varepsilon^2(\dfrac{\partial \bar{v}}{\partial \bar{t}} + \dfrac{\partial \bar{u}\bar{v}}{\partial x} + \dfrac{\partial \bar{v}^2}{\partial \bar{y}}) = -\cos\alpha - \dfrac{\partial \bar{p}}{\partial \bar{y}} + \sin\alpha\varepsilon\dfrac{\partial \bar{\tau}_{yy}}{\partial \bar{x}} + \sin\alpha\dfrac{\partial \bar{\tau}_{yx}}{\partial \bar{y}} \end{cases}$$

$$p = -\rho g \cos\alpha(\eta(x,t) - y) \qquad \tau_{xy} = \rho g H \sin\alpha \bar{\tau}_{xy}$$

$$\rho U_0^2/L \longleftrightarrow -\frac{\partial p}{\partial x} = -\rho g \frac{\partial \eta}{\partial x}$$

$$\rho U_0^2/(H/\varepsilon) = \rho g \varepsilon.$$

$$\boxed{U_0 = \sqrt{gH}.}$$

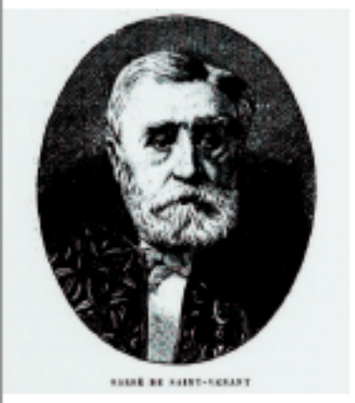

Saint-Venant Savage Hutter *Gerris*

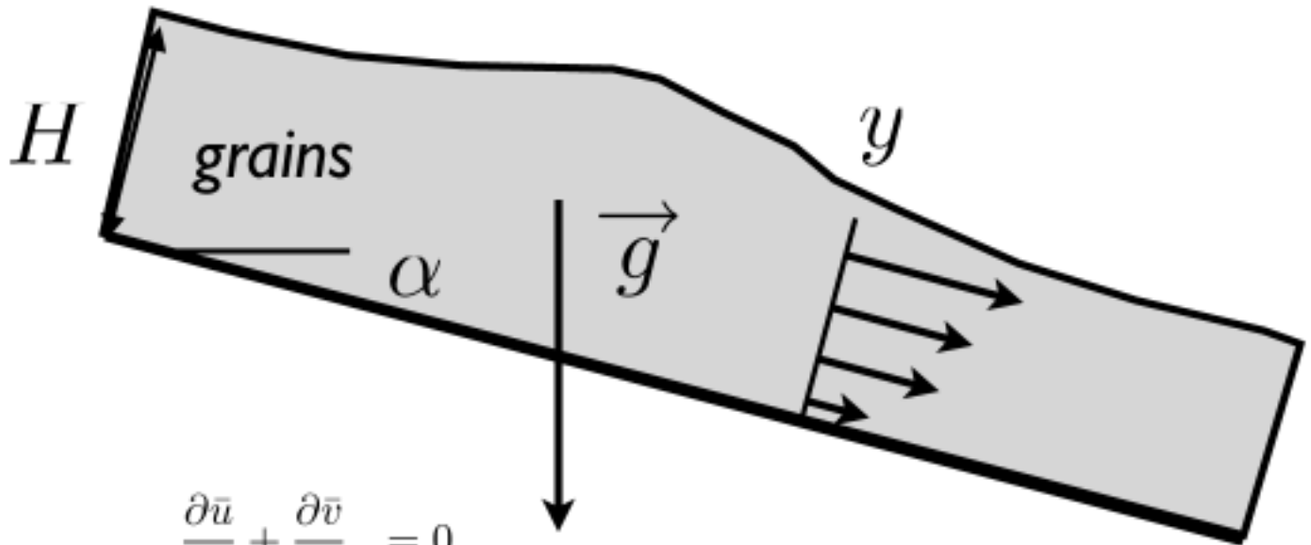

$$\begin{cases} \dfrac{\partial \bar{u}}{\partial \bar{x}} + \dfrac{\partial \bar{v}}{\partial \bar{y}} = 0 \\ \varepsilon\left(\dfrac{\partial \bar{u}}{\partial \bar{t}} + \dfrac{\partial \bar{u}^2}{\partial \bar{x}} + \dfrac{\partial \bar{u}\bar{v}}{\partial \bar{y}}\right) = -\sin\alpha - \varepsilon\dfrac{\partial \bar{p}}{\partial \bar{x}} + \sin\alpha\dfrac{\partial \bar{\tau}_{xy}}{\partial \bar{y}} \\ 0 = -\cos\alpha - \dfrac{\partial \bar{p}}{\partial \bar{y}} \end{cases}$$

$$\int \Big| dy$$

$$\frac{\partial h}{\partial t} + \frac{\partial}{\partial x}\int_f^\eta u(x,y,t)dy = 0$$

$$\frac{\partial}{\partial t}\int_f^\eta u(x,y,t)dy + \frac{\partial}{\partial x}\left(\int_f^\eta u(x,y,t)^2 dy + \cos\alpha\frac{g}{2}(h^2)\right) = -gh\sin(\alpha) - \cos\alpha gh\frac{d}{dx}f - \mu(I(0))gh\cos(\alpha).$$

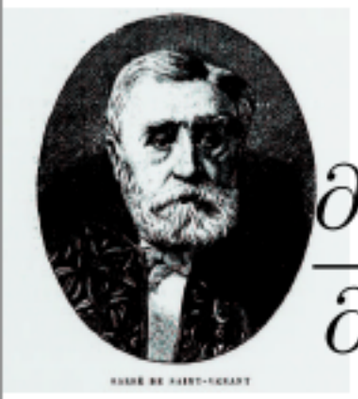

Saint-Venant Savage Hutter *Gerris*

$$\frac{\partial h}{\partial t} + \frac{\partial (Q)}{\partial x} = 0 \quad \frac{\partial Q}{\partial t} + \frac{\partial}{\partial x}(\frac{5Q^2}{4h} + \frac{g}{2}(h^2)) = -gh\mu(I)\frac{Q}{|Q|}$$

Integral over the layer of grains

```
1 0 GfsRiver GfsBox GfsGEdge { } {}
```

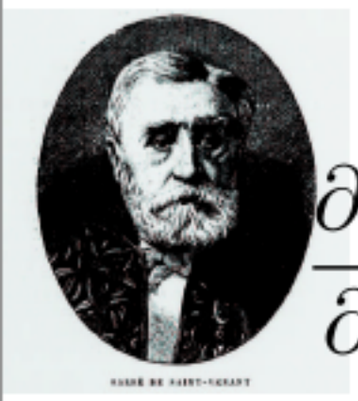

Saint-Venant Savage Hutter *Gerris*

$$\frac{\partial h}{\partial t} + \frac{\partial (Q)}{\partial x} = 0 \quad \frac{\partial Q}{\partial t} + \frac{\partial}{\partial x}(\frac{5Q^2}{4h} + \frac{g}{2}(h^2)) = -gh\mu(I)\frac{Q}{|Q|}$$

$$\frac{Q^* - Q^n}{\Delta t} + \frac{\partial}{\partial x}(\frac{Q^2}{h} + \frac{g}{2}(h^2)) = 0 \qquad \frac{Q^{n+1} - Q^*}{\Delta t} = -gh^*\mu(I^*)\frac{Q^{n+1}}{|Q^*|}$$

Audusse et al.

```
# h is P,   Q is U

Init { istep = 1 } {
        ln=(1./nbrg)*5./2.*fabs(U)/pow(P+eps,2.5)
        mu = (0.4 + 0.26/(0.4/ln +1))
        U = (U )/(1. +  dt *mu*P/(fabs(U)+eps))
 }

PhysicalParams { g = 1 }
```

Saint-Venant Savage Hutter *Gerris*

$$\frac{\partial h}{\partial t} + \frac{\partial (Q)}{\partial x} = 0 \quad \frac{\partial Q}{\partial t} + \frac{\partial}{\partial x}\left(\frac{5Q^2}{4h} + \frac{g}{2}(h^2)\right) = -gh\mu(I)\frac{Q}{|Q|}$$

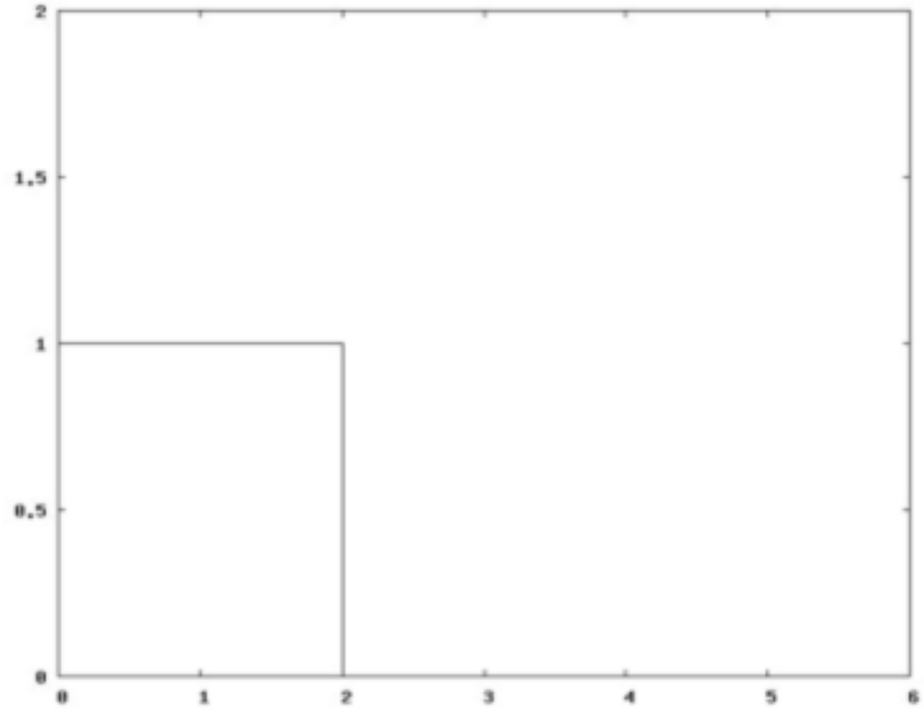

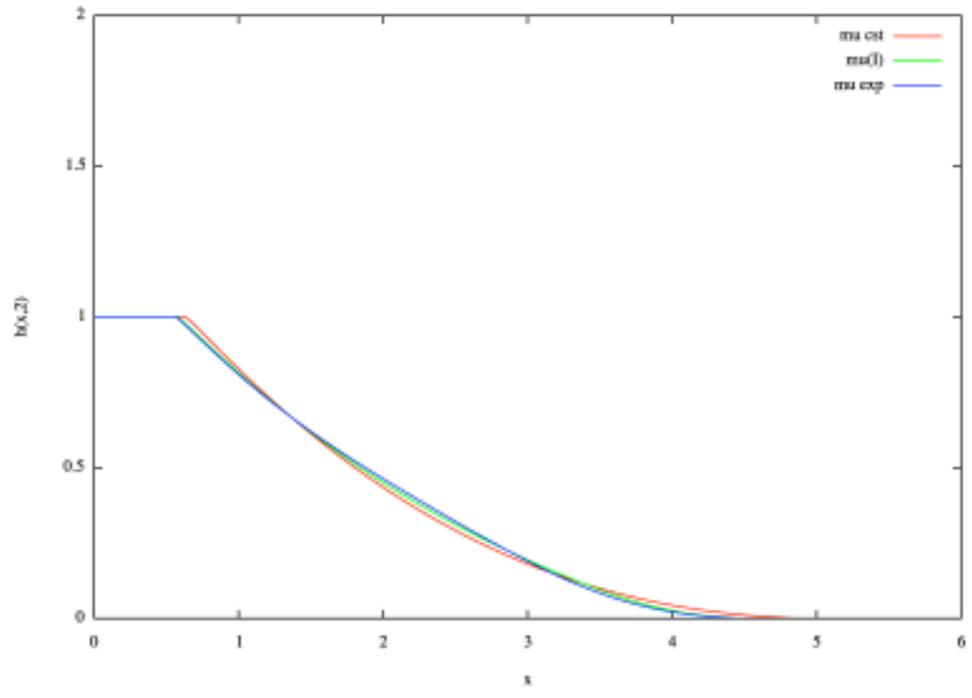

$$\mu(I) = \mu_s$$

$$\mu(I) = \mu_s + \frac{\Delta\mu}{\frac{I_0}{I} + 1}$$

$$\mu(I) = \mu_s + \Delta\mu e^{-\beta/I}$$

mu = 0.45
mu = (0.4 + 0.26/(0.4/ln +1))
mu = (0.4 + 0.26*exp(-0.136/ln))

Saint-Venant Savage Hutter *Gerris*

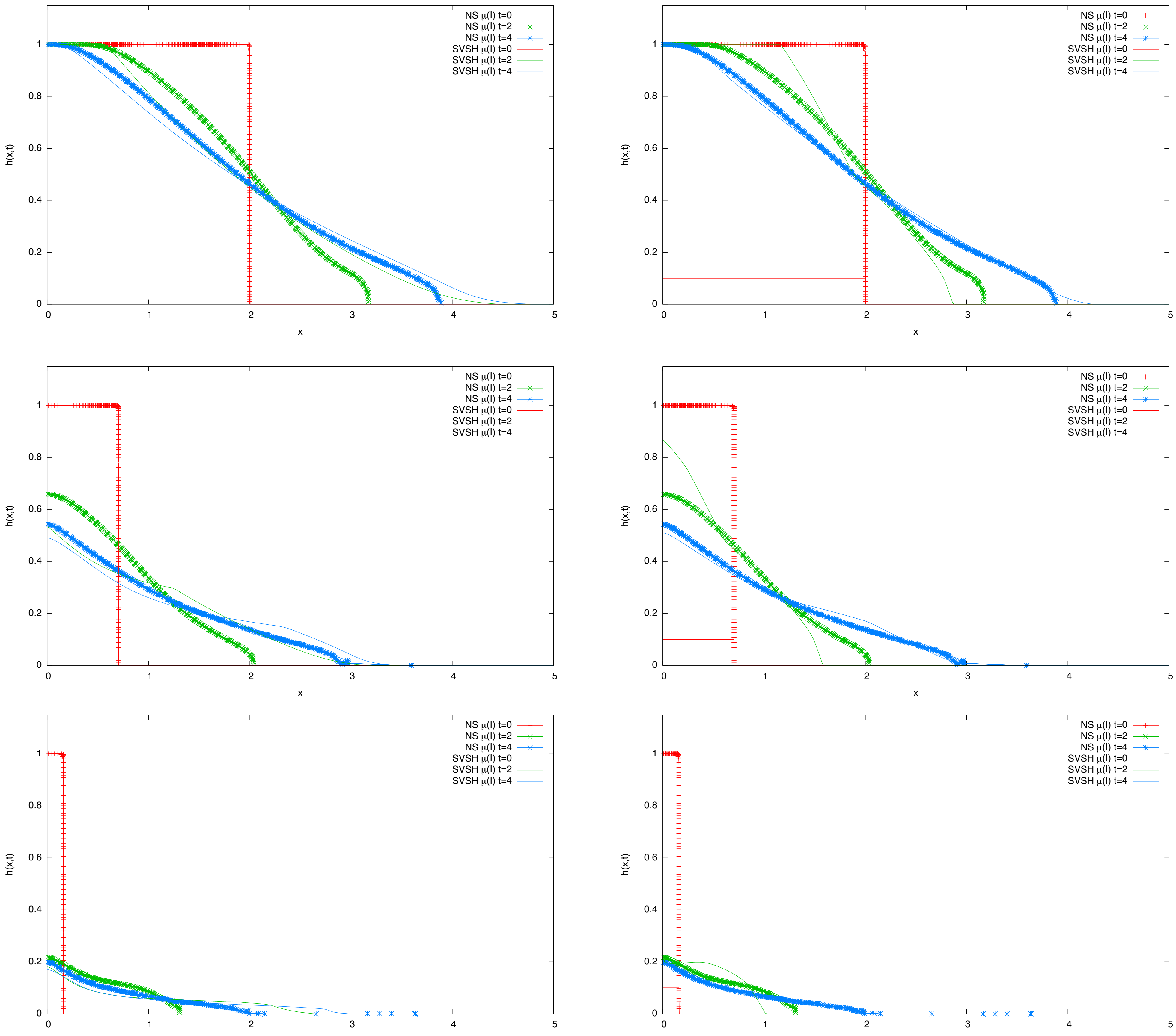

L. Satron, J. Hinch (DAMTP), A. Mangeney (IPGP), E. Larieu (IMFT)

Saint-Venant Savage Hutter *Gerris*

Saint-Venant Savage Hutter *Gerris*

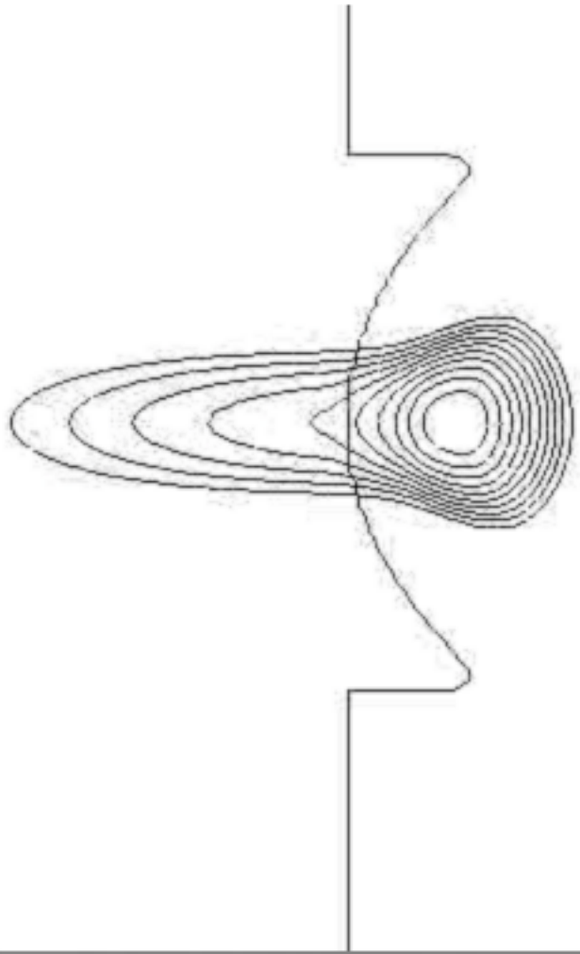

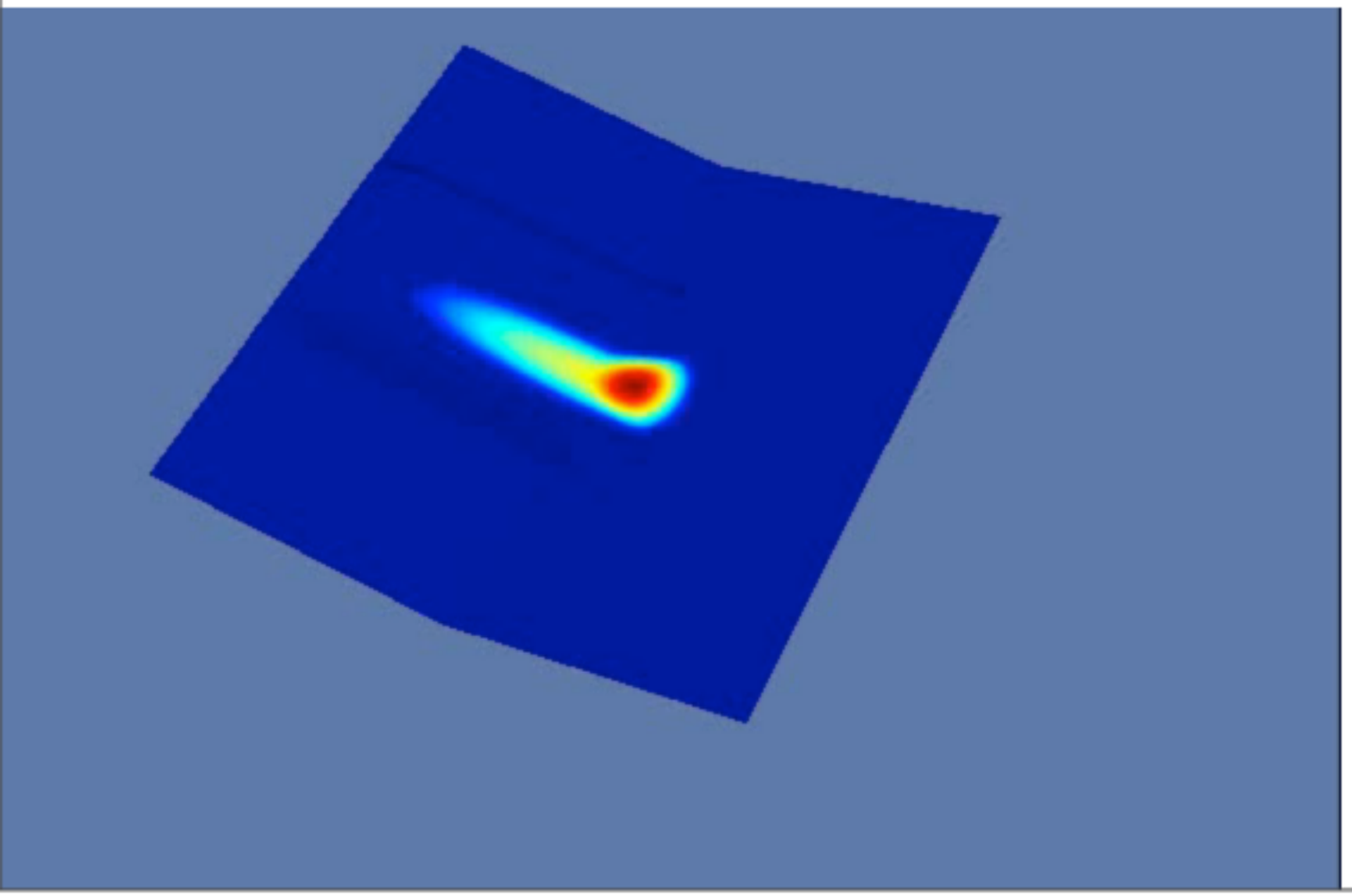

Saint-Venant Savage Hutter *Gerris*

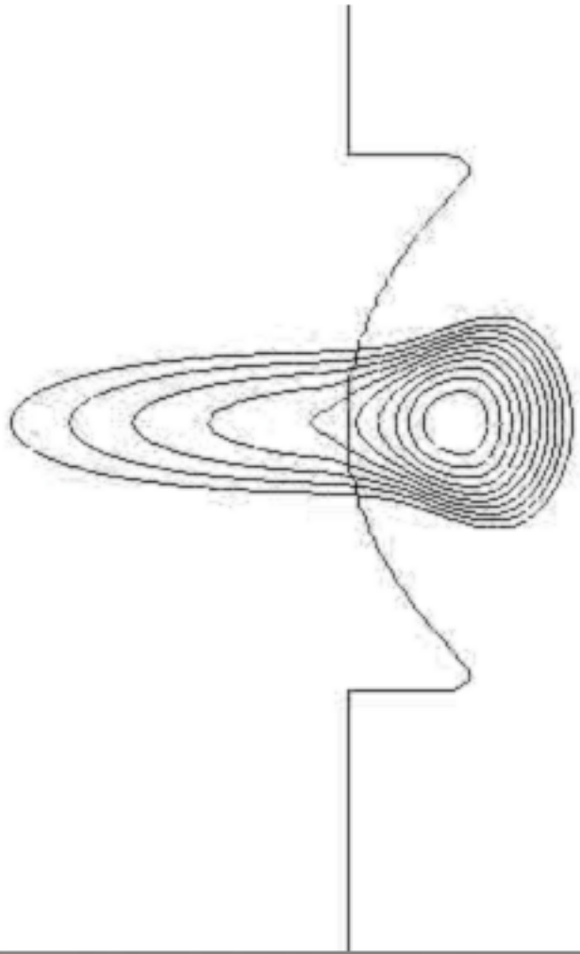

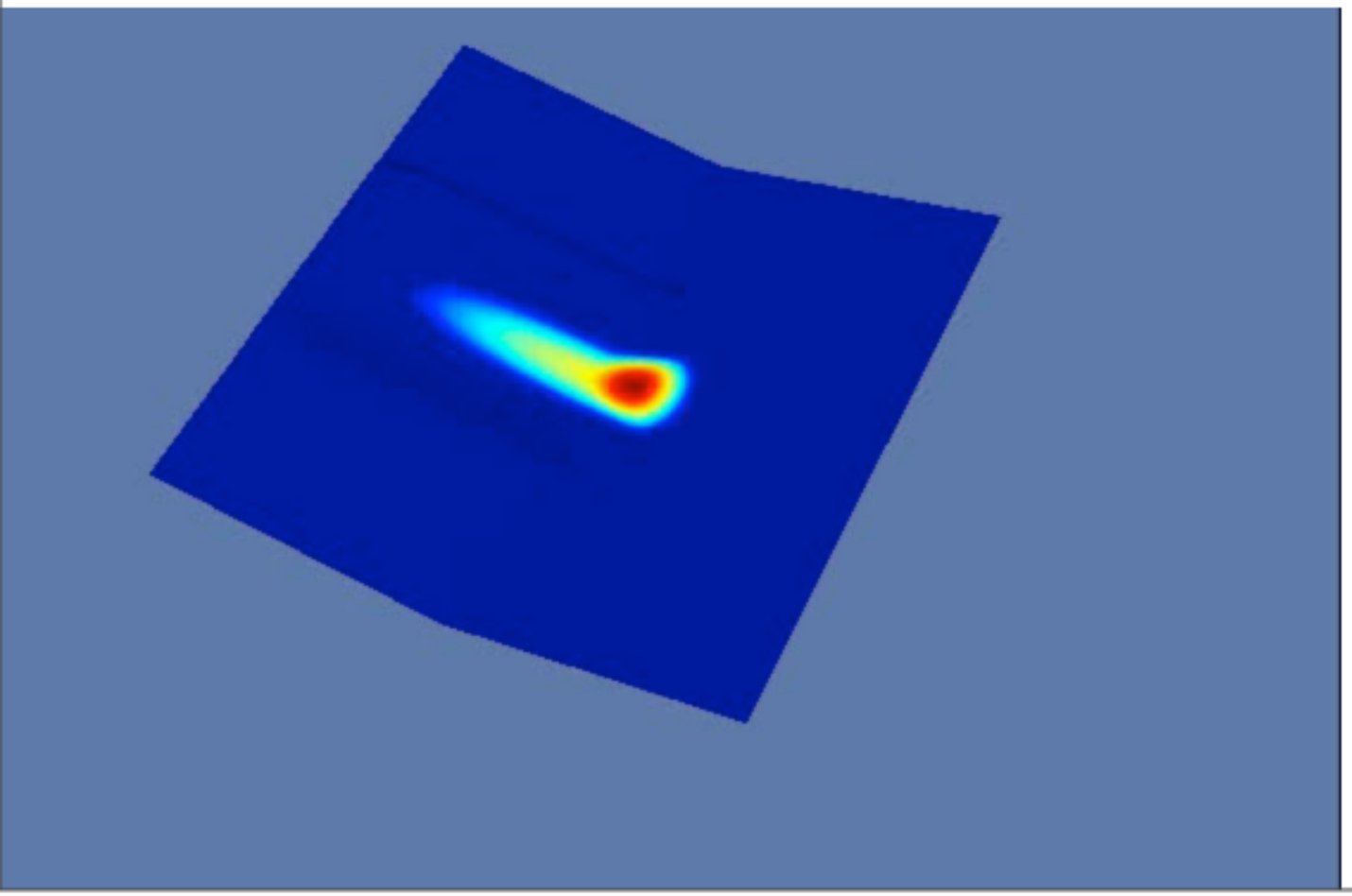

Saint-Venant Savage Hutter *Gerris*

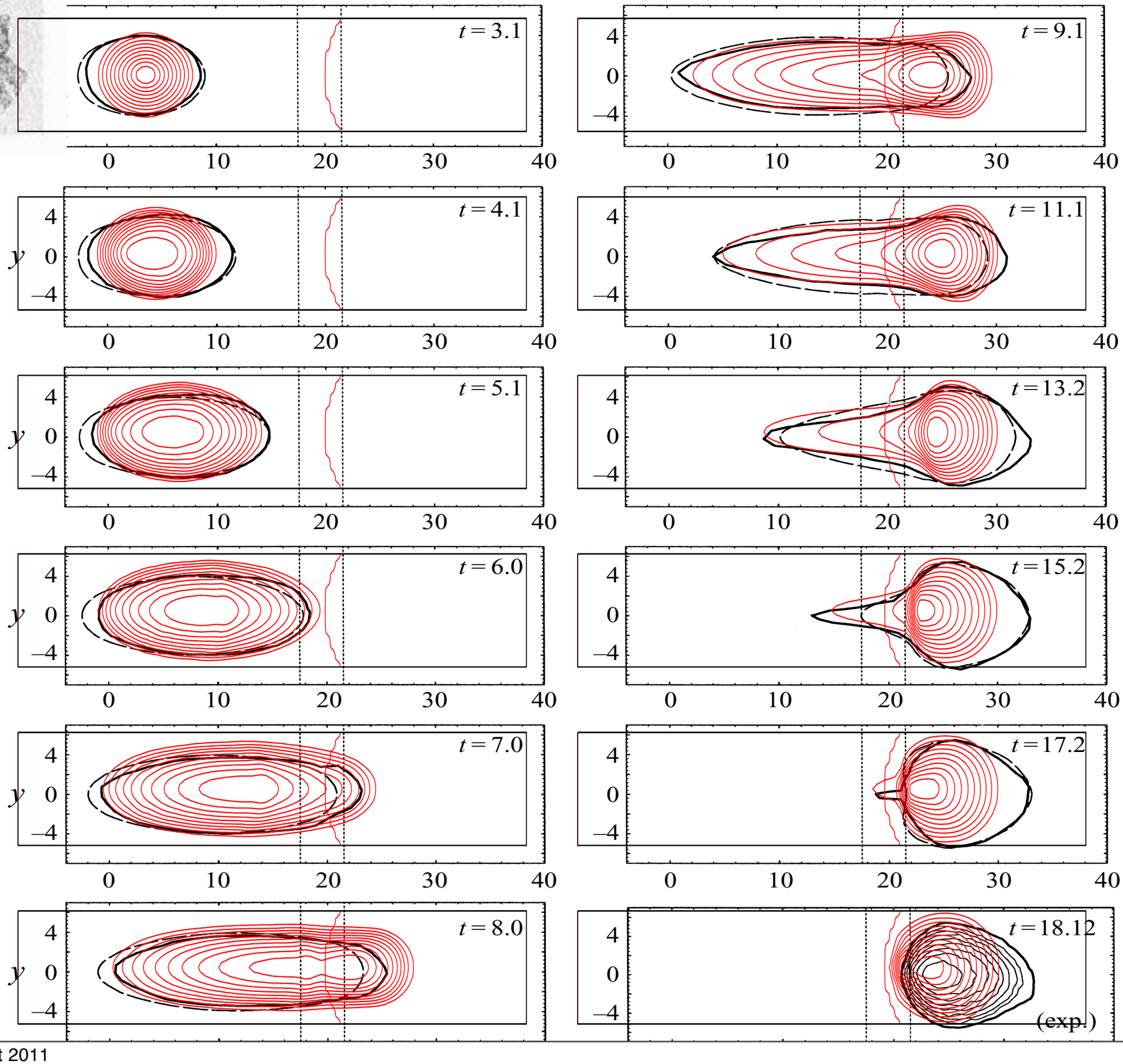

conclusion

- μ(I) obtained from experimental flows of dry granular flows [Jop et al. 06], implemented it in *Gerris*
- test case: analytical solution of steady avalanche (Bagnold solution)
- collapse of granular columns (shape as function of time compared to Discrete Simulations).
-The experimental trends of the scaling of the run out are reobtained
- Saint Venant Savage Hutter to be compared with.

This opens the door to systematic studies of granular flows using this continuum approach.

références:

P. Jop, Y. Forterre, O. Pouliquen, (2006) "A rheology for dense granular flows", Nature 441, pp. 727-730 (2006)

P.-Y. Lagrée, L. Staron and S. Popinet (subm. to J.F.M.) "The granular column collapse as a continuum: validity of a two–dimensional Navier–Stokes model with a μ(I)-rheology"

E. Lajeunesse, A. Mangeney-Castelnau, and J.-P. Vilotte, (2004) "Spreading of a granular mass on an horizontal plane», Phys. Fluids, 16(7), 2371-2381.

L. Staron & E. J. Hinch (2005) "Study of the collapse of granular columns using two-dimensional discrete-grain simulation", J. Fluid Mech. (2005), vol. 545, pp. 1–27.